9 - STAGE ARRANGEMENT
(Photograph of a Model)

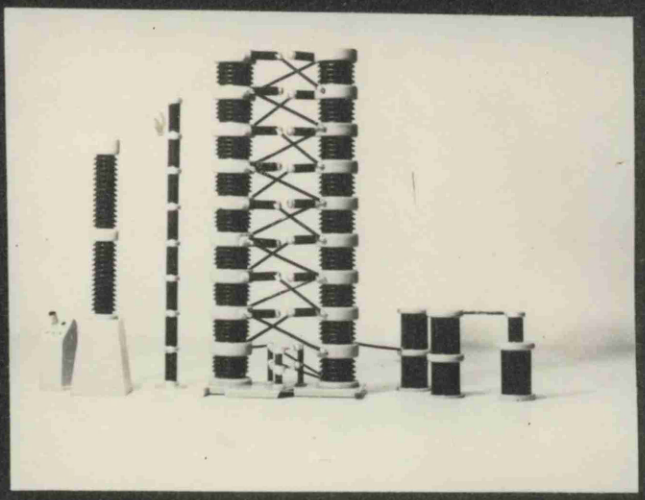

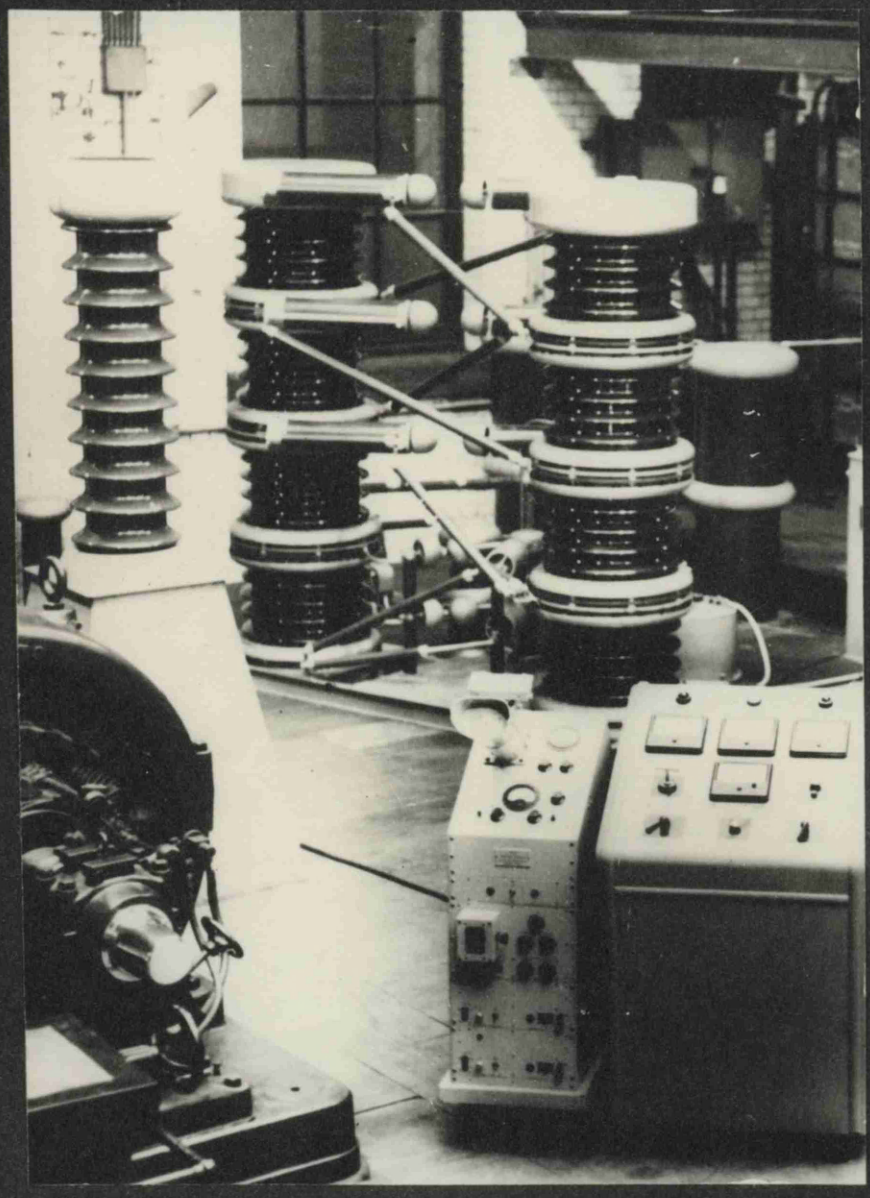

4 - STAGE
IMPULSE
GENERATOR

(Original
Tripping-
Gear shown)

FRONTISPIECE.

ProQuest LLC.
789 East Eisenhower Parkway
P.O. Box 1346
Ann Arbor, MI 48106 – 1346

ANALYSIS OF

HIGH VOLTAGE IMPULSE GENERATOR CIRCUITS

by

L. MARTIN HADDOW

B.Sc.(Eng.), A.R.C.S.T.

A Thesis Submitted to University of Glasgow

for the Degree of Doctor of Philosophy

1958.

ANALYSIS OF HIGH VOLTAGE IMPULSE GENERATOR CIRCUITS.

Resume of Thesis by L. Martin Haddow.

A study is made of transient or oscillatory voltages which arise in an impulse generator of the two-column Marx type during the firing process (i.e. between the breakdown of the first and the last spark-gap and immediately thereafter). These voltages are liable to appear on the external test and measuring equipment, but this aspect is not dealt with, nor are the spark-gap characteristics investigated systematically.

The voltages are shown to be relatively independent of the main circuit elements, but to be set up in the stray capacitative and inductive fields in the generator structure. These fields are resolved into an equivalent circuit involving measurable parameters. A matrix method is developed to analyze its dynamic properties, the solution being given in terms of eigenvalues. It is particularly suited to numerical treatment on a digital computer. The theory is extended, tentatively, to the evaluation of optimum damping resistances.

By a second approach, the generator is represented by a one-dimensional lattice circuit. Although an explicit solution is not obtained, some propagation characteristics are determined, enabling comparison to be made with the one-column type of generator (and with such analogous problems as transformer windings).

The gaps cannot in general be assumed to fire simultaneously. The transient voltages are of primary importance in causing their successive breakdown, but the instant of breakdown due to an overvoltage cannot be determined from present data. Again, the firing of the gaps constitutes the excitation to the circuit, but it is doubtful whether they behave as ideal switches. These two factors make a complete solution impracticable.

The experimental work made use of a four-stage generator. Voltages calculated from measured parameters are compared with oscillographic measurements. Sources of error in the capacitance-divider circuit are investigated and compensation for the connecting leads shown to be desirable.

FOREWORD.

I have first to express my gratitude to the Sir James Caird's Travelling Scholarships Trust for awarding me a Senior Scholarship for three years, supplemented in the first year by a Greenock Research Scholarship awarded by the Royal College of Science and Technology, Glasgow. I have to thank Professor F.M. Bruce for his continuous support and encouragement in the course of my researches. I also acknowledge the assistance of Mr. A.S. Husbands, who was my supervisor during the earlier stages, and of the other members of staff and research students in the Electrical Department of the College, almost every one of whom gave me help or advice in some form.

My thanks are also due to C.A. Parsons & Co. Ltd., Newcastle-on-Tyne, for permission to complete the writing of this thesis during my employment, and for the typing and printing; also to Mr. E. Smart and staff of the Applied Mechanics Laboratory for resolving the dynamical matrix of Section 2.2.6 on a digital computer.

L.M.H.

ANALYSIS OF HIGH VOLTAGE IMPULSE GENERATOR CIRCUITS.

SECTION 1 : THESIS

SECTION 2 : MATHEMATICAL THEORY.

SECTION 3 : EXPERIMENTAL WORK.

NOTE. Section 1 consists of an integration of the complete study, since the sub-sections of 2 and 3 cannot be arranged in a strictly logical order. The sub-sections are also shown schematically in Figure 1. The remaining figures are numbered roughly in order of first appearance in Sections 2 and 3.
List of Symbols on next page.

List of Symbols used in Section 2.1.

A	=	a diagonal matrix, in Equation 9.
B	=	a matrix in Equation 19.
$c(t)$	=	diagonal matrix of cos $\omega_r t$ - terms (Equ. 9).
$C_1, C_2 \ldots$	=	partial capacitances.
C	=	symmetrical matrix of capacitance coefficients C_{ij}.
D	=	d/dt.
$e(t)$	=	(column-matrix of) impressed emf(s) e_1 e_2 ...
$E(p)$	=	£ e(t).
f	=	frequency.
$f(w), f(z)$	=	characteristic matrices of U, Y Equ. 4(a,b).
$F(w), F(z)$	=	adjoints of f(w), f(z).
h_r	=	modal row, or eigenvector, of mode r.
h	=	square matrix formed of rows h_r.
$i(t)$	=	mesh currents.
I_n	=	unit matrix of order n.
k_r	=	modal column of mode r.
k	=	square matrix formed of columns k_r.
K	=	matrix conjugate to k.
L	=	symmetrical matrix of inductance coefficients L_{ij}.
£	=	"Laplace transform of".
n	=	No. of conducting gaps = order of matrix.
p	=	transform parameter.
$q(t)$	=	(matrix of) charge displacements in arbitrary meshes.

List of Symbols used in Section 2.1 (continued).

$\bar{q}(t)$	=	ditto in normal meshes.
$Q(p)$	=	£ $q(t)$.
r	=	typical mesh number.
R	=	resistance matrix.
S	=	C^{-1} = matrix of elastance coefficients, S_{ij}.
t	=	time.
U	=	CL = dynamical matrix (square).
$v(t)$	=	voltage difference across terminal pairs.
$V(p)$	=	£ $v(t)$.
w	=	$-1/p^2 = 1/\omega^2$.
W	=	diagonal matrix formed by w_1 w_2 ...
x	=	arbitrary column matrix in Equ. 17.
Y	=	$L^{-1} C^{-1} = U^{-1}$.
z	=	$-p^2 = \omega^2$; z_r = root of $\Delta(z) = 0$.
Z	=	diagonal matrix formed of z_1, z_2 ...
ω	=	$2 \pi f$.
$\Delta(w)$, $\Delta(z)$	=	determinant of $f(w)$, $f(z)$.
$\Delta'(w)$, $\Delta'(z)$	=	$d\Delta(w)/dw$, $d\Delta(z)/dz$.

Suffixes to e, i, q refer to arbitrary meshes.

" " h, k, $\bar{q}$, w, z, ω refer to normal modes or meshes.

Double Suffixes to C, L, S refer to mutuals between arbitrary meshes.

List of Symbols used in Section 2.3.

a	=	wave number = 1/wavelength in sections.
b	=	cos k = parameter in Equations 6 and 8.
C	=	capacitance from node to earth.
C_1, C_2 ...	=	capacitances at ends (Figure 8).
f	=	frequency.
k	=	$2\pi a$.
K_1 K_2	=	capacitance between adjacent, alternate nodes.
L	=	inductance per section.
n	=	section number.
N	=	total number of sections.
p	=	parameter of Laplace transform with respect to t.
q	=	constants in Equation 4.
t	=	time.
$U(p,z)$	=	transform of $v(t,n)$ with respect to both t and n.
$v(t,n)$	=	voltage from node n to earth at time t.
$V(p,n)$	=	Laplace transform of $v(t,n)$.
$V_1, V_2 \ldots V_N$	=	ditto at nodes 1, 2, ... N.
V_{mn}	=	voltage across Gap m following firing of Gap n.
y	=	constants in Equation 1.
z	=	parameter of sequence transform with respect to n.
ω	=	$2\pi f$.

SECTION 1 - THESIS.

1.1 Introduction.

The analytical work that has been done elsewhere on the multi-stage impulse generator has been concerned mainly with the "external" phenomena, viz. with the wave-shaping and test-load circuits connected to its terminals, and the main series circuit through the generator after it has fired. It is rather fortuitous that equipment based on Marx's original circuits should tend to work at all, even though the processes involved have been only incompletely and imperfectly understood. A paper by Edwards, Husbands and Perry (Reference 4) describes the development of the machine over about 25 years. In that time, three or four basic physical arrangements of the main components have emerged, and it is now a standard piece of high-voltage equipment in both research laboratory and industrial test-house. Yet even now there is no thorough understanding of what takes place internal to the generator between the firing of the first and the last spark-gap. Transient oscillations, overvoltages, and photo-irradiation effects are all involved.

The successful operation of the generator depends on the several spark-gaps firing simultaneously, or with very little time-lag between them. Actually, this tends to occur automatically provided the gaps are reasonably well adjusted. Nevertheless, generators having designs that appear suitable for the intended output, have been found, when assembled and tested, to operate anomalously. The authors of Reference 4, for instance, mention an 8-stage, 1000 kV. generator "which could not be made to work consistently at charging voltages in excess of 60 kV. when arranged to deliver a wave of 5 microsec. wavetail". The overvoltages appearing across the first two or three successive gaps were then calculated, taking into consideration certain stray capacitances and tail resistors. This led to a better understanding of that particular anomaly, and hence to improvement in

the machine's performance. Goodlet, (Reference 6) also discusses the influence of the gaps on the output wave-shape, as have many others in the field.

With the early oscillographic methods, high-frequency superimposed oscillations due to transients within the generator were either not recorded at all, or were indistinguishable from spurious oscillations produced in the measuring circuit itself. Improvements both in high-speed oscillographic equipment and in the associated potential dividers have made for far more precision in impulse work, as for instance in fault detection in machine windings. There has thus arisen the need for purer and smoother output voltages, and hence a real interest in the behaviour of the internal elements of the impulse generator.

Many of these circuit elements exist, however, more by accident than by design. Apart from the spark-gaps, they include the inductances of connecting links, and capacitances of insulated supports and of the air-space between the main electrodes and the earthed surroundings. Although never the same for any two installations, the predominant elements are characteristic for each basic physical arrangement of generator components. This thesis will deal only with the type of generator shown in the photographs and in Figure 2, which comprises stage capacitors and spacers arranged alternately in two vertical columns.

A certain amount of work has already been done on the internal analysis of generators in addition to that mentioned in Reference 2. Elsner (Reference 5) regards the generator stack as a transmission-line type of network, with infinitely small batteries spaced between the uniformly-distributed parameters. Partial differential equations are set up to give a system of travelling waves. These waves appear as oscillations superimposed on the terminal impulse voltage, but seemingly they do not agree well with the recorded oscillations. Provoost (Ref. 19) extends the same theory to show how travelling waves can be made aperiodic by the insertion of terminating resistance.

In an attempt to obtain a truer representation of the machine, Miller, in a Thesis to London University (Ref. 15) reviewed by Professor John (Ref. 12), regards it as a ladder network, having the same number of stages as there are generator stages, and made up of lumped parameters. Finite batteries between sections represent the charged capacitors. Difference equations are set up, which are successfully manipulated to take account of the superposition of transients produced by the simultaneous firing of several gaps. To obtain a solution, however, the capacitances of the spacers have to be neglected, although they are several times the inter-stage capacitances that have been included. Further, his theory does not set out to determine the over-voltages across the gaps prior to their sparking over, all gaps being assumed to fire at time $t = 0$. There is room for further improvement in the agreement with the measured output voltage.

What appears to be required now is, on the one hand, an extended and more analytical study of the problem discussed in Reference 4 of the firing of the successive gaps, and, on the other, an improved analysis in terms of oscillations in an extended network. A general theory should result from a successful meeting of these two approaches to the problem.

1.2 DIGEST OF STUDY.

1.2.1 Scope.

1.2.2 Scheme of Work and Preliminaries.

1.2.3 Matrix Analysis.

1.2.4 Lattice Analysis.

1.2.5 Oscillographic Measurements.

1.2 DIGEST OF STUDY.

1.2.1 Scope.

In the present study of the impulse generator, only the firing process will be dealt with. This covers the events between the firing of the first and the last spark-gap, and the oscillations arising therefrom, the charging process being completed prior to this. The external components used to control and measure the waveshape applied to a test-object, and the test-object itself, will not be involved, although the analysis should make it possible to determine the internal oscillations that are liable to be impressed on them.

Such superimposed or picked-up oscillations can be troublesome in practice, and a knowledge of their origin is an advantage. Generally, each type of generator, and even each installation, has its own characteristic features. Here, the primary concern will be with the two-column, Marx type, the one used in the experimental work being a 4-stage machine (actually part of a 9-stage installation; see Section 3.1 and Figure 2).

The object of the mathematical theory is to determine the pattern of internal voltages, and hence the gap overvoltages. The latter are of particular interest in understanding the tripping range and consistency of cascading. The ultimate aim is to make possible a stage-by-stage analysis, whereby the overvoltage on the second gap due to the firing of the first is first obtained, and then, after arriving at the instant at which the second gap fires, to find the overvoltage on the third due to the firing of the first two; and so on. Clearly, with each successive stage, the complexity of the system will increase, and the method should be applicable to generators of perhaps a dozen or more stages.

1.2.2 Scheme of Work and Preliminaries.

The various sub-divisions of the work are indicated diagrammatically in Figure 1. This shows how the three basic elements in terms of which the generator is first seen, viz. physical structure, damping and loading components, and spark-gaps, are re-interpreted into the more abstract elements of passive parameters, arbitrary connections, and switches and excitation functions. The precise natures of the latter elements have to be defined before combining them in a mathematical analysis.

The passive parameters are discussed in Sections 3.2 and 3.3. When frequencies of 20 - 30 mc/s. are involved in a structure of this size, retarded-potential and energy-radiation factors become significant. Nevertheless, it is shown that to assume "near-zone" conditions does not introduce significant error, and allows of ordinary circuit theory to be used.

There is no unique system of passive parameters by which the electro-magnetic complex can be described. One may be more suitable for measurement purposes, and another for the mathematical treatment, and it thus becomes necessary to transform from one to another. Again, apart from the fact that both are involved in the numerical calculations, there is a close relationship between the measured values and the choice of mathematical analysis. For, the suitability of the latter may depend on the relative unimportance of some complicating parameter-element, which only the measurements can disclose. The result, in the present instance, are the alternative equivalent circuits of Figures 3, 4 and 8.

The spark-gaps are discussed in Section 3.4. In general, their firing is not assumed to occur simultaneously, but to depend on the over-voltages appearing across them. Since these over-voltages take the form of short-duration pulses superimposed on a steady voltage, the breakdown characteristics are very uncertain. This makes it almost impossible, with present

knowledge, to predict the instants of breakdown, given the over-voltages and the gap settings. Thus only in certain simple conditions can the theoretical and experimental results be com pared.

When a gap fires, it changes from a non-conducting to a conducting state, and at the same time cancels the voltage across it. An ideal gap can therefore be regarded either as a simple switch, or as the source of a voltage chop; in either case it will excite the passive network. But also discussed in Section 3.4 is the possibility that the change is a more gradual transient; also that there may be appreciable energy absorbed by the spark-formation.

The arbitrary connections mainly consist of opening out, shorting, or precise setting of spark-gaps, and of arrange-ments to charge one or more of the main capacitors. They apply both to the cases considered in the mathematical analysis, and to the experiments in which the voltages are measured oscillographic-ally. The latter will be discussed presently.

There are, broadly, two approaches to the problem:- either to regard the generator as a single unit, or as a series of similar, recurrent units. The former is the more strictly correct in any case, since the floor, ceiling, and surrounding laboratory equipment prevent the stages from being exactly similar units. More especially is this so when there are only four stages available, which also puts a limit to correlation of an extended network analysis. But with a large number of stages, a recurrent pattern in the parameter values should appear, and a recurrent network analysis would have certain advantages.

1.2.3 Matrix Analysis.

The method of analysis described in Section 2.1 uses the first of these approaches. It combines Laplace-transforms and matrix techniques for the solution of the simultaneous differential equations for the equivalent circuit. The matrix methods follow closely those described in "Elementary Matrices" by Frazer, Duncan and Collar (Reference B6) to which direct reference is made for definitions and proofs of theorems. References 3, 22 and 24, were also of assistance here.

As a result of the preliminary study of Section 3.2 the complete generator can be represented by the equivalent circuit of Figure 3. When the effects of the resistances are ignored, and the stage capacitors left out of account in the oscillatory circuit, the result is the simplified analytical network of Figure 4(a). This represents a linear conservative system, having Lagrange-type of equations for mesh currents. When in general matrix form, these equations can refer to any number of generator stages, although their solution will depend on the ability to deal with matrices of high enough order. Thus, for the charge-displacements round the meshes, q(t), we have

$$(L\,D^2 + S)q \quad = \quad e \quad \ldots \quad \text{Equ. 1 of Section 2.1}\ ^{*}$$

together with the supplementary or boundary conditions. The number of equations, and therefore the order of the matrices, equals the number of conducting (or shorted) spark-gaps. The solution consists of finding the latent roots of the dynamic matrix CL (or its reciprocal), and its model matrix k. (These are also known as eigenvalues and eigenvectors respectively.) When CL is expressed with numerical elements, a numerical solution is possible, and an iterative method is described. The result of one calculation for a 4-stage case done on a digital computer is included.

* See List of Symbols.

The latent roots represent the frequencies of oscillation of the network, while the modal matrix governs their relative amplitudes in each mesh. For the conditions assumed (gaps acting as simple switches, closing at t = o), and given an initial charge distribution q(o), the solution has the form

$$q(t) = k\, c\, k^{-1}\, q(o) \quad \ldots \quad \text{Equ. 13 of Section 2.1}$$

where c is a diagonal matrix of elements $\cos \omega_r t$.

A similar solution in terms of the voltages is

$$v(t) = K\, c\, K^{-1}\, v\,(o) \qquad \text{Equ. 23 of Section 2.1.}$$

It is shown that these two are closely related, so that we can write $k'K = 1$. By means of these modal matrices, the complete original system can be transformed into a system of normal or "primitive" networks, each involving only one frequency. It is then suggested that this property enables an optimum arrangement of resistances to be found which will damp out these oscillations to any desired degree. This suggestion is quite tentative, without proof or experimental confirmation, however, and the resulting resistance network cannot necessarily be incorporated in a practical generator.

The method in general can take account of one or more gaps firing at t = o, and gives the voltage at any point in the generator, including the over-voltages across the unfired gaps (still ignoring the effects of all resistances). The same method, repeated stage by stage, could also deal with the case of the gaps firing at given intervals of time. In that case, currents as well as charge-displacements at the instant of firing of a gap would be involved in the boundary conditions, these being evaluated from the solution of the previous stage. The practical problem does, however, depend on knowing the instants of firing of the successive gaps and, as discussed in Section 3.4, this appears to be beyond present information on their spark-over characteristics.

The approach adopted was to assume various arbitrary modes of firing of the gaps, and to try to reproduce them in the generator, so that the calculated and the oscillographically measured responses could be compared. In the general case, one group of gaps is assumed to be conducting, the rest remaining non-conducting. Usually, only one of the former, say Gap N, is assumed to fire at t = o, the others, say the first N-1 gaps in the column, being already conducting (or made so by shorting to simulate the test condition). Simultaneous firing can be represented by super-positioning, the modal analysis being the same for all cases having the same N conducting gaps.

1.2.4 Lattice Analysis.

As the number of stages increases, so does the work of resolving the matrices, and an analysis in terms of a one-dimensional lattice becomes more attractive. This is discussed in Section 2.3, and is based on "unified" parameters of stray capacitance (see Section 3.2.4 and Figures 8 and 13). These comprise equal shunt capacitances, C, from each stage to earth, and equal coupling capacitances, K1 and K2, between adjacent and alternate stages along the lattice respectively. Coupling between more remotely separated stages is ignored. There are capacitance terminations at each end. The node-points are connected through the spark-gaps and inductances in a single line (Figure 8). The same circuit can alternatively be regarded as identical 6-terminal sections in cascade (Figure 11).

The former type of circuit has been studied quite extensively by Rudenberg (Ref. 20) and others (Ref. 14, 18, 25) in connection with surges in transformer windings, The characteristic equations are partly differential with respect to time, t, and partly of finite differences with respect to the stage number, n, and two theories have been developed, interpreting the solutions in terms of standing waves and travelling waves respectively. Lewis, in Reference 14, discusses the relationship between the two.

A feature common to all the above papers, however, is to ignore capacitance coupling other than that between adjacent sections (K_1), although considerable attention has been devoted to more-remote mutual inductances. Elsner and Miller (Refs. 5 and 15) also ignore K_2 in the circuit for the impulse generators. But although this may be justified for the single-layer transformer winding and for the single-column generator, in the case of the 2-column type of generator, K_2 is mainly the capacitance of the spacers between the main capacitors, and the measurements of Section 3.3.1 make K_2 about three times K_1. On the basis of steady-state voltages, alone, the characteristics of the two are very different (Section 2.3.2).

The problem has been more adequately dealt with by Brillouin in Reference B.3 for the analogous system of a row of particles having equal masses, and inter-acting forces between them extending over any distance. His work is mainly concerned with the propagation characteristics at any section of the lattice, and he points out that reflections at the terminations make the complete solution extremely complicated. In the present problem, couplings across three sections (K_3) and beyond are ignorable, and a solution seemed feasible. The work of Section 2.3 is the result, but an explicit solution of the voltage equation was not achieved. The difficulties were algebraic, however, and may yield to different treatment. The recurrent-section method was also not pursued far, although it might likewise respond to more advanced treatment. A recent paper by Waldvogel and Rouxel (Ref. 25) suggests that an extended matrix form of solution may be used.

1.2.5 Oscillographic Measurements.

The second major part of the work was to obtain sets of oscillograms of the voltages from the various points on the generator to earth. Each set was for arbitrary circuit conditions, chosen because it revealed some characteristic feature of the performance, or corresponded to a conveniently calculated

condition. It was hoped to obtain correlation of both frequencies and amplitudes of the component oscillations, although the decrements would be governed by the rather indeterminate losses.

Considerations of recording with a capacitance divider are given in Section 3.6. The divider itself was required to have a low gross capacitance, both to avoid unduly disturbing the field of stray capacitances, and to enable it to respond to the high frequencies. That used (Figure 21) was of quite simple construction. Numerous tests indicated that the screening of the middle electrode was adequate. The gross capacitance was estimated at 15 pF. Since all voltage amplitudes could be related to the charging voltage of the first stage, a knowledge of the exact value of the divider-ratio was not required, provided this ratio remained constant with, or could be corrected for, variations in voltage and frequency (or rate of change of voltage). The capacitance unit itself appeared to be sufficiently linear, but a major source of non-linearity was introduced by the inductance of the loop formed by the connections, and by the series resistance required to damp out the oscillations in this loop.

A response-frequency calibration of the complete divider was attempted, but was not satisfactory for the higher range of frequencies (above about 5 mc/s.). A theoretical response curve was calculated, and the correction factors, when applied to the recorded amplitudes, gave much improved correlation with calculations for the simplest generator arrangements (one and two stages). But this is not considered a sufficiently sound basis for comparison, especially in the more complex waveforms that are obtained from multi-stage arrangements. Additional uncertainty arises because the possible characteristics of the spark-gaps can also cause the large initial decrements, (Section 3.4), which are the main feature of the divider-response.

1.3 CONCLUSIONS.

The four principal features of the investigation are the following:-

(a) Resolution into, and measurement of the passive circuit parameters.

(b) Mathematical analysis into oscillatory modes, assuming step-function excitation.

(c) Representation of spark-gaps for both time-lag and nature of breakdown.

(d) Oscillographic measurement.

(a) The various impedance matrices and equivalent circuits appear to have been formed satisfactorily except possibly for the inductances. Mutual inductances might have improved the correlation of frequencies. Dissipation has not been included in the original parameters. The validity of the Lattice equivalent circuit requires to be confirmed after measurements of partial capacitances on a generator of more than four stages, and a further study of the inductances of an extended generator.

(b) Given the equivalent circuit, and the assumptions relating to gap breakdown, the matrix analysis developed in Section 2.1 is put forward as a satisfactory and quite general method of solution. It is not dependent on any special pattern existing in the stray capacitances and inductances. The treatment depends on numerical analysis, unlike the methods used previously in impulse generator, transformer, and other analogous problems, (except in some very recent papers on the application of computers) in which the solution is given in symbolic form. It is therefore particularly adapted for solution on a digital computer, and avoids the need for major approximations in the equivalent circuit. Further, provided the relationship between gap over-voltage and gap breakdown is known, a stage-by-stage solution could be carried out quite economically. Dissipation

factors could not be introduced very easily, in the initial solution, although resistance values for optimum damping can probably be evaluated.

The one-dimensional lattice and the recurrent network circuits of Section 2.3 are only to be regarded as sketches of methods which may offer advantages in the case of a very large number of stages. The difference equations, involving a new system of voltages, might be formed into matrices which are easier to resolve than those of Section 2.1, while an analytic solution might reveal a pattern in the frequencies which the numerical method obscures. Both the steady-state voltage distributions and the propagation characteristics indicate that the firing process of the 2-column construction of generator is markedly different from that of the single-column type, and this does not appear to have been revealed in previous work.

(c) Although the analysis enables the frequencies which can occur to be calculated, the amplitudes of oscillation under normal operating conditions cannot be predicted without a detailed knowledge of the gap-breakdown characteristics. This is also a factor which seems to be ignored in previous analytical investigations. The instant of breakdown, the nature of the change to a conducting state, and the possible effects on the decrements are unknown factors, outwith the scope of this thesis, and probably of present-day knowledge. Some of the problems raised might form subjects of future investigations.

(d) Further work is also required on the oscillographic measuring technique. The construction of an inherently linear divider circuit does not appear to be feasible, and a frequency calibration up to at least 20 mc/s., with a view to compensating the lower arm, would seem to be the most hopeful approach. Nevertheless, the very simple construction of capacitance divider, used with an ordinary commercial oscilloscope enabled much relevant information to be obtained on the firing process.

2.1 MATRIX ANALYSIS OF OSCILLATORY NETWORK.

The List of Symbols used in Section 2.1 follow the Contents Page.

2.1.1 Introduction.

In the present mathematical approach, the generator is to be analysed as a single, complex unit as shown in Figure 4. The natural modes of oscillation and the frequencies and amplitudes due to the firing of the spark-gaps in any arbitrary manner are to be found. The immediate objective is to do the analysis for the 4-stage generator shown, but with a view to extending the method to a larger number of stages. In order to make the work manageable, the analysis will be done for the equivalent conservative system, in which series resistors are shorted out, and shunt resistors removed (or, in tests, increased to very large values). Figure 4 shows the result, which is a system of capacitances and a system of inductances. The two are completely segregated except at the terminal points.

Each spark-gap will be interpreted, arbitrarily, in one of the following ways:- as an open circuit, when the voltage across it corresponds to an over-voltage; as a short circuit, because it has fired at some previous instant (or has been shorted for the test); or as a source of excitation for the whole system, because, in firing, it cancels any voltage across it, and closes a mesh.

2.1.2 Formation of Equations.

A 2-stage generator (or any generator in which two gaps are conducting) will be used occasionally to illustrate the method. Ignoring resistances, it can be visualized as three main electrodes (in reality, stage capacitors) with a capacitance-field between them, and having two inductive connections through the spark-gaps, (Figure 5(a). The field is fully described by the partial capacitances C_1, C_2, C_3, (or by their reciprocals, the elastances S_1, S_2, S_3), Figure 5(b). The straightforward method of analysing this circuit would be to choose three meshes, including, say, one round the three capacitances, and set up three equations. Since, however, there is no initial displacement round this mesh, it can be ignored provided the capacitance network is re-described by a matrix of self and mutual capacitance or elastance coefficients relative to the "external" meshes 1 and 2.

$$C = \begin{bmatrix} C_{11} & , & C_{12} \\ C_{21} & , & C_{22} \end{bmatrix} = \begin{bmatrix} (C_1 + C_3) & , & C_3 \\ C_3 & & (C_2 + C_3) \end{bmatrix}$$

$$\text{and} \quad C^{-1} = S = \begin{bmatrix} S_{11} & , & S_{12} \\ S_{21} & . & S_{22} \end{bmatrix}$$

The general method of obtaining the C- or S- matrix is given in Section 3.2.2. The capacitance network can then be shown as a "box" with pairs of access terminals, as in Figure 4(a). A similar "box" represents the inductance system, which, when connected to the same pairs of terminals, enclose the two meshes.

Mutual inductance terms will be included when setting up the equations, but later neglected. The equations will be in terms of the charge displacements, q(t), round the arbitrarily chosen meshes, and the impressed voltages e(t), and can be written

$$(D^2 L_{11} + S_{11})\, q_1(t) + (D^2 L_{12} + S_{12})\, q_2(t) = e_1(t)$$
$$(D^2 L_{21} + S_{21})\, q_1(t) + (D^2 L_{22} + S_{22})\, q_2(t) = e_2(t)$$

$$\therefore\ D^2 \begin{pmatrix} L_{11} & L_{12} \\ L_{21} & L_{22} \end{pmatrix} \cdot \begin{pmatrix} q_1 \\ q_2 \end{pmatrix} + \begin{pmatrix} S_{11} & S_{12} \\ S_{22} & S_{22} \end{pmatrix} \cdot \begin{pmatrix} q_1 \\ q_2 \end{pmatrix} = \begin{pmatrix} e_1 \\ e_2 \end{pmatrix}$$

$$(L D^2 + S)\, q = e \qquad \ldots\ldots\ (1)$$

where $D = d/dt$, so that a mesh current equals

$$i(t) = \dot{q} = Dq = dq/dt.$$

If mutual inductances are neglected, $L_{12} = L_{21} = o$, and L becomes a diagonal matrix. The order of the matrices is equal to the number of meshes (or conducting gaps).

2.1.3 Resolution of Modes of Oscillation.

The solution of $(LD^2 + S)q = e$ consists of the complementary function, which is the solution of $(LD^2 + S)q = o$ and involves the initial conditions q(o) and $\dot{q}(o)$, and the particular integral, which involves e(t). In the general problem, dealing with spark-gaps firing at different instants, both initial conditions and impressed voltages would have to be taken into account, but, for the present, the case of only one gap firing in a quiescent circuit will be considered. This can be done in two ways. In one, Heaviside's conditions can be assumed, viz. that there is neither charge nor current in the circuit at t = o, when the firing of a gap impresses a unit-step voltage (say $e_r = 1$). The other approach assumes that there are

initial charges q(o) (calculated from the steady voltage across the gap before it fires), but no impressed voltages. The currents begin to flow at t = o as the system seeks a new condition of equilibrium.

This distinction ceases to exist when the Laplace transform is taken of the whole equation. In doing this, the time-functions e(t) and q(t) become the p-functions E(p) and Q(p) according to the following relations.

The Laplace transform of $q(t) = \pounds\, q(t) = Q(p)$, where

$$Q(p) = p \int_o^{\infty} \varepsilon^{-pt}\, q(t)\, dt \text{ , (and likewise for } E(p) \text{).}$$

$$\pounds\, \dot{q}(p) = \pounds\, Dq = p\, Q(p) - p\, q(o)$$

$$\pounds\, \ddot{q}(p) = \pounds\, D^2 q = p^2\, Q(p) - p^2\, q(o) - p\, \dot{q}(o)$$

where $q(o)$ and $\dot{q}(o)$ are the values of charge and current at t = o,

Hence Equation 1 becomes

$$(L\, p^2 + S)\, Q(p) = L\, p^2\, q(o) + L\, p\, \dot{q}(o) + E(p) \quad . \quad . \quad . \quad (2)$$

Symbols denoting the same matrices as before.

In the present case, all currents are initially zero. If the second approach is used, E(p) = o, but there are voltages v(o) initially across the capacitance-terminals, corresponding to charges q(o) = C v(o). The voltages, v(o), are numerically identical with -E(p) if the latter represents only shorted gaps or step-functions (Figure 5b).

There are two slightly different ways of writing the transformed equation; both will be useful in determining the oscillations:

$$(L\, p^2 + S)\, Q(p) = p^2\, L\, q(o) \quad . \quad . \quad . \quad . \quad . \quad (3a)$$

$$(L\, p^2 + S)\, Q(p) = E(p) = -v(o) = -S\, q(o) \quad . \quad (3b)$$

From (3a) $(p^2 I + L^{-1} C^{-1}) Q = p^2 q(o)$

$\therefore \quad (z I - Y) Q = z q(o) \quad . \quad . \quad . \quad . \quad (4a)$

and from (3b) $(\frac{1}{p^2} I + CL) Q = -\frac{1}{p^2} q(o)$

$\therefore \quad (w I - U) Q = - w q(o) \quad . \quad . \quad . \quad . \quad (4b)$

where $S = C^{-1}$, $Y = L^{-1} C^{-1}$, $U = CL$

$z = - p^2$, $w = - 1/p^2$, I = unit matrix of the same order, n, as the system.

The Equations (4a) and (4b) are of the same form, all the system characteristics being contained in either Y or U. (U is sometimes known as the dynamical matrix of the system). $f(z) = z I - Y$ is called the "characteristic matrix" of Y

$\therefore f(z)Q = z q(o), \qquad \therefore Q(p) = z f^{-1} q(o) \quad . \quad . \quad . \quad (5).$

The problem is to resolve the right-hand-side into explicit functions of p.

Let $F(z)$ = adjoint of $f(z)$ (the adjoint being the transpose of the matrix made of the co-factors of the original).

and $\Delta(z) =$ determinant of $f(z)$
$= (z - z_1)(z - z_2) \ldots\ldots (z - z_n)$

It will be assumed that $z_1, z_2 \ldots z_n$, the roots of $\Delta = o$ (also called the latent roots of Y) are all distinct.

Also let $\left(\frac{d \Delta}{d z}\right)_{z = z_r} = \Delta'(z_r)$

Then $f^{-1}(z) = \frac{F(z)}{\Delta(z)}$

$$= \sum_r \frac{F(z_r)}{\Delta'(z_r)} \quad \frac{1}{z - z_r}$$

Sec. 2.1.3.

If we put $z_r = \omega_r^2$, then

$$\frac{z}{z - z_r} = \frac{p^2}{p^2 + \omega_r^2} = \text{Laplace transform of } \cos \omega_r t$$

$$\therefore \text{ from (5), } q(t) = \sum_{r=1}^{n} \frac{F(z_r)}{\Delta'(z_r)} \cos \omega_r t \,.\, q(o) \quad . \quad . \quad . \quad (6)$$

Thus the charges oscillate in n characteristic modes.

Now, since $\Delta(z_r) = o$ (z_r all different), $f(z_r)$ is a simply degenerate matrix, having n-1 independent rows. Then (see Ref. B6 Section 3.5) its adjoint, $F(z_r)$ must have only one independent row, the others being in proportion. It can therefore be expressed as a product of a column and a row, say

$$F(z_r) = k_r h_r \quad . \quad . \quad . \quad . \quad . \quad . \quad . \quad . \quad . \quad . \quad . \quad . \quad (7)$$

$$\therefore \quad q(t) = \sum_{r} k_r \cdot \frac{\cos \omega_r t}{\Delta'(z_r)} \cdot h_r \; q(o) \quad . \quad . \quad . \quad . \quad (8)$$

and by simple summation

$$\therefore \quad q(t) = k \,.\, A \,.\, c(t) \,.\, h \,.\, q(o) \quad . \quad . \quad . \quad . \quad . \quad . \quad . \quad (9)$$

where k and h are square matrices made up of the columns k_r and the rows h_r respectively, and A and c(t) are diagonal matrices formed of the terms $1/\Delta'(z_r)$ and $\cos \omega_r t$ respectively.

Again (see Ref. B6 Section 3.8) it can be proved that

$$h_r k_r = \Delta'(z_r) \quad . \quad . \quad . \quad . \quad . \quad . \quad . \quad (10)$$

$$\therefore \; h\,k = A^{-1}, \qquad \therefore \; h = A^{-1} k^{-1}$$

$$\therefore \quad q(t) = k \,.\, c(t) \,.\, k^{-1} q(o) \quad . \quad . \quad . \quad . \quad . \quad . \quad . \quad (11)$$

It is now apparent that definite ratios exist between the amplitudes of a particular frequency-component in the various meshes which are given by the modal column, k_r. The column k_r can be chosen proportional to any non-zero column of $F(z_r)$, or, as explained later, can be found by a numerical iterative method from Y.

The alternative form of the transformed equation gives a similar result.

$$\therefore (w\,I - U)\,Q = w\,.\,q(o) \quad . \quad . \quad . \quad . \quad . \quad . \quad . \quad (4b)$$

Setting up similar functions f, F, Δ gives

$$Q(p) = \sum_r \frac{F(w_r)}{\Delta'(w_r)} \cdot \frac{w_r}{w - w_r}\, q(o) \quad . \quad . \quad . \quad . \quad (12)$$

If $w_r = 1/\omega_r^2$, $\dfrac{w_r}{w - w_r} = \dfrac{p^2}{p^2 + \omega_r^2} = \mathcal{L} \cos \omega_r t.$

Hence $q(t) = k.A\,.\,c(t).h.q(o) = k.c(t).k^{-1}.q(o)$ . . (13)
which is in the same form as before, although note that the actual matrices k, h, A, etc. are now different.

2.1.4 Normal Co-ordinates.

If now new co-ordinates (i.e. system of meshes) $\bar{q}$, are adopted, given by $q = k\,\bar{q}$

$$\bar{q}(t) = c(t)\,\bar{q}(o) \quad . \quad . \quad . \quad . \quad . \quad . \quad . \quad (14)$$

i.e. $\bar{q}_1(t) = \bar{q}_1(o) \cos \omega_1 t.$

$\bar{q}_2(t) = \bar{q}_2(o) \cos \omega_2 t,$ etc.

The meshes in which the displacements $\bar{q}$ occur are known as the normal co-ordinates or meshes. Each involves only one characteristic frequency, the amplitude of which is equal to the initial charge displacement in that mesh. As a rule, such normal meshes cannot be readily identified on the equivalent circuit of the system. An interesting result follows from putting $L_1 C_1 = L_2 C_2$

in the 2-stage case, when the two normal meshes can be easily located, (see Section 2.1.9).

2.1.5 Iterative Treatment.

Although the form of solution given by Equ. 11 (or 13) is very convenient, the practical difficulty lies in obtaining the roots of $\Delta(z) = o$ and in evaluating $F(z_r)/\Delta'(z_r)$ by ordinary algebra. However, a numerical iteration method is given in Ref. B6 Chap. 10 whereby the roots (or frequencies) and the modal columns can be obtained directly from the original equation

$$(D^2 I - Y)\, q(t) = 0$$

Substituting $q(t) = k\, c(t)\, k^{-1}\, q(o)$

$$\therefore (-k\, Z\, c(t).\, k^{-1} + Y\, k.c(t).\, k^{-1})\, q(o) = o$$

where Z is the diagonal matrix formed by $z_1, z_2, \ldots z_n$

since $D^2 \cos \omega_r t = -\omega_r^2 \cos \omega_r t = -z_r \cos \omega_r t.$

This is true for all t, so put $t = o$

$$-k\, Z\, k^{-1} + Y\, k\, I\, k^{-1} = o$$

$$\therefore Y = k Z k^{-1} \qquad \ldots\ldots\ldots\ldots (15a)$$

$$\therefore Y^2 = k Z k^{-1} . k Z k^{-1} = k Z^2 k^{-1}$$

$$\therefore Y^m = k Z^m k^{-1} \qquad \ldots\ldots\ldots\ldots (16)$$

For convenience, let this be post-multiplied by an arbitrary column of constants x

$$Y^m x = k Z^m . k^{-1} x.$$

Now, if there is one dominant root z_1, corresponding to a maximum frequency component ω_1 (where $z_1 = \omega_1^2$) so that $z_1 \gg z_2$ etc. then z_2^m, etc. will be negligible by comparison with z_1^m provided m is large enough.

$$\therefore Y^m x = \begin{pmatrix} k_1 & k_2 & \dots \end{pmatrix} \begin{pmatrix} z_1^m, & o, & o \dots \\ o, & o, & \dots \\ o, & o, & \dots \\ \dots & \dots & \dots \end{pmatrix} k^{-1} x$$

$$= k_1 \cdot z_1^m \cdot \underline{k}_1 \cdot x \qquad \dots\dots\dots (17)$$

where $\underline{k}_1$ is the first row of k^{-1}, making $\underline{k}_1 x$ a scaler. Thus the column $Y^m x$ is proportional to the first modal column k_1, and further pre-multiplation of it by Y multiplies the result by $z_1 = \omega_1^2$.

The procedure for finding the maximum frequency and its modal column is to pre-multiply an arbitrary column of constants, say $\begin{pmatrix} 1, & 1, & 1 & \dots \end{pmatrix}$, by $Y = L^{-1} C^{-1}$ repeatedly until the ratios of the elements in the resulting column become sufficiently constant. This can be observed by dividing out say the top element at each stage. In the end, this factor will approach $z_1 = \omega_1^2$ and the remaining column can be taken to be k_1.

The alternative form of transformed equation would have given $U = k W k^{-1}$ ..... (15b) where $U = CL$, W = diagonal matrix formed of $w_1 = 1/\omega_1^2$, $w_2 = 1/\omega_2^2$ etc. The above procedure would then result in ω_1 being the <u>lowest</u> or fundamental frequency, and k_1 its modal column.

The dynamical matrix $U = CL$ contains all modes of oscillations as its latent roots. In order to evaluate the first sub-dominant root by the present method, it is necessary to modify U (or Y) so that it will represent a system in which the

dominant frequency is absent. This is done by introducing an equation of constraint for the first normal mesh.

$$\bar{q}_1 = \underline{k}_1 \cdot q = 0 \quad \ldots\ldots\ldots \quad (18)$$

where $\underline{k}_1$ is the first row of k^{-1}. This reciprocal cannot be calculated directly from the k_1 - column already found, but we have

$$U = k\, W\, k^{-1}, \quad \therefore \quad W = k^{-1}\, U\, k = k^{-1}\, C\, L\, k.$$

Since C, L, W, are symmetrical matrices, it follows that k^{-1} must be proportional to either $k'\, C^{-1}$ or $k'\, L$ in order to preserve the symmetry# (i.e. $k^{-1} = a\, k'\, L$, say, where a is a diagonal matrix). For the present purpose, therefore, we can take $\underline{k}_1 = k_1'\, L$, where k_1' is the transposed of k_1. (The same conditions hold for the alternative form $Y = k\, Z\, k^{-1}$.)

This equation of constraint, $\underline{k}_1\, q = o$, can be re-expressed as follows:

$$q_1 = -\frac{\underline{k}_{12}}{\underline{k}_{11}} q_2 - \frac{\underline{k}_{13}}{\underline{k}_{11}} q_3 - \ldots.$$

$$\therefore\ q = \begin{pmatrix} o & , & -\underline{k}_{12}/\underline{k}_{11} & , & -\underline{k}_{13}/\underline{k}_{11} & , & \ldots \\ o & , & 1 & & o & & \\ o & , & o & & 1 & & \\ \vdots & & \vdots & & \vdots & & \end{pmatrix} \begin{pmatrix} q_1 \\ q_2 \\ q_3 \\ \vdots \end{pmatrix} \quad \ldots\ldots \quad (19)$$

or write $q = R\, q$, say, and then $D^2 q = B\, D^2 q$.

Sect. 1.13 of Ref. B6.

Substituting this in one side of the differential equation

$$(D^2 I - Y)\, q = o, \quad \text{i.e.} \quad D^2 q = Y q$$

we get $D^2 q = YBq$, $\therefore (D^2 I - YB)\, q = o$ . . . (20)

Thus multiplying by B transforms Y for the original system to YB for a system constrained so that there is no displacement, $\bar{q}_1$, round the normal mesh 1. The dominant root and mode of this system can be found by the same iterative method, and will be the first sub-dominant of the original. The procedure can be repeated to yield the other roots.

2.1.6 Conjugate Voltage Solution and Normal Transformation.

The mesh equations and their solution given above are in terms of the charge-displacement functions and the initial charges, but no currents. They can therefore be re-stated in terms of voltage functions and initial voltages, since $q(t) = Cv(t)$, and $q(o) = Cv(o)$.

Equation 4 becomes

$$(p^2 I + C^{-1} L^{-1})\, V(p) = p^2 v(o)$$

$$\therefore \quad (z I - Y')\, V = z \cdot v(o) \quad . \; . \; . \; . \; (21)$$

and Equ. 11 becomes

$$(I/p^2 + LC)\, V = v(o)/p^2$$

$$\therefore \quad (w I - U')\, V = w \cdot v(o) \quad . \; . \; . \; . \; (22)$$

Y' and U' being the transposed matrices of Y and U, since L and C are symmetrical. These equations are of exactly the same form as before, and yield solutions of the same form, viz.

$$v(t) = K C K^{-1} v(o) \quad . \; . \; . \; . \; . \; . \; . \; . \; (23)$$

It should be noted that these are voltages across node-pairs and not in the meshes. It will be convenient in future to regard q as charge-displacement between node-pairs, and in the present case, this can be done without change.

The modal matrices k and K are related as follows. Equation 11 gives

$$q = C\,v = k\,c\,k^{-1}\,q(o) = k\,c\,k^{-1}\,C\,v(o)$$

$$\therefore \quad v = C^{-1}\,k.c.k^{-1}\,C.\,v(o) = K\,c\,K^{-1}\,v(o) \quad \text{identically.}$$

Thus K must be proportional to $C^{-1}k$, and as was shown in forming Equation 19, k^{-1} is proportional to $k'C^{-1}$. And now the arbitrary proportional elements can be so chosen that

$$k'\,K = 1 \qquad \ldots\ldots\ldots \quad (24)$$

This equation indicates that there is an orthogonal relationship between the two modal matrices, and brings out the conjugate properties of the voltages and charge-displacements. In tensor algebra (see Ref. B.11) they are the co- and contra-variant quantities of the system. Further, there is a system of normal voltages, $\bar{v}$, given by $v = K\,\bar{v}$, corresponding to $q = k\,\bar{q}$.

As with the normal charges, each normal voltage involves only one frequency. The relationship between the original and normal systems can be interpreted as a transformation between the original network and a set of "primitive" networks, as shown in Figure 4(b). The capacitance matrix can be transformed as follows

$$q = C\,v\,, \qquad \therefore \quad k\,\bar{q} = C\,K\,\bar{v}$$

$$\therefore \quad \bar{q} = k^{-1}\,C\,K\,\bar{v} = K'\,C\,K\,\bar{v} = \bar{C}\,\bar{v}$$

$$\therefore \quad \bar{C} = K'\,C\,K \quad \text{and} \quad C = k\,\bar{C}\,k' \qquad \ldots\ldots \quad (25)$$

where $\bar{C}$ is the capacitance matrix of the primitive system, and is diagonal, (i.e. without mutual terms) since $K' \propto K^{-1}\ C^{-1}$

Similarly, $L = K\,\bar{L}\,K'$ and $\bar{L} = k'\,L\,k$ . . . . . (26)

The above process is analogous to that developed by Kron (Ref. B.11) to effect transformations between the original network, and a set of primitive networks, each consisting of an element of the former. In the present case, however, there is no identification of the original and normal quantities (except the frequencies, and, implicitly, the energies). In fact the latter are not even unique, but depend on an arbitrary scale-factor contained in k or K.

2.1.7 Damping of Oscillations.

It is now proposed to apply the transformation concept just developed to calculate the resistances required to effect damping in any of the natural modes of oscillation. It is suggested, by analogy, that if each primitive network be shunted by the resistance necessary to give the desired degree of damping of its mode, (Fig. 4c) the resulting resistance matrix $\bar{R}$ can be transformed to $R = K\,\bar{R}\,K$ pertaining to the original system (Figure 4d). More conveniently, if reciprocal-resistance, or conductance G is used, then $G = k\,\bar{G}\,k'$. This will be similar to the original C-matrix, which (see Figure 14) can be readily interpreted into individual admittances between terminals. The resistances have been calculated for complete damping of the 2-stage case in Section 2.2.4. The values appear to be of the right order, but the arrangement has not been tried experimentally.

2.1.8 Two-Stage Case.

For the case in which the first two gaps are conducting (one or both having fired at t = o), the expressions can be obtained more directly. Assuming $L_{12} = L_{21} = 0$

$$U = CL = \begin{pmatrix} C_{11} & , & C_{12} \\ C_{12} & , & C_{22} \end{pmatrix} \cdot \begin{pmatrix} L_{11} & , & 0 \\ 0 & , & L_{22} \end{pmatrix} = \begin{pmatrix} C_{11} L_{11}, & C_{12} L_{22} \\ C_{12} L_{11}, & C_{22} L_{22} \end{pmatrix}$$

$$\therefore Y = L^{-1} C^{-1} = \frac{1}{\Delta_o} \begin{pmatrix} C_{22} L_{22} & , & - C_{12} L22 \\ -C_{12} L_{11} & , & C_{11} L_{11} \end{pmatrix}$$

where $\Delta_o = (C_{11} C_{22} - C_{12}^2) L_{11} L_{22}$

$$f(z) = f(p^2) = \begin{pmatrix} z - C_{22} L_{22}/\Delta_o , & C_{12} L_{22}/\Delta_o \\ C_{12} L_{11}/\Delta_o ; & z - C_{11} L_{11}/\Delta_o \end{pmatrix}$$

$$F(z) = \begin{pmatrix} z - C_{11} L_{11}/\Delta_o , & - C_{12} L_{22}/\Delta_o \\ - C_{12} L_{11}/\Delta_o , & z - C_{22} L_{22}/\Delta_o \end{pmatrix}$$

$$\Delta(z) = z^2 - z (C_{11} L_{11} + C_{22} L_{22}) / \Delta_o + 1/\Delta_o$$

$$= (z - z_1)(z - z_2)$$

In this case it is easy to show that

$$F(z_1) = \begin{pmatrix} 1 \\ \dfrac{- C_{12} L_{11}}{z_1 \Delta_o - C_{11} L_{11}} \end{pmatrix} \cdot \left(z_1 - C_{11} L_{11}/\Delta_o, - C_{12} L_{22}/\Delta_o \right)$$

$$= k_1 h_1 , \text{ say, } \quad \text{(cp. Equ. 7)}$$

and similarly $F(z_2) = k_2 h_2$.

Also $A_1 = 1/\Delta'(z_1) = 1/(z_1 - z_2)$

$A_2 = 1/\Delta'(z_2) = 1/(z_2 - z_1)$

Substitutions also show that $k^{-1} = A\,h$ ... (as Equ. 10).

$$\therefore \quad q(t) = (A_1 k_1 h_1 \cos \omega_1 t + A_2 k_2 h_2 \cos \omega_2 t)\, q(o)$$

$$= k \,.\, c(t) \,.\, A.h.q(o)$$

$$\therefore \quad \underline{q(t) = k \,.\, c(t).k^{-1} \,.\, q(o)} \qquad \text{as Equ. 11.}$$

2.1.9 Special Case when $L_1 C_1 = L_2 C_2$

The special case of $L_1 C_1 = L_2 C_2$ (see Figure 7b) will be considered.

$$\Delta(z) = p^4 + \frac{p^2((C_1 + C_3) L_1 + (C_2 + C_3) L_2)}{L_1 L_2 (C_1 C_2 + C_2 C_3 + C_3 C_1)}$$

$$+ \frac{1}{L_1 L_2 (C_1 C_2 + C_2 C_3 + C_3 C_1)}$$

Substituting $L_1 C_1 = L_2 C_2$, and manipulating, gives

$$\Delta(z) = \left(p^2 + \frac{C_1 + C_2}{(L_1 + L_2)(C_1 C_2 + C_2 C_3 + C_3 C_1)} \right) \cdot \left(p^2 + \frac{L_1 + L_2}{L_1 L_2 (C_1 + C_2)} \right)$$

$$= (p^2 + \omega_1^2)(p^2 + \omega_2^2) \qquad \text{as before}$$

$$\therefore \quad \omega_1^2 = \frac{1}{(L_1 + L_2)(C_3 + C_1 C_2/(C_1 + C_2))} \,,$$

$$\omega_2^2 = \frac{1}{(C_1 + C_2) L_1 L_2/(L_1 + L_2)} = \frac{1}{L_1 C_1}$$

Substituting these in the modal matrix expression,

$$k = \begin{pmatrix} 1 & , & 1 \\ 1 & , & -L_1/L_2 \end{pmatrix}, \quad \therefore k^{-1} = \frac{1}{L_1 + L_2} \begin{pmatrix} L_1 & , & L_2 \\ L_2 & , & -L_2 \end{pmatrix}$$

$$\therefore q(t) = k\, c\, k^{-1}\, q(o)$$

$$\therefore \begin{pmatrix} q_1 \\ q_2 \end{pmatrix} = \frac{1}{L_1+L_2} \begin{pmatrix} 1, & \\ 1, & -L_1/L_2 \end{pmatrix} \begin{pmatrix} \cos \omega_1 t\ , & o \\ o, & \cos \omega_2 t \end{pmatrix} \begin{pmatrix} L_1, & L_2 \\ L_2, & -L_2 \end{pmatrix} \begin{pmatrix} q_1(o) \\ q_2(o) \end{pmatrix}$$

$$= \frac{1}{L_1+L_2} \begin{pmatrix} L_2 \cos \omega_1 t, & L_2 \cos \omega_2 t \\ L_2 \cos \omega_1 t, & -L_1 \cos \omega_2 t \end{pmatrix} \begin{pmatrix} q_1(o)L_1/L_2 + q_2(o) \\ q_1(o) \quad -q_2(o) \end{pmatrix}$$

From this result, it is apparent that ω_1 refers to an oscillation round Mesh 1' , Figure 7(c), through the two inductances in series. The q-matrix shows that the current of this component flows with equal amplitude in Meshes 1 and 2. None of this current flows in the connection from the mid-point; in fact it is the current which would flow if this connection were opened. Similarly, ω_2 refers to opposing oscillations in the meshes formed by L_1C_1 and L_2C_2. The current in the common connection divides in the two meshes in the ratio $L_2:L_1$, making the voltage-component across C_3 zero, so that it could be opened without affecting ω_2.

2.2 NUMERICAL CALCULATIONS.

2.2.1 Steady-State Voltages.

2.2.2 One-Stage oscillations.

2.2.3 Two-stage oscillations.

2.2.4 Two-stages : normal networks and damping.

2.2.5 Iterative Solution of 2-Stage case.

2.2.6 Four-Stage oscillations.

In this section, the theory of Section 2.1 and the measured parameters of Section 3.3 will be used to evaluate the transients in the 4-Stage generator for a number of arbitrary conditions (i.e. arrangements of connections). These are to be compared with oscillographic measurements in Section 3.7.

2.2.1 Steady State Voltages.

From the C- and S- matrices alone, it is possible to calculate the steady-state components of the over-voltages produced across the unfired gaps by the firing of the others. If the voltage changes are Δv, corresponding to charge displacements Δq (and assuming there is no charge lost through resistive leaks)

$$\underset{(1,r)}{\Delta q} = \underset{(r,r)(1,r)}{C.\Delta v}, \qquad \text{where } r \text{ is the number of conducting gaps}$$

$$\therefore \underset{(1,4)}{\Delta v} = \underset{(r,4)(1,r)}{S.\Delta q} = \underset{(r,4)}{S} \cdot \underset{(r,r)}{S^{-1}} \cdot \underset{(1,r)}{\Delta v}$$

(The figures in the brackets indicate the number of rows, columns in the matrix. Refer also to Section 3.2.3.)

(a) Gap 1 firing alone : v_1 changes from - 1 to 0,

$$\Delta v = \begin{pmatrix} S_{11} \\ S_{21} \\ S_{31} \\ S_{41} \end{pmatrix} \frac{1}{S_{11}} = \begin{pmatrix} 1.07 \\ -0.88 \\ 0.24 \\ -0.24 \end{pmatrix} \frac{1}{1.07} = \begin{pmatrix} 1 \\ -.824 \\ 0.224 \\ -.224 \end{pmatrix}$$

Thus, if there were a voltage of -1 initially across each gap, Gaps 2 and 4 will now tend to be fired by voltages of -1.824 and -1.224 respectively, while the firing of Gap 3 will be inhibited, as shown in Figure 7(a).
(Note, the negative signs follow the conventions of Figure 3.)

(b) Gaps 1 and 2 firing (i.e. assuming Gap 4 does not fire under -1.224).

$$\Delta v = \begin{pmatrix} 1.07 & -.89 \\ -.88 & 1.90 \\ 0.24 & -1.15 \\ -.24 & 0.63 \end{pmatrix} \cdot \begin{pmatrix} 1.53 & 0.72 \\ 0.72 & 0.865 \end{pmatrix} \cdot \begin{pmatrix} 1 \\ 1 \end{pmatrix} = \begin{pmatrix} 1 \\ 1 \\ -1.28 \\ 0.46 \end{pmatrix}$$

The steady-state voltage across Gap 3 is now -2.28, while that across Gap 4 will fall to -1 + 0.46 = -0.54.

(c) Gaps 1, 2 and 3 firing. Similarly by inverting the (3,3) S-matrix gives $\Delta v = \{1 , 1 , 1 , -1,36\}$.

These results have been plotted in Figure 7. This shows that as each successive gap fires, the overvoltage on the next, unfired, gap increases.

2.2.2 One-Stage Oscillations.

Consider the case when Gap 1 fires, all other remaining non-conducting. Then L_1 will oscillate with S_{11}, giving the simple equation

$$(L_1 p^2 + S_{11})\, Q_1 = -v_1(o) = 1$$

$$\therefore\ Q_1(p) = \frac{1}{L_1 p^2 + S_{11}} = \frac{10^6}{1.8\, p^2 + 1.07 \times 10^{16}}$$

$$= 0.93\ \frac{0.77^2 \times 10^{16}}{p^2 + 0.77^2 \times 10^{16}} \times 10^{-10}$$

since from Section 3.3, $L_1 = 1.8 \times 10^{-6}$ H, $S_{11} = 1.07 \times 10^{10}$ F^{-1}

$$\therefore\ q_1(t) = 0.93(1-\cos\ \omega t).10^{-10}$$

where $\omega = 0.77 \times 10^8$ rad/sec., $f = 12.3$ mc/s.

$$\therefore\ v(t) = Sq = 0.93 \begin{bmatrix} 1.07 \\ -0.89 \\ 0.24 \\ -0.24 \end{bmatrix} (1-\cos\ \omega t) = \begin{bmatrix} 1 \\ -0.83 \\ 0.22 \\ -0.22 \end{bmatrix} (1-\cos\ \omega t)$$

With a charging voltage of 1 unit, the initial voltage across each gap will be -1 (see Figure 3).

After Gap 1 fires,

$$v(t) = -\begin{bmatrix} \cos\ \omega t \\ 1 + (0.83 - 0.83 \cos\ \omega t) \\ 1 - (0.22 - 0.22 \cos\ \omega t) \\ 1 + (0.22 - 0.22 \cos\ \omega t) \end{bmatrix}$$

Thus both Gaps 2 and 4 will tend to fire due to the transients of Gap 1, while the tendency for Gap 3 to fire will be reduced.

2.2.3 Two-Stage Oscillations.

The measured values of parameters are given in Section 3.3.

$$L_{11} = 1.8 \times 10^{-6}, \quad L_{22} = 1.3 \times 10^{-6} \text{ (Henry)}$$

$$S_{(2,2)} = \begin{pmatrix} 1.07 & -0.89 \\ -0.89 & 1.90 \end{pmatrix} \times 10^{-10} \text{ (1/Farad)}$$

$$C_{(2,2)} = \frac{\begin{pmatrix} 1.90 & 0.89 \\ 0.89 & 1.07 \end{pmatrix}}{(1.07 \times 1.90 - 0.89^2)} = \begin{pmatrix} 1.53 & 0.72 \\ 0.72 & 0.865 \end{pmatrix} \times 10^{-10} \text{ (Farad)}$$

(See Section 3.2.3)

Then, $\Delta_o = (C_{11} C_{22} - C_{12}^2) L_1 L_2$

$= (1.53 \times 0.865 - 0.72^2) \times 1.8 \times 1.3 \times 10^{-32}$

$= 1.884 \times 10^{-32}$ (Farad - Henry)^2 units.

$$\Delta(z) = z^2 + \frac{z(1.53 \times 1.8 + 0.865 \times 1.3) \times 10^{16}}{1.88} + \frac{10^{32}}{1.88}$$

$$= (z + 0.303 \times 10^{16})(z + 1,76 \times 10^{16})$$

$\therefore z_1 = -\omega_1^2 = -0.303 \times 10^{16}, \quad z_2 = -\omega_2^2 = -1.76 \times 10^{16}$

$\omega_1 = 0.55 \times 10^8, \quad \omega_2 = 1.325 \times 10^8$ (Rad/sec.)

$\underline{f_1 = 8.77 \text{ mc/s.}} \qquad \underline{f_2 = 21.1 \text{ mc/s.}}$

Also, $k = \begin{pmatrix} 1 & 1 \\ 0.59 & -2.35 \end{pmatrix}, \quad k^{-1} = \begin{pmatrix} 0.80 & 0.34 \\ 0.20 & -0.34 \end{pmatrix}$

and $K = \begin{pmatrix} 0.80 & 0.20 \\ 0.34 & -.34 \end{pmatrix}$

The initial charges must be so disposed as to give the pre-breakdown voltage across each gap about to fire at t = o, and zero across the already-conducting gaps. With the sign conventions indicated in Figure 5, the initial charges and voltages will be negative, when the stage charging voltage is, say, 1 unit positive. The charges can be calculated from $q(o) = Cv(o)$.

Case (a). Suppose Gap 1 fires on unit voltage, Gap 2 being shorted

$$\begin{pmatrix} q_1 \\ q_2 \end{pmatrix}_{t=o} = \begin{pmatrix} 1.53 & 0.72 \\ 0.72 & 0.865 \end{pmatrix} \begin{pmatrix} -1 \\ 0 \end{pmatrix} = \begin{pmatrix} -1.53 \\ -0.72 \end{pmatrix}$$

Case (b). Suppose Gap 1 is shorted, and Gap 2 fires

$$\begin{pmatrix} q_1 \\ q_2 \end{pmatrix}_{t=o} = \begin{pmatrix} -0.72 \\ -0.865 \end{pmatrix}$$

The various numerical matrices can now be substituted in

$$q = k\, c\, k^{-1}\, q(o)$$

Case (a).

$$\begin{pmatrix} q_1 \\ q_2 \end{pmatrix} = \begin{pmatrix} 1 & 1 \\ 0.59, & -2.35 \end{pmatrix} \begin{pmatrix} \cos \omega_1 t, & \\ 0 & \cos \omega_2 t \end{pmatrix} \begin{pmatrix} 0.80, & 0.34 \\ 0.20, & -0.34 \end{pmatrix} \begin{pmatrix} -1.53 \\ -0.72 \end{pmatrix}$$

$$= \begin{pmatrix} \cos \omega_1 t & \cos \omega_2 t \\ 0.59 \cos \omega_1 t\ , & -2.35 \cos \omega_2 t \end{pmatrix} \begin{pmatrix} -1.47 \\ -0.06 \end{pmatrix}$$

$$= -\begin{pmatrix} 1.47\ , & 0.06 \\ 0.87\ , & -0.14 \end{pmatrix} \begin{pmatrix} \cos \omega_1 t \\ \cos \omega_2 t \end{pmatrix}$$

Further, the voltage across each node-pair is given by $v = Sq$. If $q(t)$ for the meshes with open-circuited gaps be taken as zero, S is the first two columns of the 4 x 4 S-matrix.

$$\therefore \quad \begin{pmatrix} v_1 \\ v_2 \\ v_3 \\ v_4 \end{pmatrix} = - \begin{pmatrix} 1.07 , & -0.89 \\ -0.89 , & 1.90 \\ 0.24 , & -1.15 \\ -0.24 , & 0.63 \end{pmatrix} \begin{pmatrix} 1.468, & 0.063 \\ 0.871, & -.147 \end{pmatrix} c$$

$$= - \begin{pmatrix} 0.796 , & 0.199 \\ 0.348 , & -.335 \\ -.649 , & 0.184 \\ 0.196 & -0.108 \end{pmatrix} \begin{pmatrix} \cos \omega_1 t \\ \cos \omega_2 t \end{pmatrix}$$

At $t = o$, this gives $v \doteqdot \{-1, \ 0, \ 0.47, \ -0.09\}$

The voltages of 0.47 and -0.09 indicated to be across Gaps 3 and 4 initially are due to the charge displacements $q(o)$ in Meshes 1 and 2. If, as in normal operation, Stages 3 and 4 were charged, the initial voltage across, say, Gap 3 would be -1, i,e, due to a displacement through the charging resistors, there would be a voltage change of -1.47. Thus when Gap 1 fires, there would be additional voltages of $-(0.47 - 0.65 \cos \omega_1 t + 0.18 \cos \omega_2 t)$ superimposed on Gap 3, tending to make it fire, and $(0.09 - 0.20 \cos \omega_1 t + 0.11 \cos \omega_2 t)$ on Gap 4, tending to retard firing.

Case (b). Similarly:-

$$\begin{pmatrix} q_1 \\ q_2 \end{pmatrix} = - \begin{pmatrix} 0.871 , & -0.151 \\ 0.517 , & 0.354 \end{pmatrix} \begin{pmatrix} \cos \omega_1 t \\ \cos \omega_2 t \end{pmatrix}$$

$$\begin{pmatrix} v_1 \\ v_2 \\ v_3 \\ v_4 \end{pmatrix} = - \begin{pmatrix} 0.472 , & -0.476 \\ 0.207 , & 0.806 \\ -0.385 , & -0.443 \\ 0.117 , & 0.259 \end{pmatrix} \begin{pmatrix} \cos \omega_1 t \\ \cos \omega_2 t \end{pmatrix}$$

2.2.4 Two Stages : Normal Networks and Damping.

The parameters of the normal or primitive networks are given by

$$\bar{C} = K' C K = \begin{pmatrix} 1.47 & 0 \\ 0 & 0.063 \end{pmatrix} 10^{-10} F.$$

$$\bar{L} = k' L k = \begin{pmatrix} 2.26 & 0 \\ 0 & 9.0 \end{pmatrix} 10^{-6} H.$$

Check that $1/\bar{L}_{11}\,\bar{C}_{11} = 0.302 = \omega_1^2$ as before.

$1/\bar{L}_{22}\,\bar{C}_{22} = 1.77 = \omega_2^2$

Shunt resistance for critical damping $= \frac{1}{2}\,\omega L$,
hence completely to damp out ω_1 and ω_2 requires

$$\bar{R}_{11} = \tfrac{1}{2} \times 0.55 \times 10^8 \times 2.26 \times 10^{-6} = 62 \text{ ohms.}$$

$$\therefore \quad \bar{G}_{11} = 1/\bar{R}_{11} = 1.61 \times 10^{-2}$$

Similarly $\bar{G}_{22} = 0.168 \times 10^{-2}$

$$\therefore \quad G = k\,\bar{G}\,k' = \begin{pmatrix} 1.78 & 0.56 \\ 0.56 & 1.49 \end{pmatrix} = \begin{pmatrix} (G_1 + G_3), & G_3 \\ G_3 & , (G_2 + G_3) \end{pmatrix}$$

$$\therefore \quad G_1 = 1.22 \times 10^{-2} \qquad \therefore \quad R_1 = 82 \text{ ohms}$$

$$G_2 = 0.93 \text{ "} \qquad R_2 = 107 \text{ "}$$

$$G_3 = 0.56 \text{ "} \qquad R_3 = 178 \text{ "}$$

These are shown in Figure 5(d), and at (**e**) are in possible situations in the actual generator. It should be noted, however, that they are only about 10% of the practical values of tail resistors.

2.2.5 Iterative Solution of 2-Stage Case.

The modal matrix, k, can also be found by the iterative method, although it is not really justified for a 2 x 2 matrix.

$$U = CL = \begin{pmatrix} 1.53 & 0.72 \\ 0.72 & 0.865 \end{pmatrix} \begin{pmatrix} 1.8 & 0 \\ 0 & 1.3 \end{pmatrix} \times 10^{-16} \text{ Fd-Hy.}$$

$$= \begin{pmatrix} 2.76 & 0.935 \\ 1.3 & 1.12 \end{pmatrix} \times 10^{-16}$$

Let the arbitrary column be $x = 1, 1$

$$\text{Then } Ux = \begin{pmatrix} 2.76 & 0.935 \\ 1.3 & 1.12 \end{pmatrix} \begin{pmatrix} 1 \\ 1 \end{pmatrix} = \begin{pmatrix} 3.70 \\ 2.42 \end{pmatrix} = 3.7 \begin{pmatrix} 1 \\ 0.655 \end{pmatrix}$$

Repeated multiplication of the column by U :-

x	Iteration No.									
	1		2		3		4		5	
1	3.70	1	3.38	1	3.33	1	3.32	1	3.32	1
1	2.42	0.66	2.04	.605	1.98	.595	1.97	.593	1.96	0.59

This gives $k_1 \doteqdot \begin{pmatrix} 1 \\ 0.59 \end{pmatrix}$, while the constant factor is

$+w_1 = 3.32 = 1/\omega_1^2 \quad \therefore \quad \omega_1 = 0.55 \times 10^8$

as before. Then $\underline{k}_1 = k_1^1 L = \begin{pmatrix} 1.8 & 0.76 \end{pmatrix}$

$$= 1.8 \begin{pmatrix} 1 & 0.426 \end{pmatrix}$$

$$\therefore \quad B = \begin{pmatrix} 0 & -0.426 \\ 0 & 1 \end{pmatrix}$$

$$\therefore \quad U_2 = U_1 B = \begin{pmatrix} 2.76 & , & 0.935 \\ 1.3 & , & 1.12 \end{pmatrix} \begin{pmatrix} 0 & , & -.426 \\ 0 & , & 1 \end{pmatrix} = \begin{pmatrix} 0 & , & -0.240 \\ 0 & , & 0.566 \end{pmatrix}$$

$$U_2 x = \begin{pmatrix} -0.24 \\ 0.566 \end{pmatrix} = -0.24 \begin{pmatrix} 1 \\ -2.35 \end{pmatrix}$$

$$U_2^2 x = \begin{pmatrix} 0.566 \\ -1.33 \end{pmatrix} = 0.566 \begin{pmatrix} 1 \\ -2.35 \end{pmatrix}$$

The result is thereafter constant.
The column matrix is k_2 , and $+ w_2 = 0.566 = 1/\omega_2^2$,
$\therefore \omega_2 = 1.33 \times 10^8$ rad/sec. both the same as by direct calculation.

2.2.6 Four-Stage Oscillations.

The following results in resolving the 4-Stage case have been obtained with the aid of the Ferranti "Pegasus" computer at King's College, Newcastle, by another person in the course of experimental programme work. Only the latent roots and modal columns were obtained on the machine, the rest being done by slide-rule, although the latter, too, could have been computed with a small extension to the programme. The form of matrix equation developed in the last Section (actually Equation 22 was used) appears to be particularly suitable for solution by computer. The programme, once made, will deal with any dynamical matrix, U' = LC, up to about the 16th order (and possibly to twice this order, by operating on the inverse matrix Y'). Mutual terms in the inductance matrix would present no difficulty, but damping or dissipation could not be readily dealt with.

Inductance matrix, $L = \begin{pmatrix} 1.8 & 0 & 0 & 0 \\ 0 & 1.3 & 0 & 0 \\ 0 & 0 & 1.3 & 0 \\ 0 & 0 & 0 & 1.3 \end{pmatrix}$ $(10^{-6}$ Henry)

Capacitance matrix as given in Figure 14.

Latent roots, w, of $U^1 = LC$, and equivalent frequencies:-

Mode	$w = 1/\omega^2$	ω $(10^8/\text{sec})$	$f = \omega/2\pi$ (mc/s)
1	4.9183 ...	0.489	7.79
2	1.6138 ...	0.787	12.55
3	0.7427 ...	1.16	18.5
4	0.2951 ...	1.84	29.3

Vector columns as computed:-

Mode 1	Mode 2	Mode 3	Mode 4
1.0	-.9259 ...	-.6747 ...	-.3049 ...
0.6594 ...	0.1538 ...	1.0	0.7378 ...
0.4655 ...	1.0	-0.0398	-0.9293 ..
0.1663 ...	0.6120 ...	-.9234	1.0

Changing ratios of columns, for convenience, gives

$$k = \begin{pmatrix} 1 & -1 & -1 & -1 \\ 0.66 & 0.17 & 1.48 & 2.43 \\ 0.47 & 1.08 & -0.06 & -3.05 \\ 0.17 & 0.66 & -1.37 & 3.29 \end{pmatrix}$$

$$\therefore k^{-1} = \begin{pmatrix} +.513 & +.469 & +.334 & +.113 \\ -.314 & +.067 & +.462 & +.277 \\ -.149 & +.309 & -.012 & -.286 \\ -.030 & +.093 & -.116 & +.122 \end{pmatrix}$$

Now, by Equation 23, $v(t) = k\ c\ k^{-1}\ v(o)$.

Consider only the case where Gap 1 closes at t = o, all others being conducting (or shorted). Then v(o) = 1, 0, 0, 0 so that the last three columns of k^{-1} can be omitted. Writing out the 2nd order expressions (showing the elements of k^{-1} underlined)

$$\begin{pmatrix} v_1 \\ v_2 \end{pmatrix} = \begin{pmatrix} k_{11} & k_{12} \\ k_{21} & k_{22} \end{pmatrix} \begin{pmatrix} c_1 & 0 \\ 0 & c_2 \end{pmatrix} \begin{pmatrix} \underline{k}_{11} \\ \underline{k}_{12} \end{pmatrix}$$

$$= \begin{pmatrix} k_{11} & \underline{k}_{11} , & k_{12} & \underline{k}_{12} \\ k_{21} & \underline{k}_{11} , & k_{22} & \underline{k}_{12} \end{pmatrix} \begin{pmatrix} \cos \omega_1 t \\ \cos \omega_2 t \end{pmatrix}$$

In the same way, for the 4-stage case, we get

$$\begin{pmatrix} v_1 \\ v_2 \\ v_3 \\ v_4 \end{pmatrix} = \begin{pmatrix} .51 & .31 & .15 & .03 \\ .34 & -.05 & -.22 & -.07 \\ .24 & -.34 & .01 & .09 \\ .09 & -.21 & .20 & -.10 \end{pmatrix} \begin{pmatrix} \cos \omega_1 t \\ \cos \omega_2 t \\ \cos \omega_3 t \\ \cos \omega_4 t \end{pmatrix}$$

The expressions for voltages to earth (corresponding to the measured quantities) are

$$\begin{pmatrix} v_1 \\ v_1 + v_2 \\ v_1 + v_2 + v_3 \\ v_1 + v_2 + v_3 + v_4 \end{pmatrix} = \begin{pmatrix} .51 & .31 & .15 & .03 \\ .85 & .26 & -.07 & -.04 \\ 1.09 & -.08 & -.06 & .05 \\ 1.18 & -.29 & .14 & -.05 \end{pmatrix} \begin{pmatrix} \cos \omega_1 t \\ \cos \omega_2 t \\ \cos \omega_3 t \\ \cos \omega_4 t \end{pmatrix}$$

Two of these have been plotted in Figure 28.

2.3 ANALYSIS AS ONE-DIMENSIONAL LATTICE.

The List of Symbols in Section 2.3 follows the Contents Page.

2.3.1 Introduction.

The equivalent circuit of a generator extended to a large number of stages is shown in Figure 8 (Section 3.2.4). Before attempting a dynamic analysis, the hypothetical distributions of steady-state voltage as each gap fires will be considered, Figure 6. These are based on the uniform stray capacitances derived from Figure 13, and ignoring the inductances and resistances.

2.3.2 Hypothetical Steady State Voltages.

The upper diagrams are for coupling between adjacent stages only, K_1 being comparable with C. This is the circuit condition studied by Elsner (Ref. 5) and Miller (Ref. 15). It corresponds more to the single-column generator than to the present 2-column type. There is the usual hyperbolic distribution, so that a positive over-voltage appears at each unfired gap as soon as Gap 1 fires, that at Gap 2 being the greatest. The over-voltage across an unfired gap increases as more of the preceding gaps fire. Thus, by very careful adjustment, it is

possible for Gap 1 to cause all the remaining gaps to fire practically simultaneously. On the other hand, unless K_1 is small compared with C, the over-voltages, and hence the tripping range, will be small, and firing may be irregular.

In the lower diagrams, only capacitance coupling between alternate nodes, K_2, is assumed. This corresponds more closely to the 2-column type of impulse generator and has quite a different voltage-distribution characteristic. After Gap 1 fires, a positive over-voltage appears across Gaps 2, 4, 6, etc., while at the odd-numbered gaps the voltage change tends to inhibit firing. (e.g. V_{31}). This pattern is reversed when Gap 2 fires (increasing the voltage across Gap 3 to V_{32}), and again with the firing of the others. Because, in practice, these changes do not occur instantaneously owing to the inductances and resistances, the whole firing process may take an appreciable time, if the gaps fire strictly in turn. If, however, the gaps are very critically set, so that V_d is only slightly greater than V_c, it is conceivable that all the even-numbered gaps fire simultaneously. The remaining gaps should thus fire at the next swing of the voltage distribution. Compared with the previous case, the over-voltages do not decrease as K_2 is increased, and in practice are likely to be greater, at the start. V_{21}, for instance, can approach 200% of V_c.

When both K_1 and K_2 are present, the distribution characteristic will be intermediate between these two. In the generator the estimated values are

$$K_1 = 10 \text{ pF}, \quad K_2 = 33 \text{ pF}, \quad C = 30 \text{ pF}.$$

so that the second characteristic will predominate. Distributions calculated from the capacitance matrices, are given in Section 2.2, and Figure 6 can be seen to agree with this. One or two points found experimentally are also in agreement.

This shows the importance of taking K_2 into account with the 2-column type of generator. It also shows how the

measured values of parameters determine the choice of mathematical technique. The influence of K_2 will again be discussed later in this Section in connection with the propagation characteristics of Figure 9.

2.3.3 Dynamical Analysis of Lattice.

Turning again to the equivalent circuit of Figure 8, the one-dimensional dynamical lattice extends from Node 0 to Node N, and is excited by the firing of a gap between Nodes N-1 and N. The terminations consist of C_1, C_2, C_3, C_4, as shown. Equating to zero the branch currents flowing into node n using the "operational" or transformed voltages.

$$p K_2(V_{n+2} + V_{n-2} - 2V_n) + (\frac{1}{pL} + p K_1)(V_{n+1} + V_{n-1} - 2V_n) - p C V_n = 0$$

$$\therefore \quad y_2(V_{n+2} + V_{n-2}) + y_1(V_{n+1} + V_{n-1}) - y_o V_n = 0 \qquad . \; . \; . \; . \; . \; (1)$$

where $y_2 = p K_2$, $y_1 = \frac{1}{pL} + p K_1$

$$y_o = \frac{2}{pL} + 2 p K_2 + 2 p K_1 + pC$$

$$= 2y_2 + 2y_1 + pC.$$

It is proposed to attempt a solution of this difference equation, using the sequence transform given in Reference 13 by Lawden. If $u = u(mT)$ is a function of time known by samples taken at intervals T, so that $t = mT$, then u can be transformed into a new function

$$U(z) = \sum_{m=0} u. \; z^{-m}$$

This is a generalized Laplace transform, and reverts to it in the limit (T = 0). It has the property that the transform of

$$u(mT + xT) = z^x U(z) + \sum_{r=0}^{x-1} u_r z^{x-r} \quad \ldots\ldots (2)$$

where u_o , u_1 , ... u_{x-1} are the initial conditions (m=0). The transform is also used by Barker (Reference 2) and, in a slightly different form, by Gardner and Barnes (Ref. B7, Chap. 9), both of whom give useful tables of transformed functions. (Also References 16 and 23).

In the present application, the transform has to be made with respect to the node-number n (instead of time). Let the voltages at the first few functions be $V(p,0) = V_o$, $V(p,1) = V_1$, etc., and restate Equation 1 for Node (n + 2), for convenience,

$$\therefore \quad y_2 V_{n+4} + y_1 V_{n+3} - y_o V_{n+2} + y_1 V_{n+1} + y_2 V_n = 0 \quad \ldots\ldots (3)$$

Applying the sequence transform

$$\begin{aligned} & y_2 (z^4 U + z^4 V_o + z^3 V_1 + z^2 V_2 + z V_3) \\ & + y_1 (z^3 U + z^3 V_o + z^2 V_1 + z V_2) \\ & - y_o (z^2 U + z^2 V_o + z V_1) \\ & + y_1 (z U + z V_o) + y_2 U = 0 \end{aligned}$$

$$\therefore \quad U(p,z) = - \frac{(q_3 z^3 + q_2 z^2 + q_1 z + q_o)z}{y_2 z^4 + y_1 z^3 - y_o z^2 + y_1 z + y_2} \quad \ldots\ldots (4)$$

where
$$q_3 = y_2 V_o$$
$$q_2 = y_1 V_o + y_2 V_1$$
$$q_1 = -y_o V_o + y_1 V_1 + y_2 V_2$$
$$q_o = y_1 V_o - y_o V_1 + y_1 V_2 + y_2 V_3$$

V_o , V_1 ... have to be interpreted in terms of the boundary conditions at the ends of the lattice, which comprise the capacitances C_1, C_2, C_3, C_4, and the impressed voltage $V_N - V_{N-1} = 1$.

At the base-end, $V_o = 0$, $\therefore$ $q_3 = 0$

Since $C_1 = K_2$, the equation for currents into Node 1 is

$$y_1(V_2 - V_1) + y_2(V_3 - V_1) - (y_1 + y_2 + pC) V_1 = 0$$

$$\therefore \quad - y_o V_1 + y_1 V_2 + y_2 V_3 = 0$$

But this also equals q_o , $\therefore$ $q_o = 0$.

V_1, V_2 need to be stated in terms of the conditions at the other end, but meantime:-

$$U(p,z) = - \frac{y_2 V_1 z^3 + (y_1 V_1 + y_2 V_2)z^2}{y_2 z^4 + y_1 z^3 - y_o z^2 + y_1 z + y_2} \quad . \quad . \quad . \quad (5)$$

Since the denominator is a reciprocal function in z, it can be factorized in the form

$$y_2 (z^2 - 2b_1 z + 1)(z^2 - 2b_2 z + 1)$$

$$\therefore \; U(p,z) = \frac{y_2 V_1 z^2 + (y_1 V_1 + y_2 V_2)z}{2(b_2 - b_1)y_2} \left(\frac{1}{z^2 - 2b_1 z + 1} - \frac{1}{z^2 - 2b_2 z + 1} \right)$$

. . . . . (6)

Barker, (Reference 2) gives the sequence transform pairs:-

$$U(z) \quad :: \quad V(n)$$

$$\frac{z}{z^2 - 2bz + 1} \quad :: \quad \frac{\sin kn}{\sin k} \qquad \text{where } \cos k = b < 1$$

$$:: \quad \frac{\sinh kn}{\sinh k} \qquad \text{where } \cosh k = b > 1$$

$$\frac{z^2}{z^2 - 2bz + 1} \quad :: \quad \frac{\sin(k+1)n}{\sin k} \quad \text{or} \quad \frac{\sinh(k+1)n}{\sinh k}$$

Hence the inverse transform of $U(p,z)$, assuming $b < 1$, is

$$V(p,n) = y_2 v_1 \left\{ \frac{\sin k_1(n+1)}{\sin k_1} - \frac{\sin k_2(n+1)}{\sin k_2} \right\} + \left\{ + (y_1 V_1 + y_2 V_2) \left\{ \frac{\sin k_1 n}{\sin k_1} - \frac{\sin k_2 n}{\sin k_2} \right\} \right\}$$

$$2 y_2 (\cos k_2 - \cos k_1) \qquad \ldots (7)$$

In order to eliminate V_1 and V_2 from this equation, it is apparently necessary to find first the expressions for V_N, V_{N-1}, etc. and substitute in the equations for currents at Nodes N and N-1. No way has been found of doing this without involving extremely cumbersome expressions. And even then, the poles of the resulting expression for $V(p,n)$ have to be determined in order to find the inverse Laplace transform $v(t,n)$, and hence to interpret the solution in physical terms.

2.3.4 General Propagation Characteristics.

Nevertheless, the general propagation characteristics of the lattice can be found from an examination of the parameters b_1, b_2. By equating coefficients of the denominators of Equations 5 and 6, we get

$$b_1 + b_2 = - y_1/2\, y_2 \quad , \quad 2 + 4\, b_1\, b_2 = - y_o/y_2$$

$$\therefore \quad 4\, y_2\, b^2 + 2 y_1\, b - 2\, y_2 - y_o = 0 \quad . \quad . \quad . \quad . \quad (8)$$

This is a quadratic containing both roots for $b = \cos k$.

Assuming the solution is made up of travelling-wave components, so that

$$v(t,n) = \sum A\, e^{j(\omega t - kn)} \quad . \quad . \quad . \quad . \quad . \quad . \quad (9)$$

we can, by putting

$$p = j\omega = j\, 2\pi f \text{ , where } f = \text{frequency}$$

and $$k = 2\pi a, \text{ where } a = \text{wave number (or reciprocal of the wavelength in sections)}$$

and substituting for y_o, y_1, y_2 , write

$$\omega^2 = \frac{2\,(1 - \cos k)/L}{C + 2\,K_1 + 4\,K_2 - 2\,K_1 \cos k - 4\,K_2 \cos^2 k}$$

$$= \frac{2\,(1 - \cos k)/L}{C + 2\,K_1(1 - \cos k) + 2\,K_2(1 - \cos 2k)} \quad . \quad . \quad . \quad (10)$$

This is the general propagation equation for travelling waves in the lattice, and takes no account of the end-conditions. The significance of this relationship between the frequency, f, and the wave-member, a, is discussed in the earlier

chapters of Reference B3 by Brillouin, It allows the separate effects of K_1 and K_2 to be found, as shown graphically in Figure 9, using values for the circuit elements estimated in Section 3.3.

When $K_1 = K_2 = 0$, the lattice is that of a simple artificial line, and

$$\omega^2 = \frac{2(1 - \cos k)}{LC}, \quad \therefore f = \frac{\sin \pi a}{\pi\sqrt{LC}}$$

This shows that there is then a cut-off frequency of $f_{max} = 1/\pi\sqrt{LC} = 51$ mc/s. Any component of a higher frequency would be attenuated with distance from the point at which it is impressed. The cut-off frequency corresponds to $a = \frac{1}{2}$, or a wavelength of 2 sections. This is in accordance with general theory: in the analagous mechanical system of particles discussed by Brillouin, the minimum wavelength equals twice the distance between the particles. It can also be regarded as the natural frequency of a section comprising inductance L and two capacitors C/2 in series. As a travelling wave, the velocity is f/a, and therefore varies with frequency. The minimum velocity is therefore about 100×10^6 sections/second.

When the coupling coefficients K_1 and K_2 are introduced, the maximum frequency occurs when

$\cos k = -1$, $k = 2\pi a = \pi$, $a = \frac{1}{2}$, as before.

Then $\omega^2_{max} = \frac{1}{L(K_1 + C/4)}$, giving $f_{max} = 33$ mc/s. (approx.

This mode of oscillation is independent of K_2, and corresponds to current in the mesh shown in Figure 10(a). The introduction of K_1 thus reduces the maximum frequency which can be propagated in the lattice.

A thorough search for the natural modes of oscillation on this basis has not been attempted, but two others are shown.

One is given for $a = \frac{1}{4}$ $\cos k = 0$, and then

$$\omega^2 = \frac{1}{2L(K_1/2 + K_2 + C/4)}$$ and f = 14 mc/s. (Figure 10b).

Another is for $\cos k = 1 - \sqrt{C/4\ K_2}$, and

$$\omega^2 = \frac{1}{L(K_1 + 4\ K_2)} = \frac{1}{NL(K_1/N + 4\ K_2/N)}$$, and f = 12 mc/s.

This is equivalent to an oscillation along the whole length of the lattice, as shown in Figure 10c. It is not immediately apparent why this should be independent of the value of C, since the C's will gain or lose charge during a cycle. It probably depends on the initial distribution of the voltage being along the whole lattice.

These natural modes of propagated waves correspond to the standing waves discussed by Lewis (Ref. 14). They cannot necessarily be interpreted on the equivalent circuit (compare the discussion on the 2-mesh case in Section 2.1.9). The propagation equation cannot give a complete analysis for this reason, and also because it takes no account of the boundary conditions.

2.3.5 Note on Recurrent-Section Analysis.

The recurrent section is shown in Figure 11 from which the admittance matrix has been directly derived. By simple manipulation, this has been converted to a matrix relating the "input" to "output" quantities. The response of N such sections in cascade would be given by the Nth power of this matrix. However, the matrix does not appear to be amenable to such treatment, and the method has not been pursued further.

3.1 DESCRIPTION OF IMPULSE GENERATOR.

The impulse test plant used for the experimental work is shown in the photographs (frontispiece), its electrical disposition being given in Figure 2. When permanently installed, the impulse generator will have 9 stages, giving a nominal output of 1500 kV with a stored energy of 10.5 kW-sec. It is of the two-column type; each column is made up of a stack of outwardly-identical porcelain containers consisting of the stage-capacitors, (0.085 μF each) and oil-filled spacers, arranged alternately. The principal dimensions are: column-centres 6 ft., height 22 in. per stage, diameter of units 28 in. Connections to the horizontally mounted spark gap are made through clip-on shorting rods. Resistors (usually of 25 ohms each) can be substituted for internal series damping and wavefront control. The charging and tail resistors are mounted diagonally between the flanges. The number of stages can therefore be increased, within limits, by merely increasing the number of units in the columns. A recent installation of this design is of 18 such stages, with a nominal output of 4000 kV.

During the present investigation, only the first four stages could be erected, owing to limitations of space in the laboratory - mainly roof-truss ties. The proximity of other equipment would be about normal, so that a fairly typical system of stray capacitances should have obtained for these four stages. The most prominent sources of stray-capacitance fields were the corona-shielded flanges between the units. This is further discussed in Section 3.2.

For most of the tests, the 25 ohm wave-front resistors were not inserted. Although of a "non-inductive" wire-wound construction, they were found to have about 5 μH inductance, which considerably altered the frequencies of oscillation, while providing no appreciable damping effect. (See Section 3.3.3). Again, the normal wavetail resistors were sometimes replaced by higher-value carbon resistors, mainly to increase the duration of over-voltages.

The normal surge potentiometer consisted of two 600 kV units of about 60 pF each in the upper arm. It was unsuitable for inter-stage measurements because its capacitance was large enough to disturb the stray-field system, and inductance in both the upper-arm loop and in the lower arm unit made its response too slow for 20-30 mc/s. The divider used is described in Section 3.6.

The high frequencies and low divider capacitance also made it undesirable to use a delay cable. The original trip-control system, (shown in the photographs), which consisted of two sets of 3-electrode gaps, could not be made consistent enough for recording on fast time-sweeps, and it was replaced by a Trigatron-controlled gap (Section 3.5). Although consistent enough, the behaviour of this device under certain conditions was somewhat anomalous.

Two transient recorders were used, Southern Instruments models "T.R.10" and "T.R.12", both using 10 kV tubes (G.E.C. 908 BCC). Most of the work was done when only the former was available. Triggering of its time-sweep was through a 3-electrode magnesium gap, with 1 microsec. maximum sweep speed. The T.R.12 model had electronic triggering, with a maximum sweep speed of 0.2 microsec.

3.2 RESOLUTION INTO PASSIVE PARAMETERS.

3.2.1 General.

The impulse generator used in the investigation is described in Section 3.1. Figure 2 is a diagram of the main circuit connections (in the 9-stage arrangement) the components of which control the output wave-shape. None of them plays a major part in the analysis of the firing process, the phenomena of which are principally rooted in the physical structure of the generator and its surroundings, and in the characteristics of the spark-gaps. The present object is to visualize this electro-magnetic complex in terms of suitable mathematical parameters,

A cursory series of oscillograms was made of the voltages appearing at the more obvious points of the 4-stage generator. These showed that frequencies of about 20 mc/s. could occur. At that frequency, it becomes questionable whether normal circuit theory can be applied. The problem is discussed in Reference B.10. A general field system can be resolved into the mathematical components of induction and radiation fields. Under so-called "near-zone" conditions, of small physical dimensions and low frequencies, the latter field is negligible, and the former leads to conventional circuit elements. The criterion is that the maximum separation of currents and charges that exert a significant and uncancelled effect on one another be much smaller than v/ω, where v is the velocity characteristic of the medium between them, and $\omega = 2\pi f$. Here, $\omega \doteq 10^8$ rad./sec., so that for the error due to the neglect of the radiation field not to

exceed 1%, the separation must not exceed 3 cm.: for an error of 10%, 30 cm.

Clearly, the actual dimensions will, at these frequencies, bring the system into the intermediate zone, in which radiation and potential retardation should be taken into account. The solutions of problems in this zone are seldom practicable, although in the border-line region, the effects are mainly to alter the values of the lumped-circuit parameters as measured at low frequencies, and still allow the use of circuit theory. In the case of a loop conductor, the effect would be to reduce the inductance slightly, and to introduce a radiation equivalent resistance. For a square loop of 1 m. sides, this resistance is in the order of $\frac{1}{4}$ ohm for $\omega = 10^8$, and this is probably negligible. Further, when discussing over-voltages across spark-gaps, the electrodes of which are fairly close together, retardation of potentials induced by other parts of the system may be unimportant. The effect on the potentials of more widely separated parts of the system, although difficult to predict, is likely to be only of second order, because the interactions between them must decrease with the separation.

On the whole, therefore, it seems justified to use the near-zone conditions of ordinary circuit theory, and to assume that parameters measured at low frequencies can be applied at 20-30 mc/s. without much error. The structure is to be resolved into a capacitance system between a number of electrodes, and inductive (and possibly resistive) connections between them.

The preliminary oscillograms showed that transient voltages on either side of the main .085 μF capacitors were practically identical. Their internal impedance can therefore be neglected at these frequencies, and each regarded as a single electrode. One of these capacitors is mounted on the earthed base-plate, and hence forms part of the earthed surroundings.

There are also the capacitances associated with 15-cm. diameter spark-gap hemispheres and their mountings. These are strictly speaking separated from the above by inductive connections (which may consist of 25 ohm resistors) but considering their relatively small values it seems justified to lump them in with the main capacitors to which they are connected.

The capacitance system of the 4-stage generator now consists of four isolated electrodes and the earthed surroundings. This can be resolved either into the 10 inter-electrode, partial capacitances shown in Figure 12; or into a set of Maxwell's coefficients of capacitance or elastance (i.e. reciprocal capacitance). The former (which include the capacitances of the spacer units) were the most convenient to obtain by bridge measurements, (Section 3.3.1) and can be transformed into any other set mathematically. First, however, the other components of the generator will be dealt with.

The main interconnections between the electrodes are through those spark-gaps which are either shorted or conducting at the time being considered (Figure 3). The whole of the inductance in the system is assumed to be located in these connections. A rough calculation indicated that mutual inductances between adjacent connections would be less than 10% of the self-inductances, so that it seemed justified in ignoring them in the analysis.* Self-inductance values were estimated as in Section 3.3.2. The wave-front control resistors also normally form part of these connections, but in most of the tests they were replaced by shorting links.. Their damping effect at the frequencies concerned was negligible (25 ohms compared with a critical damping in the order of 500 ohms) whereas the self-inductance of the normal resistors (Section 3.3.3) considerably altered the natural frequencies.

There remain the charging and tail resistors (R_C and R_T in Figure 2). Both are essential to the charging of the main

(* But see Corrigendum at end of Section 3.7).

capacitors, but their practical values are so large that they cannot involve any fresh oscillations, and have only a shunting effect on the transient circuit. Besides tending to damp out oscillations, this shunting increases the decrement of over-voltage pulses across the gaps, and can have an important effect on their firing. Nevertheless, any analysis of oscillatory circuits is best done without damping in the first instance, so in the experiments these resistors were made large enough not to affect the transients during firing, and they need not be included in the equivalent circuit at the present stage. Their omission leads to the simplified oscillatory network of Figure 4a.

3.2.2 Capacitance Field System.

The theory developed in Section 2.1 requires the capacitance field system to be described in terms of capacitance or elastance coefficients. These have to be calculated from the inter-electrode capacitances already found. Treating the system as a "box" with four pairs of access terminals, the voltages and currents will be related by an elastance-matrix, as follows:-

$$\begin{pmatrix} V_1 \\ V_2 \\ V_3 \\ V_4 \end{pmatrix} = \frac{1}{p} \begin{pmatrix} S_{11} & S_{12} & S_{13} & S_{14} \\ S_{21} & S_{22} & S_{23} & S_{24} \\ S_{31} & S_{32} & S_{33} & S_{34} \\ S_{41} & S_{42} & S_{43} & S_{44} \end{pmatrix} \begin{pmatrix} I_1 \\ I_2 \\ I_3 \\ I_4 \end{pmatrix}$$

that is, $V = \frac{1}{p} S I$, in ordinary matrix notation.

Now if $I_2 = I_3 = I_4 = 0$

$$\begin{pmatrix} V_1 \\ V_2 \\ V_3 \\ V_4 \end{pmatrix} = \frac{I_1}{p} \begin{pmatrix} S_{11} \\ S_{21} \\ S_{31} \\ S_{41} \end{pmatrix} \quad \therefore \begin{pmatrix} S_{11} \\ S_{21} \\ S_{31} \\ S_{41} \end{pmatrix} = p \begin{pmatrix} V_1/I_1 \\ V_2/I_1 \\ V_3/I_1 \\ V_4/I_1 \end{pmatrix}$$

Each elastance coefficient, say S_{21}, is given by p-times the ratio of the voltage appearing across (2) and the current impressed on terminals (1), all terminal-pairs other than (1) being open-circuited.

But this response is not easy to calculate directly from the partial capacitances. On the other hand, the response based on the capacitance matrix can be written down by inspection using the relationship $I = p\,C\,V$.

If $V_2 = V_3 = V_4 = 0$

$$\begin{pmatrix} I_1 \\ I_2 \\ I_3 \\ I_4 \end{pmatrix} = V_1\, p \begin{pmatrix} C_{11} \\ C_{21} \\ C_{31} \\ C_{41} \end{pmatrix} \quad \therefore \begin{pmatrix} C_{11} \\ C_{21} \\ C_{31} \\ C_{41} \end{pmatrix} = \frac{1}{p} \begin{pmatrix} I_1/V_1 \\ I_2/V_1 \\ I_3/V_1 \\ I_4/V_1 \end{pmatrix}$$

Thus the capacitance coefficient C_{21}, for instance, is given by $1/p$ times the ratio of the current flowing in terminal-pairs (2), and the voltage impressed across terminals (1), all terminal pairs other than (1) being short-circuited.

The result of making these short-circuits can be seen in Figure 14. The current through each short-circuit is simply that through one or a number of parallel capacitors, so that, for instance, $C_{21} = C_{12} = C_5 + C_8 + C_{10}$.

Now the equation $I = pCV$ can be inverted to give $V = \frac{1}{p} C^{-1} I$, and this must be identical with $V = \frac{1}{p} S I$,

$\therefore S = C^{-1}$. Thus S can be obtained most easily by inverting the C-matrix after substituting numerical values.

3.2.3. Matrices for Fewer than Four Stages.

The C- and S- matrices refer to a network in which all four currents are taken into account. When some of the spark-gaps remain open-circuits throughout the period considered, it is convenient to reduce the number of mesh-equations, and hence the order of the system.

When an S-matrix is involved in these equations, it is simply a sub-partition of the 4 x 4 S-matrix, the columns corresponding to the zero currents being omitted. The reduced C-matrix is not, however, a sub-partition of the 4 x 4 C-matrix, but the reciprocal of the active part of the new S-matrix. Thus, if Gaps 3 and 4 remain open,

$$\begin{pmatrix} V_1 \\ V_2 \end{pmatrix} = \frac{1}{p} \begin{pmatrix} S_{11} & S_{12} \\ S_{21} & S_{22} \end{pmatrix} \begin{pmatrix} I_1 \\ I_2 \end{pmatrix} = \frac{1}{p_{(2,2)}} .S.\ I, \quad \text{say}$$

Then $I = {}_{p(2,2)}^{C} V$ where $\underset{(2,2)}{C} = \underset{(2,2)}{S^{-1}}$

where the figures in the brackets denote the number of rows, columns in the matrix.

3.2.4 Parameters of Lattice Network.

In the case of a generator with a larger number of stages, it might be expected that a definite pattern would exist in the values of capacitances between electrodes (except, possibly, at the top and bottom of the stack). Referring to Figure 13 it is suggested that the partial capacitance from each isolated electrode (i.e. main-capacitor unit) to the earthed surroundings is C = 30 pF that between adjacent electrodes (considered in the order in which they are connected through the gaps), = K_1 = 10 pF; that between alternate electrodes (which is largely the capacitance of the spacer-unit) = K_2 = 33 pF; that between third (and more remote)

electrodes = K_3 = negligible. This pattern of capacitances requires changes of less than 10% in the values measured on the 4-stage generator (Figure 12) (except that C_{10}, which was only that of a corona shield, is increased from 17 pF to 30 pF in the extended case). It is also reasonable to suppose that the inductances of interconnections will remain constant at the value found for L_2 = 1.3 μH. Thus an approximate but very convenient equivalent circuit for a generator of any number of steps can now be drawn, and the L- and C- matrices written down by inspection, as has been done for a 9-stage generator, Figure 15.

Further, the connection of a load-capacitance C_x would only require the matrix to be enlarged by another row and column, each element of which equals C_x, and all the original elements to be increased by C_x.

More important, the circuit can now be regarded as a uniform, one-dimensional lattice network, (Figure 8), or alternatively as a row of identical sections, of the kind shown in Figure 11, in cascade. In each case there are special end-terminations. At the top there are the capacitances C_2, C_3, C_4, representing the remaining unfired stages of the generator, or some other impedances representing the external loading. At the base-end there is the capacitance of the first spacer, $C_1 = K_2$ approximately.

3.3 MEASUREMENT OF PARAMETERS.

3.3.1 Partial Capacitances.

3.3.2 Self Inductance per Stage.

3.3.3 Inductance of 25 ohm Resistors.

3.3.1 Partial Capacitances.

The capacitance system of the 4-stage generator consists of four isolated electrodes, and a fifth made up of the first stage capacitors, the generator bedplate and the earthed surroundings. The ten partial capacitances which exist between these nodes (Figure 12) were found from measurements made with the 10 kc/s substitution bridge shown in Figure 16. All measurements were of capacitance to earth from one or more of the isolated electrodes, the others being earthed. Fifteen groupings of this kind were possible, giving a like number of simultaneous equations in the ten capacitances, ten of which were then solved and checked against the other five. (Table, Figure 17).

The bridge, made up of standard screened components, needs no special explanation, but it may be noted that all connections to the generator were made through fixed wires coming to a small terminal board. All interconnections were made at this board, thus minimising changes in the lead capacitances. Then with the wires in the same positions, but disconnected from the generator, their respective capacitances to earth were measured. Allowances were made for them before solving the simultaneous equations. Such precautions were found necessary because the solution involved differences of fairly large numbers. The detection was very sensitive, and permitted indicated readings to better than 0.1 pF on the variable air capacitor when set around 500 pF. Substitution of the ten capacitance values in the five unused equations gave a consistency of better than 1% between the two sides.

The group capacitances were also measured by means of a Q-meter at 208 kc/s. and 646 kc/s. but without the precautions of using fixed connecting wires. The results were all between the "gross" and "net" values given by the above method, and the difference in the values at the two frequencies was in the order of 1%.

3.3.2 Self-Inductance per Stage.

The stage inductance of the generator (without the internal damping resistors) is that of the spark-gap assembly and connecting links and one stage capacitor. The arrangement shown in Figure 30d comprising two stage capacitors, each supported on spacers, one being in the position normally occupied by the spacer A/D, should form a loop of twice this inductance. With one gap permanently shorted, one capacitor was charged to about 20 kV, and then discharged into the other through the trigatron-controlled gap, the oscillations at the point B being recorded. (Osc. 1085). The frequency was 0.5 mc/s. and there were two - 0.085 microfarad capacitors in series, so that the loop inductance was 2.56 μH or say 1.3 μH per stage. (Q-meter measurements gave a loop inductance of 2.8 μH, but the detection was not sensitive.)

Since the first stage inductance included that of the base-plate of the generator, a separate test was made (Fig. 30e). Oscillogram 1053 indicated a frequency of 0.59 mc/s. and the loop inductance worked out to 1.8 μH. This is practically the same as the stage inductance, since the 0.08 μF capacitors were shown to have negligible inductance.

The inductance was also estimated by calculation from the dimensions, as given in Figure 18. The connections through the spark gaps are assumed to be straight conductors of $2\,r_o$ = 0.025 m. diameter, and the stage capacitors cylinders of $2R$ = 0.2m. diameter, length of conductors = a = 1.8 m., separation of conductors = b = 0.2m.

Sec. 3.3.2.

The self-inductance of the rectangular loop ABCD is proportional to the flux through it due to an equal current in the four sides. Attwood (Ref. B1, Chap.10) gives formulae for calculating the contribution of each side.
Neglecting internal flux, that due to AB is

$$L_{AB} = \frac{\mu}{2\pi} \left\{ \sqrt{a^2 + r^2} - r - a \log_e \frac{a + \sqrt{a^2 + r^2}}{r} \right\}_{r = r_o}^{r = b}$$

where r is a radius out from the axis of AB, r_o = radius of Conductor AB.
There will be a similar expression for BC, so that, after substitution, half loop inductance

$$= L_2 = L_{AB} + L_{BC} = 1.26 + 0.15 = 1.41\,\mu H$$ (compared with 1.3 μH.

Mutual inductance between adjacent loops is proportional to the flux from AB betweeb CD and EF, represented by the limits r = b and r = 2b. This gives M_{12} = 0.16 μH.

Mutual inductances can probably be neglected for the approximate calculation intended here. (But see Corrigendum to Section 3.7).

3.3.3 Inductance of 25 ohm Resistors.

The internal series (or wave-front) resistors used with the generator consist of 25 ohm wire-wound units which can be inserted in place of the tubular connecting links on either side of the gaps. They serve as damping in the whole generator circuit, which includes the load, but do not damp out the internal oscillations. When a single stage fires, the oscillation is about 12 mc/s. as indicated in Oscillograms 1112-1117, Fig. 32,a, and the estimated inductance is 1.8 μH. Inserting a 25 ohm resistor reduces this to about 6 mc/s. indicating an additional 5.4 μH in the circuit.

An approximate direct measurement was made, using a Q-meter and the arrangement shown in Figure 19. L' is a series "ballast" inductance inserted to increase the Q of the resonant circuit, which, even then, was low and the indicated resistance unreliable. L is the change of inductance caused by replacing the shorting link with the resistor, and the two values obtained, 5.3 and 4.8 μH, are considered consistent enough with the previous value.

3.4 GAP BREAKDOWN CONSIDERATIONS.

The excitation of the system arises from the cancellations of voltage across the gap electrodes, and the changes from an open-circuit to a short-circuit condition between them, when the gaps fire. Except in hypothetical treatment, the gaps cannot be assumed to fire simultaneously. The first gap-voltage to be cancelled will be the steady charging voltage V_c; but that of any later gap will involve superimposed oscillatory voltages as well. Thus, both this transient voltage function, and the instant of its cancellation need to be known in any realistic analysis. But the instant of firing of a gap appears to be governed by considerations other than the direct breakdown voltage, V_d, of, and the instantaneous voltage across, the gap.

Consider the first two stages of the generator, Figure 26(a), and equivalent circuit (b), derived from Figure 3. As stated in Section 3.2, the voltages across the stage capacitors, V_c, remain unchanged for the duration of the firing process; and are represented by "batteries". This is the situation considered by Edwards, et al (Reference 4), with the addition of the inductance. On Gap 1 firing, the voltage of B will be V_c (1 - cos ωt), neglecting damping, where $\omega/2\pi$ ~ 10 mc/s. A fraction of this voltage (actually 0.8 from Section 2.2.1) will be superimposed on V_c across Gap 2, which is set at V_d (perhaps 10% greater than V_c). The resistive losses produce exponential damping, with the result shown in Figure 26(c). If, in addition, $R_t(C_2 + C_5)$ is comparable with the period of oscillation, there will be a decrement of the axis of oscillation from 1.8 V_c to V_c, as shown at (d). (For C_2 = 9 pF, C_5 = 56 pF, R_t = 1 kilohm, this time-constant = 0.07 microsec. For R_t = 60 kilohm, T = 4 microsec.). The gap-voltage exceeds V_d as shown by the areas shown shaded in (c) and (d). Thus the overvoltage on Gap 2 is a variable function, and can consist of a series of pulses of initially about 1.5 V_d, and then of decreasing amplitude, and of less than 0.1 microsec. duration each.

Data of breakdown characteristics under these conditions are not easy to obtain. Some work by Hardy (Reference 8) shows that the initial direct potential may have a marked and very variable effect on time-lags, and in any case tends to increase the peak-value of the impulse required to cause breakdown. It is further increased by the steepness of the front (or sharpness of the pulse).

Hardy's observations are for constant irradiation. Now although Gap 2 is usually said to be irradiated by the spark of Gap 1, this irradiation does not commence earlier than 1/20 microsec. before the crest of the first pulse, and may not grow to an adequate intensity instantaneously. This question has been discussed by H.G. White (quoted in Reference B.14, Chap. 4) in explaining times of this order for breakdown with 10 - 20% overvoltage.

Thus, while Oscillograms 914-918 (Figure 31, and and see Section 3.7) show that quite long time-lags can occur within the working range of the generator, the calculation of the delays between the firing of two gaps from a knowledge of the voltage-function and gap-setting is quite complicated, and probably impossible with present data. One compromise basis for the analysis is to assume the delays are long enough for the oscillations due to the preceding gap(s) to die out, but not for the decrement of their axis (or "steady-state value") to be appreciable This condition obtained in the experiments when R_t = 60 kilohms.

In some oscillograms, particularly for Gap 1 firing alone, there is a large decrement on the first loop of the oscillation (see Osc. 912,913 in Fig. 31 a, b, and Osc. 1112-7, Fig.32,a) Its relationship to the normal exponential decrement is shown in Figure 26(e). The question is raised (Section 3.7) whether it is correct to regard the firing of a gap as an instantaneous change from a non-conducting to a conducting state. An exponential collapse, with a time-constant of 1/30 microsec. would explain the observed initial decrement. Such times (in the order of 10^{-7} sec.

for the formation of the highly-conducting part of the spark-channel seem not unreasonable, judging by published results (e.g. in Reference B.14, Chap. 4).

Another explanation of this initial decrement has been considered. The loss of energy in a conducting spark-gap through radiation, etc. would appear to be relatively small, and, being constant, can be included in the overall damping of the circuit. If, however, energy were absorbed at a very much greater rate during the formative period of the spark channel, it would account for the observed effect. Some data by J.W. Flowers are quoted (rather diffidently) in Reference B.14, page 393. In the present case, the only source from which such a block of energy can be taken is the stray capacitances. If these total 100 pF, charged to 50 kV, energy = $\frac{1}{2}$ CV^2 = 0.1 watt-second. Peak current under a 10 mc/s. free oscillation = 400A. There is also the current from the stage capacitor through the tail resistor:- about 1A. for R_t = 60 kilohm, and 60A. for R_t = 1 kilohm. These figures differ considerably from those given in the reference. Nevertheless, a closer study may well show a connection between this aspect of the breakdown mechanism and the behaviour of the generator.

Note: as described in the next Section, Gap 1 was normally a self-illuminating triggering device, or Trigatron, the behaviour of which was always suspect. But one experiment suggested that the behaviour of a simple sphere gap was no different. (Oscillograms 1356, 1358, Figure 29c).

A similar, though smaller, initial decrement can be observed in the train of oscillations set up on the firing of a sphere-gap connected across an unclamped divider. (See Osc. 846, 1237 in Figure 30c).

3.5 TRIGATRON DEVICE.

In order to provide, without the use of a delay cable, a triggering pulse to the oscilloscope in advance of the signal from the divider, "controlled firing" of the first stage of the generator was necessary. The method provided by the manufacturers consisted of two sets of 3-electrode gaps and an R-C network, and proved to be too slow and inconsistent for use with fast timesweeps. It was replaced by the well-known "Trigatron" device (see References 8 and 11), the construction and associated circuit used being shown in Figure 20.

The voltage tripping range was adequate, being as much as 50% of the self tripping voltage on - V + polarities. The tripping delay could be varied by altering the values of the resistor, r, and capacitor, c, which controlled the front of the pulse. Although not constant, it was usually sufficiently so for the purpose. The chopped pulse is shown on several of the series of oscillograms marked T. (See Sec. 3.7 for abbreviations used.)

No systematic study of the performance was made, but much time was spent on investigating anomalies in its behaviour during other tests. In some cases, with Trigatron polarity - V +, steps appeared on the tail of the wave. (Figure 29). The step is upwards in Osc. 889 (Figure 29a) when the tail resistor (B/z) is 1 kilohm, and downwards in Osc. 890 when R_t = 60 kilohm. This is further illustrated in Osc. 982-984 (Figure 29b) in which the step appeared when the point was flush with the hemisphere, and did not appear when the point was withdrawn about $\frac{1}{4}$ inch into the glass tube. The frequency of oscillation also changes, being 9 mc/s. and 12 mc/s. respectively. Apparently the point electrode T first sparked over to the opposite hemisphere B', while the step occurred when the annular gap broke down, bringing the main capacitor into circuit. The step never occurred when the polarity of the point was the same as the facing hemisphere.

However, tests in the series Osc. 1156-1170 (see Fig. 29d, e, f, g) when the trigatron was at Gap 2, showed that anomalous behaviour was possible with -V-/+V+ conditions. The figures on the traces give the main charging voltage, V_c, the tripping pulse being about 12 kV. peak. The smooth waves, sometimes leading to a step occurred when V_c was near the self-tripping value. Osc. 1170 confirms the relative polarities. These anomalies appeared to depend partly on circuit conditions, as they did not occur when the device was at Gap 1. The explanation must lie with a better understanding of the physical processes obtaining in the device than is provided by existing literature. In most of the tests the -V- condition was used, and apart from the possible cause of the initial decrement (see Sectiom 3.4) there is reasonable confidence that the Trigatron has not affected the oscillations appearing in the other oscillograms.

3.6 POTENTIAL DIVIDER FOR OSCILLOGRAPHIC MEASUREMENTS.

3.6.1 General.

3.6.2 Frequency Response of Measuring Circuit.

3.6.3 Design of Idealized Divider.

3.6.4 Bridge Measurements on Divider.

3.6.5 Oscillographic Tests.

The essential requirements of the potential divider were as follows, very approximately.

Working voltage	100 kV.
Divider ratio	1/150.
Frequency range	1-30 mc/s.
D.C. time constant	10 microsec.
Max. capacitive shunting.	15 pF.
Inherent inductance of connections	5 μH.
Desired accuracy.	$\pm$ 10%
Max. pickup of spurious voltages of order 100 kV.	10%

No delay cable was required, as the generator was operated in a controlled manner throughout. The divider was to be used in association with a Southern Instruments Ltd. "T.R.10" Oscillograph.

3.6.1 General.

Various recognized forms of potential divider were considered (Reference B.5, Chap. 9). A pure resistance divider would not be difficult to design for this voltage, but was not recommended for high frequencies on account of distributed capacitances in the upper arm, and the capacitance of the plates and connections of the oscillograph shunting the lower arm. Since the voltages most of interest were those between pairs of adjacent points, both at a potential above earth, the use of two matched dividers, in a symmetrical arrangement similar to that used by Hohl (Reference 9) might have been possible. But until a generator arrangement with a large number of stages was being studied, it offered no advantage over the single-unit capacitance divider, which was also the simplest to make. Provided the gross capacitance to earth was not more than about 15 pF it should be possible to allow for any disturbance to the waveform due to its connection. To obtain a faithful linear response was a more serious problem, however, as will be shown later.

The divider shown in Figure 21 (actually two very similar units were made) is practically the same as that incorporated in the oscillograph described by Nuttall, (Reference 17) in that it comprises a single arrangement of electrodes and a screened connection from the low voltage electrode to the plates of the oscillograph. Oil instead of air was used for the main dielectric, making for a more compact construction. It was found necessary to add a .001 μF mica capacitor across the lower arm to give the required ratio, and a resistor of 100Ω to suppress oscillations of about 100 mc/s. between it and the co-axial connection. Some adjustment of the upper-arm capacitance C_1 was possible by raising or lowering the h.v. electrode, but the smaller C_1 and C_2, the greater the chance of spurious pickup for the same screening. Further, reducing C_1 did not appreciably reduce the gross capacitance which, as will be shown later, is fixed by the voltage and the dielectric material used, and by the

basic shape and proportions of the electrodes, which are determined by the shielding required.

Figure 22(a) shows the divider reduced to an idealized form. The objective is to measure V_x without picking up a component of V_y through C_y. C_y is reduced by extending the shield upwards while still allowing sufficient clearance for the access of V_x.

3.6.2 Frequency Response of Measuring Circuit.

So far the divider would be expected to have perfectly linear response to the voltage applied between its h.v. and earth terminals. But what is required is a response to the voltage at points on the generator, and it is inevitable that the connections must form a loop of at least 1 metre square, having, therefore, an inductance in the order of 5 μH. This is liable to oscillate with the 15 pF gross capacitance at 17 mc/s., and will do so if the voltage being measured contains components greater than this frequency, so that series resistance damping is necessary. (In this case the critical resistance is about 1000 Ω). In either case the response becomes non-linear.

Howard (Reference 10) has calculated the response of a similar arrangement to a steadily rising voltage. In this work the response to a sinusoidal voltage, and in particular to $(1 - \cos \omega t)$, is required. The response can be given in terms of the voltage across the whole capacitance unit (since c_1/c_2 is constant). (see Figure 23).

Sec. 3.6.2.

Laplace transform of $(1 - \cos \omega t) = \omega^2/(p^2 + \omega^2)$

Response = voltage across capacitance, C

$$= \frac{1/pC}{pL + R + 1/pC} \cdot \frac{\omega^2}{p^2 + \omega^2}$$

$$= \frac{\omega_o^2}{p^2 + 2\omega_o r p + \omega_o^2} \cdot \frac{\omega^2}{p^2 + \omega^2}$$

where $\omega_o = 1/\sqrt{LC}$ = natural frequency, and $r = R/2\omega_o L$ = fractional-damping factor. Also let $\omega = k\omega_o$, and

$a = r - \sqrt{r^2 - 1}$, $b = r + \sqrt{r^2 - 1}$, provided $r \neq 1$,

then response-transform $= \dfrac{\omega_o^4 k^2}{(p + a\omega_o)(p + b\omega_o)(p^2 + k^2\omega_o^2)}$

$\therefore$ response time-function

$$= 1 - \frac{k^2 e^{-at}}{a(b-a)(a^2+k^2)} - \frac{k^2 e^{-bt}}{b(a-b)(b^2+k^2)} - \frac{\cos(\omega t - \Theta)}{\sqrt{(a^2+k^2)(b^2+k^2)}}$$

where $\tan \Theta = 2rk/(1-k^2)$.

In particular, the amplitude of the main oscillation, of frequency $f = \omega/2\pi$, is reduced in the ratio

$$1/\sqrt{(a^2+k^2)(b^2+k^2)} = 1/\sqrt{k^4+(4r^2-2)k^2+1} = 1/(k^2+1)$$

when $r = 1$.

This response ratio is plotted against k for a number of damping factors in Figure 23.

The distortion is considerable for all components with a frequency in the order of ω_o. For $k = 1$, $\omega = \omega_o$, and $r = 1$, the amplitude is reduced to half. The only way of obtaining even the most approximate of practical results with a divider of this form would be to increase ω_o well beyond the range of expected, and this can only be done by reducing the gross divider capacitance.

3.6.3 Design of Idealized Divider.

The gross capacitance of the idealized divider of Figure 22(a) is mainly the effective upper-arm C_1 and the "bushing capacitance", C_b. A formal analysis of the field system to relate the bushing capacitance to C_1 (and hence to optimize the conflicting requirements of access and shielding) has not been attempted.

For the present it will be assumed that if, somewhere between the h.v. electrode and the earthed shield, there is a region, sufficiently free from external coupling, in which the middle electrode can be located, the latter can be left out of account. The field system, whatever its practical shape, may be imagined to be transformed into the field between two concentric spheres (Fig. 22(b)). Their dimensions and the dielectric between them have then to be chosen to withstand 100 kV. with minimum capacitance.

From simple electrostatic theory:-

$$\frac{V}{E_1} = \left(\frac{1}{r_1} - \frac{1}{r_2}\right) r_1^2 \quad \text{and} \quad C = 4\pi K_o K_1 r_1^2 / \frac{V}{E} .$$

Minimum capacitance is obtained for $r_1 = {}^{V}/_{E}$, $r_2 =$ infinity, and then $C_{min} = 4\pi K_o ({}^{K_1}/_{E}).V.$

Minimum overall size requires $r_1 = 2({}^{V}/_{E})$, $r_2 = 4({}^{V}/_{E})$

and then $C = 4\ C_{min}$.

The curves of Figure 22(c) give relative dimensions and capacitance values between these two extremes, and a practical compromise would probably be to make $r_1 = 1.2\ (^{V}/_{E})$ or thereabouts.

A more significant point is that for a given voltage, the capacitance is controlled by the factor $(^{K1}/_{E})$, i.e. by the dielectric material. The Table gives the results for various commonly-used materials. There is very little to choose between air and transformer oil, both indicating that the capacitance will be in the order of 5 and 7 pF. for an idealized capacitance with $r_1 = 1.2\ ^{V}/_{E}$. Assuming a practical divider could be designed to have the same gross capacitance as this, the frequency range could only be increased by about 50%.

Certain other dielectric materials appear attractive from this point of view, Pyrex glass and carbon-tetrachloride (CCl_4) being outstanding. No proper investigation of the use of these materials has been made here, although a very crude divider incorporating a 1" dia. test-tube filled with CCl_4 was put together, and generator oscillations of about 50 kV. were observed visually. The results, although promising, were too late to affect the rest of the work.

3.6.4 Bridge Measurements on Divider.

The above discussion indicates that a divider with pure capacitances in the lower arm cannot, for present purposes, give a linear response. Further, the use of the mathematical formula as a means of applying a correction to the amplitudes of the recorded oscillations is not altogether satisfying, unless the formula can be confirmed experimentally. What is considered necessary is to add inductance and resistance in the lower arm in such proportions that the ratio and phase-angle of the divider remains constant with frequency. About 8 ohms and 0.05 μH would need to be added, and accurate measurements of the small capacitances and inductances would be very uncertain by any direct method.

Sec. 3.6.4.

An overall frequency calibration of the divider was therefore attempted. A similar calibration had already been done in the Electrical Engineering Department on a 300 pF divider by Aked, Reference 1. The maximum frequencies used were 2-3 mc/s., beyond which the limitations of the supply- and detector-components of the bridge were reached. Figure 24 shows the response, or transfer function, of the present divider with a connection to the upper arm of approximately the usual size, but without damping resistance, made with the same equipment.

The apparatus is shown in its final form in Figure 25 after a series of modifications. One arm of the bridge, viz. the upper arm of the divider, and its connecting lead, had to remain unscreened. Pick-up to this arm was not considered to be very important as a high degree of accuracy was not required. The detector had however to be screened very thoroughly because of the strong electric and magnetic fields. The symmetrical detector input, after passing through a de-coupling transformer, was amplified by a tuned anode stage before being fed into the probe-unit of a valve milli-voltmeter. The probe-unit and batteries supplying the 8D3 Valve were all contained in an outer box. The design of the transformer was an adaption of that described by Sinclair (Reference 21).

In order to have about 1 mV detector signal for 1% sensitivity, an output of about 20 volts was required. This represented quite a large power with a load of about 50 pF at 20 mc/s. Two "807" Pentodes were used in parallel in a tuned-anode/cathode-follower power unit supplied from a signal generator. The cathode resistance was about 1000 ohms.

The bridge now appeared to be satisfactory technically, but useful results were still not obtained. The response of the divider with damping resistor of 1000 ohms is also shown in Figure 24, and the ratio is seen to increase with frequency, and to be indeterminate beyond about 7 mc/s. This is contrary to the

theory, see Figure 23, and to observations of oscillograms. The work was terminated before any more definite results could be obtained, but enough was done to show that a bridge-calibration up to even 20 mc/s. would be quite difficult with the equipment available.

3.6.5 Oscillographic Tests.

The disturbance-level of the measuring circuit is indicated by the pick-up recorded when the divider is connected to "earth". The divider and oscilloscope were earthed to a point Z_b on the generator base directly below B. (Figure 21). The trace when the divider is connected to Z_b (Osc. 1097, Figure 32b) is therefore due to electrostatic (and possible electro-magnetic) pickup. It differs slightly from that at Z_a (a point below A) and at the c.r.o. chassis (Osc. 1111 and 1098). However, the pickup is considered to be small enough to make corrections unnecessary.

Another effect is the disturbance of the electrostatic field system due to the capacitance of the divider. Its magnitude was assessed by noting the effect of connecting the other divider, regarded as a capacitor of about the same value, to the same point. This was done for a number of conditions, the most severe effect being at H, where the steady-state level was reduced by about 20%, the oscillations being practically unaffected This is the expected result of connecting 15-20 pF between H and Z, and the divider itself can therefore be assumed to have about the same effect. (See Figure 30b, Osc. 1234, 1236).

The natural frequency of oscillation of the divider circuit was found as indicated in Figure 30c. It was dependent on the size of the connecting loop through the sphere-gap: in Osc. 846 the loop was about 1 metre square, and the frequency 17 mc/s. A minimum loop gave about 23 mc/s. The appearance of this frequency in the record when an undamped divider is used for

voltage measurements has been mentioned in Section 3.7 (Osc. 1215-1236, Fig. 30b). A damping resistor of 1000 ohms appears from Osc. 845, 1239 (Fig. 30c) to be slightly less than critical, which agrees with a gross capacitance of 15 pF. Its effect on the response is further discussed in Section 3.7.

3.7 DISCUSSION OF OSCILLOGRAMS.

Reproductions of selected oscillograms are given in Figures 29-33. Except where otherwise indicated, the records were made with the arrangement of Figure 21, the letters A, A' ... Z corresponding to the points shown on the outline of the generator, the Oscillogram number being given alongside. Data on the generator stage connections and other conditions are given in the small tables, in which the following abbreviations have been used.

T	=	gap triggered by Trigatron device.
F	=	gap fired by overvoltage, etc.
S	=	gap made conducting by being shorted.
O	=	gap non-conducting by being opened out.
'x'cm	=	gap spacing approximately.
V_d	=	corresponding direct breakdown voltage (by meter)
V_c	=	charging voltage.
R_t	=	tail resistor value.
c.r.o.	=	nominal timesweep and timing oscillation.
Trig.	=	Trigatron polarity arrangement.*

All series resistors were replaced by normal shorting links. Charging resistors were 60 kilohms each. When a stage was not charged, the charging resistor was removed, and a resistor of about 150 kilohms connected across the stage capacitor.

* The first $\pm$ sign is the polarity of the main electrode B', the second $\pm$ sign that of the pulse applied to the trigger-point T, both relative to the main electrode A'. V indicates that A' is at the charging voltage above earth. Thus with V_c positive, and a negative tripping pulse, Trig = -V-.

Sec. 3.7.

Before analysing the oscillations for normal 1, 2 and 4 stage conditions, various factors influencing the firing of Gap 2 will be discussed, see Figure 31. In Osc. 914-918, Gap 2 was set with V_d 65% greater than V_c, with the result that Gap 2 fires a considerable time after Gap 1. The two events appear in the voltage waves at all points on the generator. Before Gap 2 fires, the oscillations are the same as when Gap 1 fires alone (compare traces from Osc. 912, 913, in (a), (b)). Thereafter a new double-frequency oscillation appears. The delays are progressively shortened as V_d is reduced to 41% (e,f.) and 13% (h,i) above V_c.

The voltage at B' always follows closely that at A' apart from the steady voltage on A, which is not recorded. The same applies between C' and D' after Gap 2 fires, at which instant D' increases by approximately 2 V_c. Before Gap 2 fires, the difference between the transients at C' and D' is the over-voltage across Gap 2. The mean voltage at C' is raised by V_c above its original value; that at D' by 0.2 V_c, due to the position of Capacitor III (D,E) in the capacitance field. Thus the average overvoltage is 0.8 V_c and remains fairly steady owing to the large value of R_t (60 kilohms).

After Gap 2 fires, a similar condition occurs between E' and F' at Gap 3 (which is not allowed to fire). The mean overvoltage is now about 1.4 V_c (see j) and remains fairly constant when R_t = 660 kilohms between D,F.

The effect of the tail resistors on the overvoltage is shown in (g), where R_t = 1 kilohm between D,F. Point F' now returns to the potential of E' (less V_c) with a time-constant of about 1/5 microsec., which makes the overvoltage pulse quite short. The same applies at (c,d). The effect is explained theoretically in Section 3.4.

The records show that the maximum overvoltage occurs on the gap adjacent to the one that has just fired. The next gap has a small, negative overvoltage (see c,k) and the next again a

small positive overvoltage (see d).

In all cases, the transient voltages on either side of a main stage capacitor are the same, the charging voltage, if present, not being recorded by the arrangement of Figure 21. This shows that these capacitors present negligible impedance to the transient currents.

The oscillograms in Figures 32, 33, form the basis for correlation with the results of the theory of Section 2. There are two methods of comparison. The mathematical result can be drawn out graphically, and the waveform compared, more or less qualitatively with the oscillogram; or the recorded wave can be analysed into its steady-state level, and the component frequencies, amplitudes and decrements of its oscillations.

The second method, which has been adopted for the 1 and 2 stage cases, follows mainly that given in Manley's "Waveform Analysis" (Reference B.12, Chap. 4), although there is here the additional factor of decrements. All amplitudes are referred to the stage charging voltage, generally indicated by the level of the axis of oscillations of the voltage at B or C. Two component frequencies are separated as follows. The lower frequency is sketched on tracing paper in such a way that when placed either above or below the composite wave it forms an envelope to the higher frequency component. The distance between the two envelopes is the double-amplitude of the latter. See Figure 27(b). The results of this analysis on the oscillograms in Figures 32,33, for a variety of conditions in which one and two gaps are conducting, are given in the Table at the end of this Section.

The simplest arrangement (gap condition "T,0,0,0") comprises only one inductive loop oscillating with the stray capacitances. Assuming that none of the inductance is directly between point B and the datum Z (and in fact there is only the oil-filled spacer and external strays) the voltage-oscillation at B (Osc. 1113, Fig. 32a) should theoretically have an initial amplitude of unity, measured from the axis of oscillations, followed by

exponential decrement. In fact there is a large initial decrement (see also Figure 26e). Allowing for an exponential decrement of about 0.7 per half-cycle, the initial amplitude is only about 0.15.

Non-linearity of the measuring circuit would tend to distort the recorded waveform in this way, as discussed in Section 3.6, but the calculations indicate that the response to 12 mc/s. oscillation should be at least 0.7 of its original amplitude, for the critically-damped divider. The voltage was again measured with the damping resistance removed, and the result (Osc. 1187, Figure 30a) appears much more reasonable. Nevertheless, the curves for $r = R/2\omega_o L = 0$. (Figure 23) show that the response should be considerably magnified. (In that case, $k = \omega/\omega_o$ = 12 mc/s/15 mc/s. = 0.8.) The result is therefore quite unreliable, and further if the original component frequencies exceed 15 mc/s., the divider oscillations will predominate (see Osc. 1215-1236, Fig. 30b).

An alternative explanation is that Gap 1 does not break down instantaneously, but takes in the order of 1/30 microsec. to become conducting. The difference between A' and B' in Osc. 1112, Fig. 32a) in fact gives a "front" of about this duration, instead of a unit step. (Figure 27a). This is discussed in Section 3.4. Again, slight variations in the initial amplitude occur between one trace and another, which would agree with irregularities in firing. The Trigatron device in Gap 1 was frequently suspected of causing these effects, and indeed often behaved anomalously, see Figure 29. Nevertheless, Osc. 1356, 1358, show that it <u>could</u> behave the same as a sphere-gap (Fig. 29c)

Most of the steady-state voltages agree approximately with those calculated. The overvoltage across Gap 2 is about 0.8.

Sec. 3.7.

The generator with two gaps conducting can be excited in a number of different ways, the normal one being when both capacitors are charged and both gaps fire without appreciable delay between them. (T,F,0,0, in Osc. 1097-1111, Fig. 32b). Analyses of the voltages at the main capacitors are given in the Table (see also Figure 27b). The two frequencies are fairly close to the theoretical values as is the steady-state level at F,G (it is rather too low at H). The amplitudes again do not compare well, even after allowing for the divider response.

It can be seen from the records of Figure 31 that the oscillations are much the same, whatever instant Gap 2 fires. This is understandable if it is the "slow" firing Gap 1 which inhibits the oscillation in the first loop. The condition actually obtaining, therefore, is one in which Gap 2 fires on an approximately steady voltage of 1.8, Gap 1 being merely conducting. This condition (S,T,0,0) has been calculated in Section 2,2, and the results are compared in the Table with the analysis of Osc. 1171-1175 (Fig. 33d). The comparison is again not very good, possibly because of the large initial decrement, but multiplying the theoretical values by 1.8 gives a rather closer comparison with the measurement of the lower frequency component for the T,F,0,0 case (Osc. 1097-1111)(Fig. 32a).

A similar condition holds for Osc. 1122-1126, (Figure 33a) in which Gap 2 fires under the over-voltage alone. The oscillations are of correspondingly smaller amplitude, but of much the same shape. The condition T,S,0,0 of Osc. 1132-1135 (Fig. 33c) was done because it was of an easily calculated form. The slower oscillations are of the expected amplitudes, relative one to another, but only about 0.4 of the calculated values.

Two conditions in which all four gaps are conducting, the excitation being by one gap only in each case, are given in Osc. 1137-1141 (Fig. 33b) and Osc. 1142-1147 (Fig. 33e). Four frequencies would be expected, but only one of about 6 mc/s. appears predominantly. The higher components are likely to be

attenuated by either (or both) the effects already mentioned. The conditions for the former series are the same as for the calculations in Section 2.2 for the 4-Stage case, the resolution of the dynamic matrix of which was done on a digital computer. The theoretical waveforms contain predominant frequencies of 7.8, 12.6, 18.5 mc/s. and are plotted for two points in Figure 28 for comparison with Oscillograms 1137 and 1141. (Those of 29.3 mc/s. are of less than 10% in amplitude and are ignored.) No correlation can be claimed here; even the predominant frequency in the oscillograms (6.2 mc/s. and 5.5 mc/s. respectively) is considerably lower than the calculated value. Assuming the measured frequencies to be correct, the discrepancy might be put down to inaccuracy of inductance (including omission of mutuals).

Corrigendum.

After the work had been brought to a close, it became apparent to the writer that the conception of the inductances given in Section 3.3.2 is not correct. The field of self-inductance round one of the horizontal connectors cannot be said to extend only as far as an adjacent connector, (Figures 18 and 30d), since the latter does not necessarily form the return path for any part of the current through it. The return current can flow through non-adjacent conductors and through the various partial-capacitance fields. Strictly speaking, it would be fallacious to state any definite value of inductance for a conductor that is not part of a single, closed, current path. The lumped parameters given in the equivalent-circuit analysis are approximate, and depend on the inductance field being concentrated close to the conductor. In a horizontal connector, nearly 90% lies between radii r_o and b, and this space should contain only a small part of the displacements in the capacitance field system. Nevertheless, the discrepancies in the frequencies may well be due to such errors in assessing the parameters.

TABLE OF CALCULATED AND MEASURED COMPONENTS OF VOLTAGES.

All voltages are relative to the charging voltage, V_c, as given by the steady-state level at B (or at D in the STOO case).

The response factor, q, of the divider is obtained from Figure 23, assuming ω_o = 15 mc/s.

I.G. CONDITION		T,O,O,O (Rd = 1 kilohm)				T,O,O,O (Rd = O)			
OSCILLOGRAMS		1112 - 1117				1185 - 1190			
GENERATOR POINT		B,C	D,E	F,G	H	B,C	D,E	F,G	H
STEADY STATE LEVEL	calc.	1	0.17	0.39	0.17	1	.17	.39	.17
	meas.	1	0.2	0.29	0.14	1	0.2	.29	.14
OSCILLATION FREQUENCY (mc/s)	calc.	12.3	-	-	-	12.3	"	"	"
	meas.	12	12	12	12	12	"	"	"
Amplitude	calc.	1	0.17	0.39	0.17	1	0.17	0.39	0.17
calc. x (q = 0.7, 1.6)		0.7	0.12	0.28	0.12	1.6	.27	.63	.27
	meas.	0.2	0.05	.05	.05	0.9	0.2	0.28	0.13

Table continued.

TABLE (cont'd.)

I.G. CONDITION		T, S, 0, 0				S, T, 0, 0			
OSCILLOGRAMS		1132 - 1135				1171 - 1175			
GENERATOR POINT		B,C	D,E	F,G	H	B,C	D,E	F,G	H
STEADY STATE LEVEL.	calc.	1	1	0.53	0.61	0	1	0.17	0.54
	meas.	1	1	0.4	0.4	0	1	0.2	0.35
LOW FREQUENCY COMPONENT (mc/s)	calc.	8.74	"	"	"	8.74	"	"	"
	meas.	9.1	"	"	"	8.3	"	"	"
Amplitude	calc.	0.81	1.15	0.50	0.69	0.48	0.68	0.29	0.41
calc. x (q = .75)		0.61	0.86	0.37	0.52	0.35	0.51	0.22	0.31
	meas.	0.25	0.4	0.17	0.2	0.17	0.20	0.10	0.1
HIGH FREQUENCY COMPONENT (mc/s)	calc.	21	"	"	"	21	"	"	"
	meas.	nil				nil			
Amplitude	calc.	0.19	0.15	0.04	0.07	0.48	0.32	0.12	0.13
calc. x (q = .35)		0.07	0.05	0.01	0.03	0.17	0.11	.04	.05
	meas.	nil	-	-	-	nil	-	-	-

Table continued.

TABLE (cont'd.)

I.G. CONDITION		T, F, O, O				T, F, O, O *			
OSCILLOGRAMS		1097 - 1111				1097 - 1111			
GENERATOR POINT		B,C	D,E	F,G	H	B,C	D,E	F,G	H
STEADY STATE LEVEL	calc.	1	2	0.71	1.2	1	2	0.71	1.2
	meas.	1	2	0.63	0.77	1	2	0.63	0.77
LOW FREQUENCY COMPONENT (mc/s)	calc.	8.74	"	"	"	8.74	"	"	"
	meas.	8.8	8.3	8.8	8.6	8.8	"	"	"
Amplitude	calc.	1.28	1.83	0.79	1.1	0.87	1.25	0.52	0.75
calc. x (q = 0.75)		0.96	1.37	0.59	0.82	0.65	0.94	0.39	0.56
	meas.	0.50	0.64	0.30	0.34	0.50	0.64	0.30	0.34
HIGH FREQUENCY COMPONENT (mc/s	calc.	21	"	"	"	21	"	"	"
	meas.	18.7	19		18.9	18.7	"	"	"
Amplitude	calc.	0.28	0.17	0.08	0.06	0.87	0.58	0.23	0.24
calc. x (q = 0.35)		0.1	0.06	0.03	0.02	0.32	0.2	0.08	0.09
	meas.	0.12	0.20	nil	0.07	0.12	0.20	0	0.07

* In this case, the calculations are based on Gap 2 firing on a steady voltage of 1.8, the oscillations (but not the steady-state components) due to the firing of Gap 1 having died out.

LIST OF REFERENCES.

1. Aked, A: "Peak Voltage Measurements of Standard Impulse Voltage Waves," Proc. I.E.E., Pt.C, 103, (1956), 186-

2. Barker, R.H.: "The Pulse Transfer Function and its Application to Sampling Servo Systems," Proc. I.E.E., Pt.IV, 99, (1952), 302-317.

3. Duncan, W.J. & Collar, A.R.: "A Method for the Solution of Oscillatory Problems by Matrices," Phil.Mag., Ser.7, 17, (1934), 865.

4. Edwards, F.S., Husbands, A.S. & Perry, F.R.: "The Development and Design of High Voltage Impulse Generators," Proc. I.E.E., Pt.II, 98, (1951), 155.

5. Elsner, R.: "Die Berechming der Zundschwingung eines vielstufigen Marxschen Stossgenerators," Archiv. fur Elektrotechnik, 30, (1936) 445-455.

6. Goodlet, B.L.: "Electromagnetic Phenomena in High Voltage Testing Equipment," Jour. I.E.E., 74(1934), 377.

7. Hardy, D.R. & Wroe, H.: "The Breakdown of Pre-stressed Air at Atmospheric pressures," Brit.Jour.Appl.Phys., 5, (1954), 335-39.

8. Hardy, D.R. & Broadbent, T.E.: "The Control of High Voltage Impulse Generators," BEAMA. Jour., 62, (1955), 63-68.

9. Hohl, H.: "Der Hochspannungsteiler beim Kathodenstrahloszillographen," Arch. Elektrotech. 31, (1941), 663.

10. Howard, P.R.: "Errors in Recording Surge Voltages," Proc. I.E.E., Pt.II, 99, (1952), 371-383.

11. Husbands, A.S. & Higham, J.B.: "The Controlled Tripping of High Voltage Impulse Generators," Jour.Sci. Instrum., 28, (1951), 243.

12. John, Prof. W.J.: Transmission Section Chairman's Address, Jour. I.E.E., Pt.I, 95, (1948), 167-171.

13. Lawden, D.F.: "The Function $\sum_{n=1}^{\infty} n^r z^n$ and Associated Polynomials," Proc.Camb.Phil.Soc., 47, (1951), 309.

14. Lewis, T.J.: "The Transient Behaviour of Ladder Networks of the type representing transformer and machine windings," Proc. I.E.E., Pt.II, 101, (1954), 541-53.

15. Miller, J.L.: "A Theoretical and Experimental Study of the Inter-Stage Phenomena in the Marx-type Impulse Generator," Ph.D. Thesis to London University 1947.

16. Neufeld, J.: "On the Operational Solution of Linear Mixed difference-differential equations," Proc.Camb. Phil.Soc., 30, (1934), 389-391.

17. Nuttall, A.K.: "A C.R. Oscillograph for the direct measurement of high-voltage transients," Jour.I.E.E. 78, (1936), 229.

18. Pirenne, J.: "Théorie générale des phénomènes oscillatoires dans les enroulements de transformateurs," Revue Générale de l'Electricite, 47, (1940) 19.

19. Provoost, P.G.: "Travelling Waves in Surge Generators," (in Dutch), Electrotechnick, 33, (1955) 177-81.

20. Rudenberg, R.: "Performance of travelling waves in coils and windings," Trans. A.I.E.E., 59, 1940, 1031.

21. Sinclair, D.B.: "A R.F. Bridge for Impedance Measurement from 400 Kc/s. to 60 mc/s." Proc.Inst. Radio Engrs., 28, (1940), 497.

22. Stigant, S.A.: "Direct Setting up of Z_d for Closed-Mesh Networks from the Network Diagram," BEAMA Jour. 54, (1947), 28 and 65.

23. Stone, W.M.: "A Note on a paper by Durant" (on a finite difference equation). Phil.Mag., 39, (1948), 988-991.

24. Vowels, R.E.: "Matrix Methods in the Solution of Ladder Networks," J.I.E.E., Part III, 95, (1948), 40-50.

25. Waldvogel, P. & Rouxel: "Predetermination by Calculation of the Electric Stresses in a Winding Subjected to a Surge Voltage," C.I.G.R.E., 1956, No. 125.

BOOK REFERENCES.

B.1. Attwood, S.S.: "Electric and Magnetic Fields," London 1956.

B.2. Bewley, L.V.: "Travelling Waves in Transmission Systems," London 1933.

B.3. Brillouin, Leon: "Wave Propagation in Periodic Structures, New York 1946.

B.4. Carslaw, H.S. & Jaeger, J.C.: "Operational Methods in Applied Mathematics," Oxford 1947.

B.5. Craggs, J.D. & Meek, J.M.: "High Voltage Laboratory Technique," London 1954.

B.6. Frazer, R.A., Duncan, W.J. & Collar, A.R.: Elementary Matrices," Cambridge 1938.

B.7. Gardner, M.F. & Barnes, J.L.: "Transients in Linear Systems," Vol.I, Lumped-Constant systems. New York 1947.

B.8. Guillemin, E.A.: "Communication Networks"(2 Vols.) New York 1935.

B.9. Hartshorn, L.: "Radio-Frequency Measurements by Bridge and Resonance Methods," London 1940.

B.10. King, R.W.P.: "Electromagnetic Engineering, Vol, I. New York 1945.

B.11. Kron, G.: "Tensor Analysis of Networks," New York 1939.

B.12. Manley, R.G.: "Waveform Analysis," London 1945.

B.13. McLachlan, N.W.: "Modern Operational Calculus with Applications in Technical Mathematics," London 1949.

B.14. Meek, J.M. & Craggs, J.D.: "Electrical Breakdown of Gases." Oxford 1953.

B.15. Weber, Ernst.: "Linear Transient Analysis," Vol,I. New York 1954.

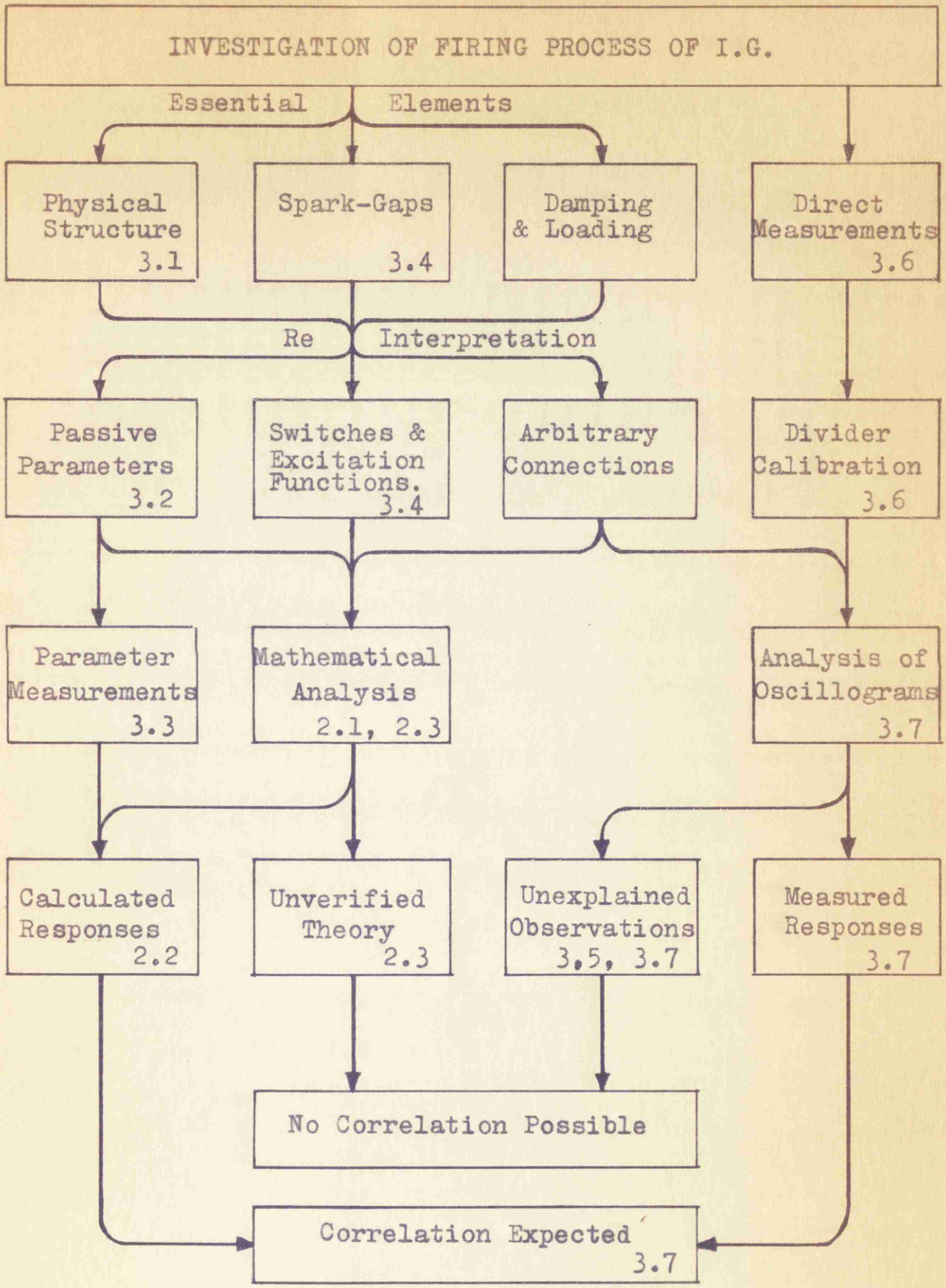

SCHEME OF INVESTIGATION. FIGURE 1.

(The numbers refer to Sub-Sections of the Text)

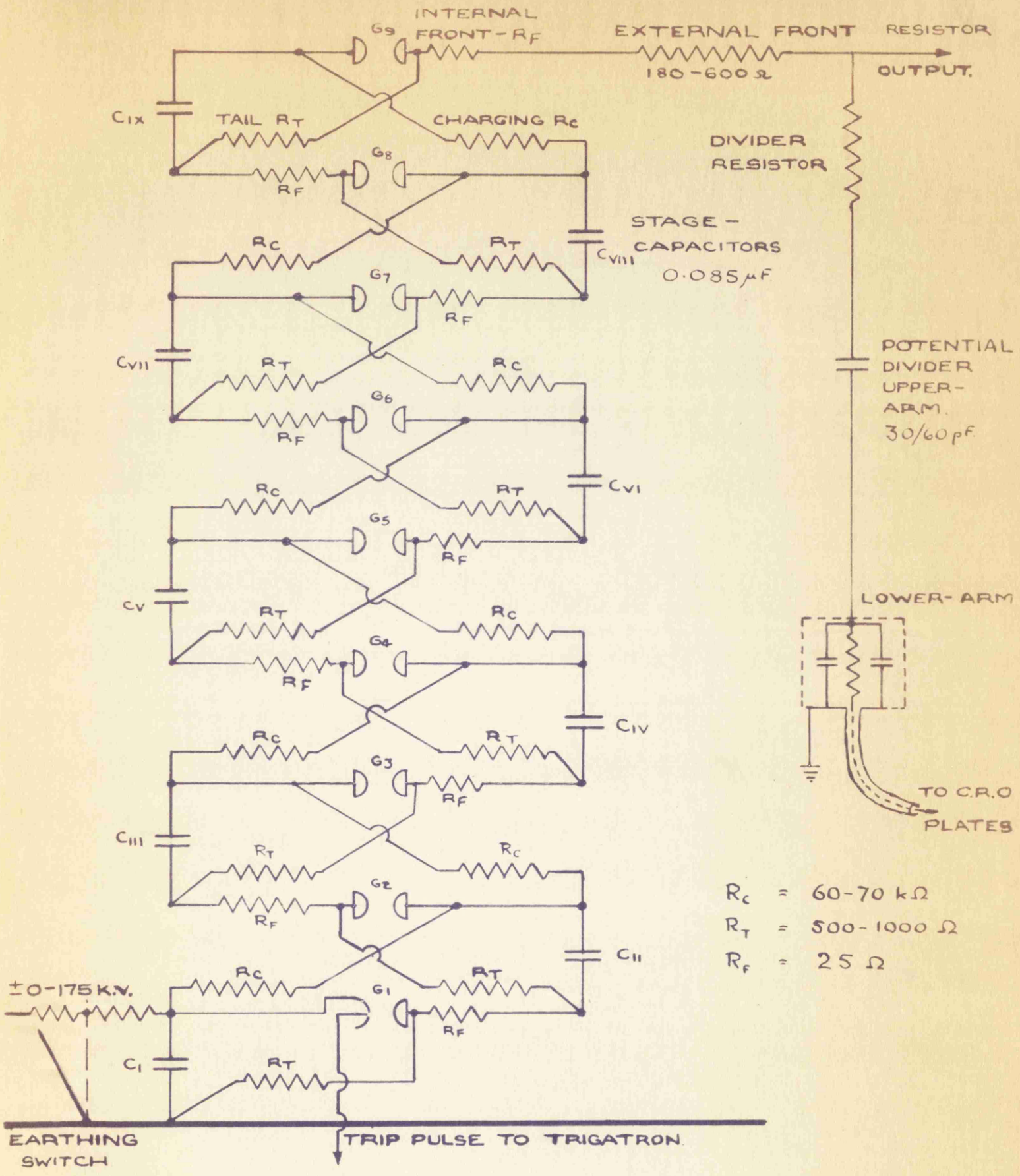

NINE-STAGE IMPULSE GENERATOR CONNECTIONS. FIGURE 2.

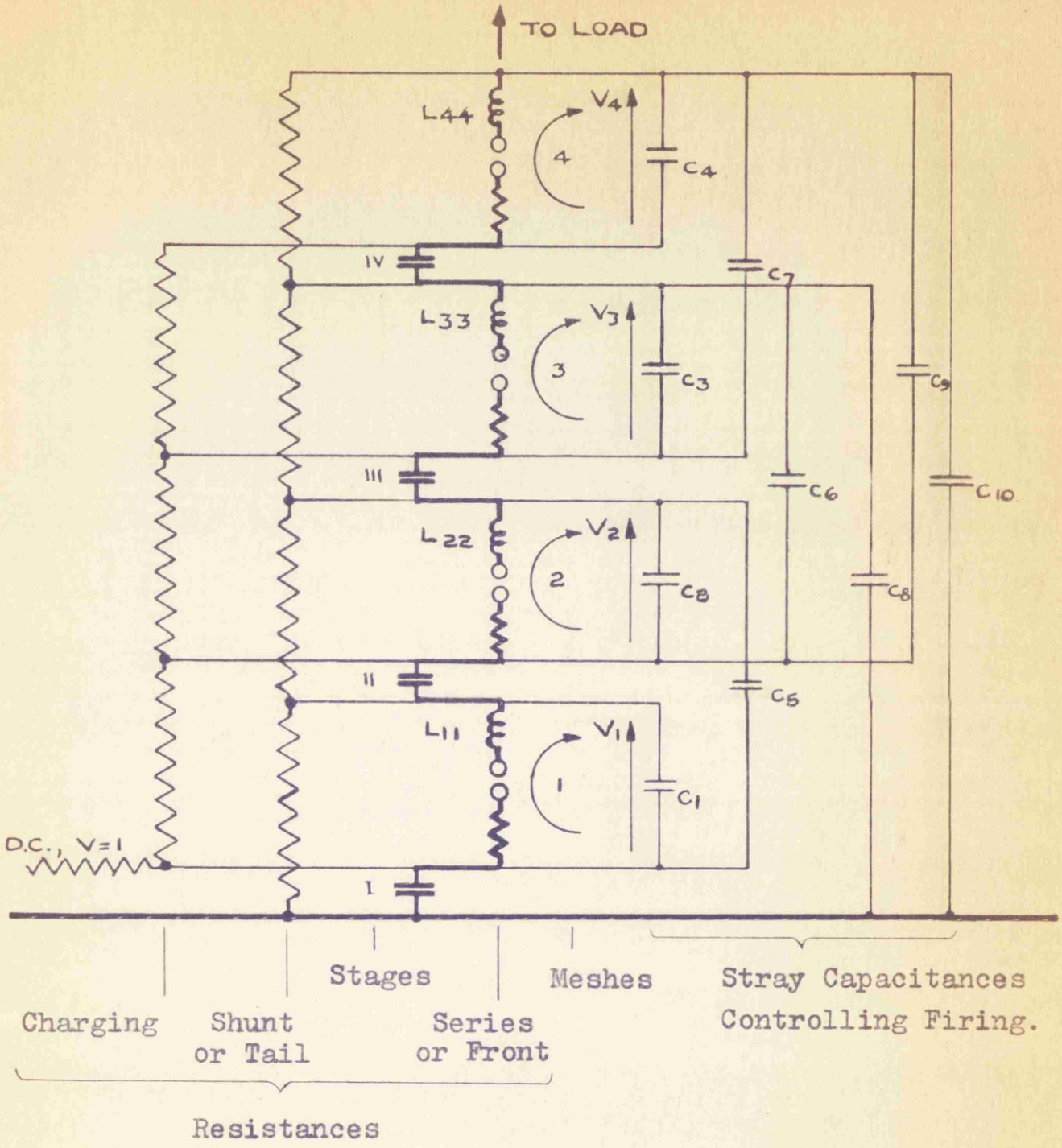

4-STAGE I.G. EQUIVALENT CIRCUIT. FIGURE 3.

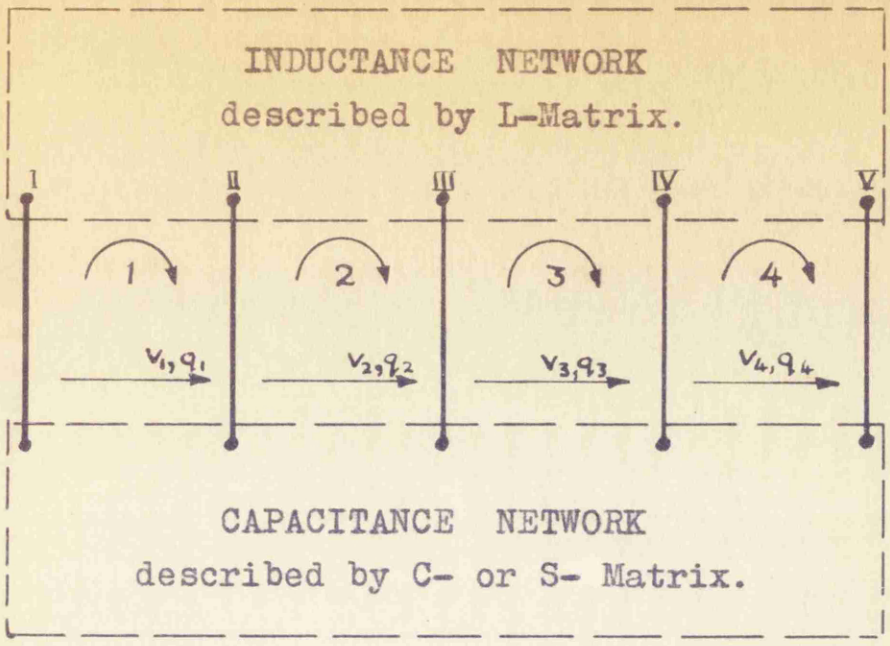

Meshes and Original Terminal-Pairs.

(a) Connection of Segregated L and C Networks.

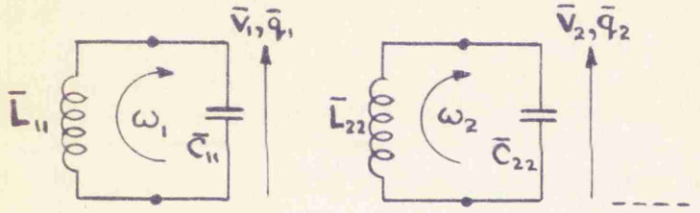

(b) Normal-Terminal-Pair Networks.

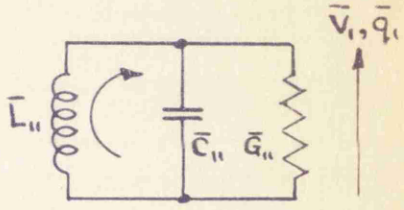

(c) Damped ω_1-Network.

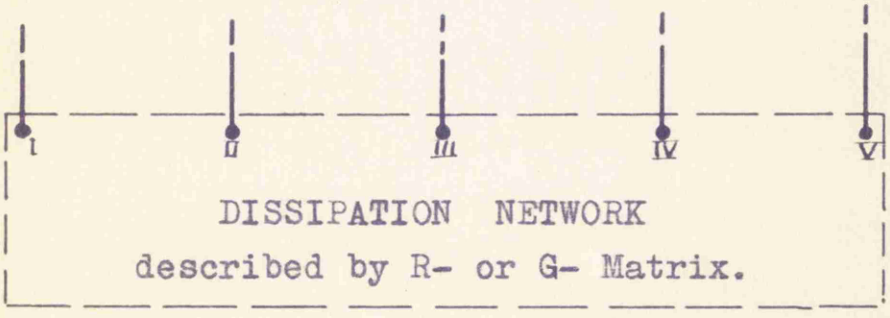

Connections to Original Terminal-Pairs.

(d) Derived Damping Network.

4-STAGE I.G. ANALYTICAL NETWORKS. FIGURE 4.

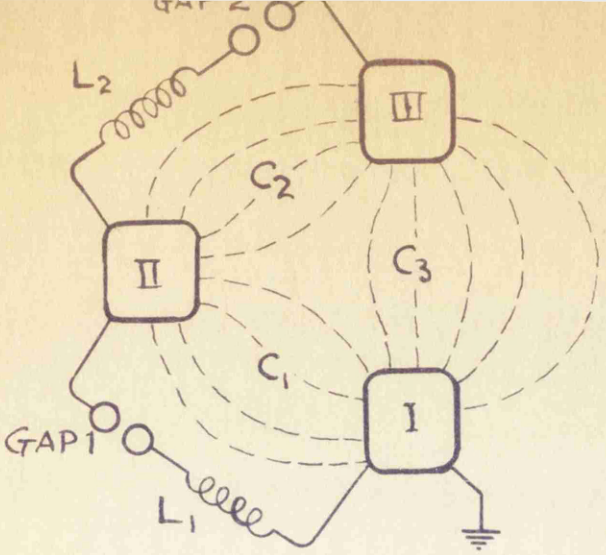

(a) Electrostatic Fields.

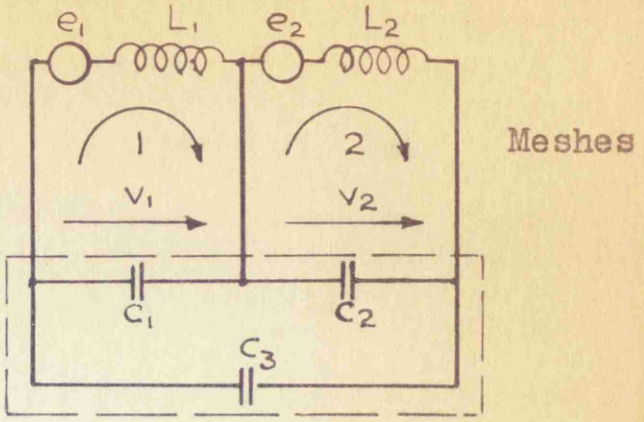

(b) Equivalent Circuit.

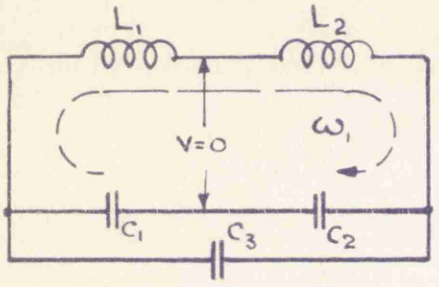

Normal Mesh $\bar{1}$

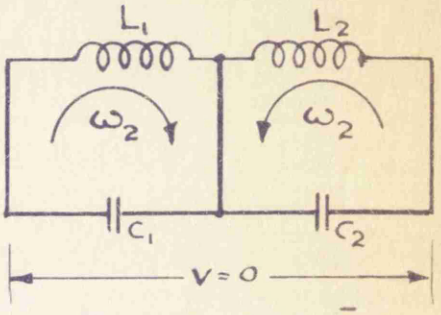

Normal Mesh $\bar{2}$

(c) Special Case, $L_1C_1 = L_2C_2$, Normal Meshes.

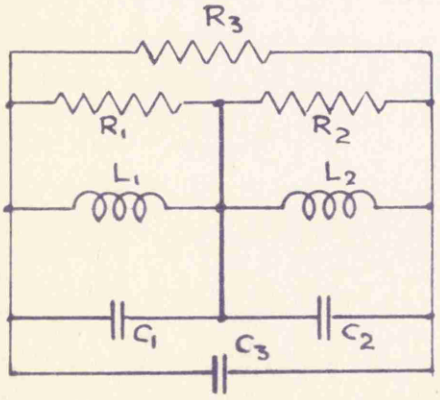

(d) Damped Circuit.

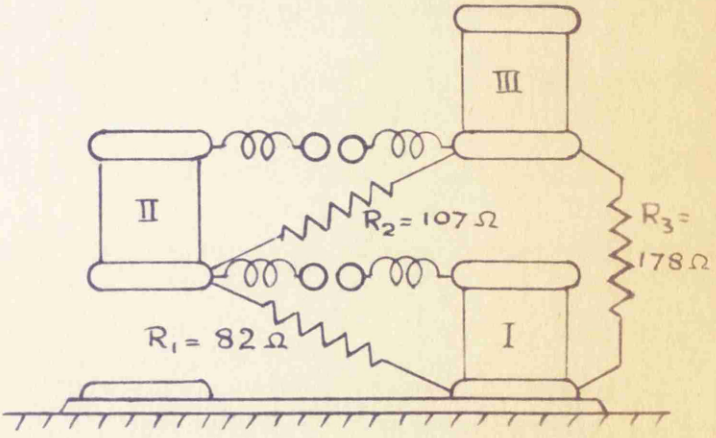

(e) Estimated Resistance Values for Critical Damping.

TWO-STAGE I.G. THEORY. FIGURE 5.

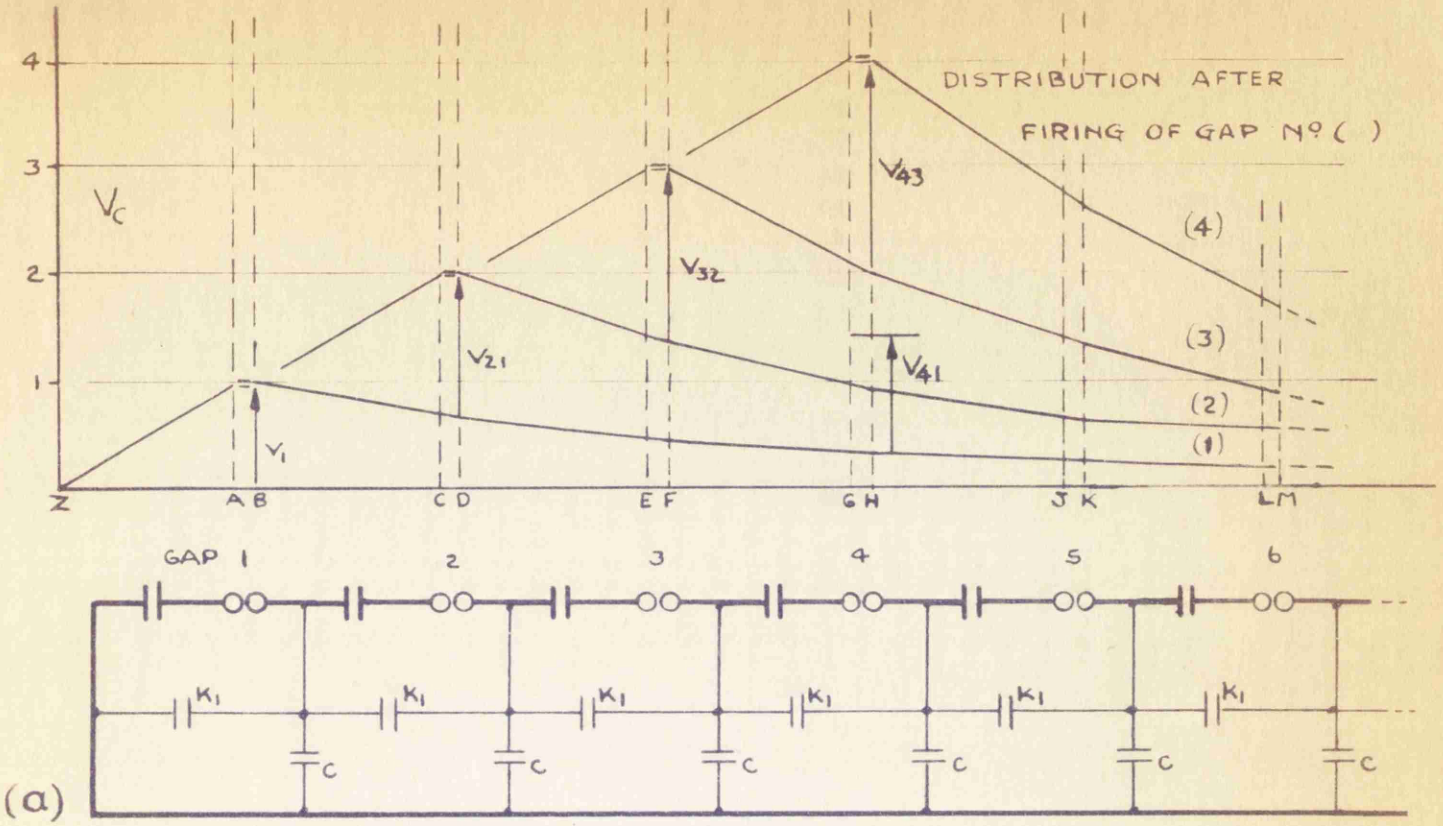

(a)

Note: V_{41} = "Voltage across Gap 4 following Firing of Gap 1", etc.

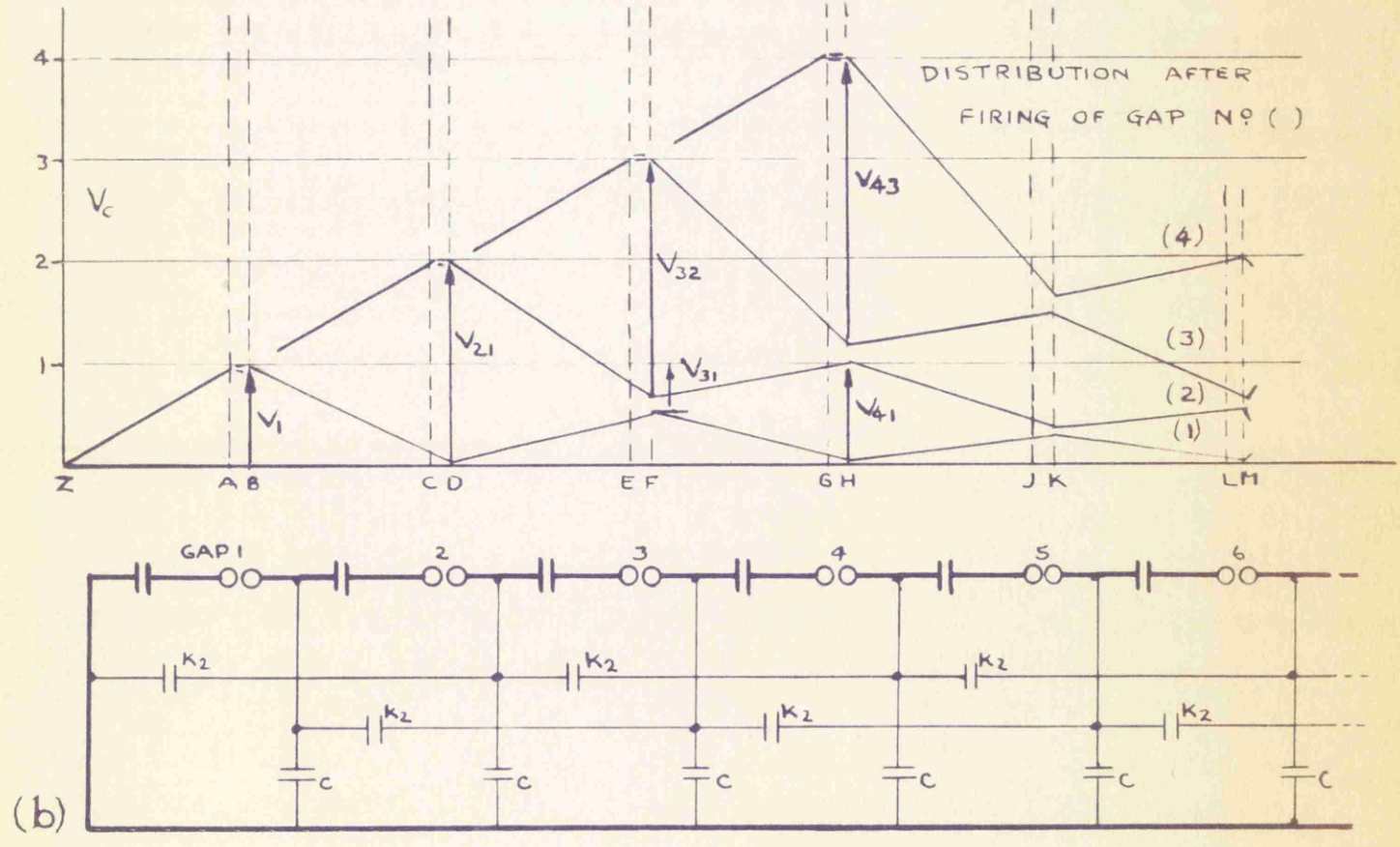

(b)

HYPOTHETICAL VOLTAGE DISTRIBUTIONS. FIGURE 6.

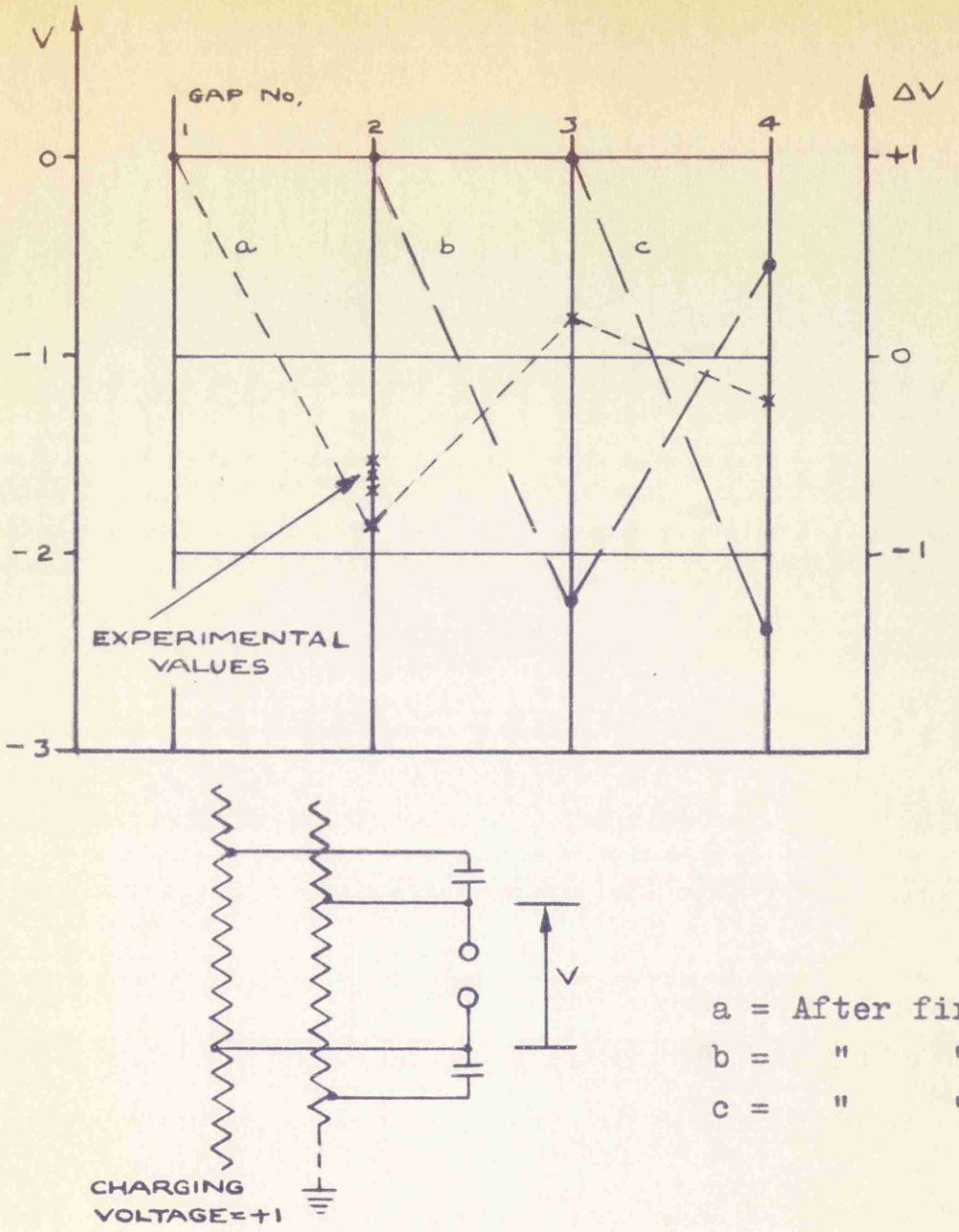

a = After firing of Gap 1.
b = " " " Gaps 1,2.
c = " " " Gaps 1,2,3.

For Experimental points, $v = V_d/V_c$, where

V_d = d.c. spark-over voltage of Gap 2.

V_c = charging voltage giving 50% spark-over of Gap 2 following firing of Gap 1.

STEADY-STATE VOLTAGES ACROSS GAPS. FIGURE 7.

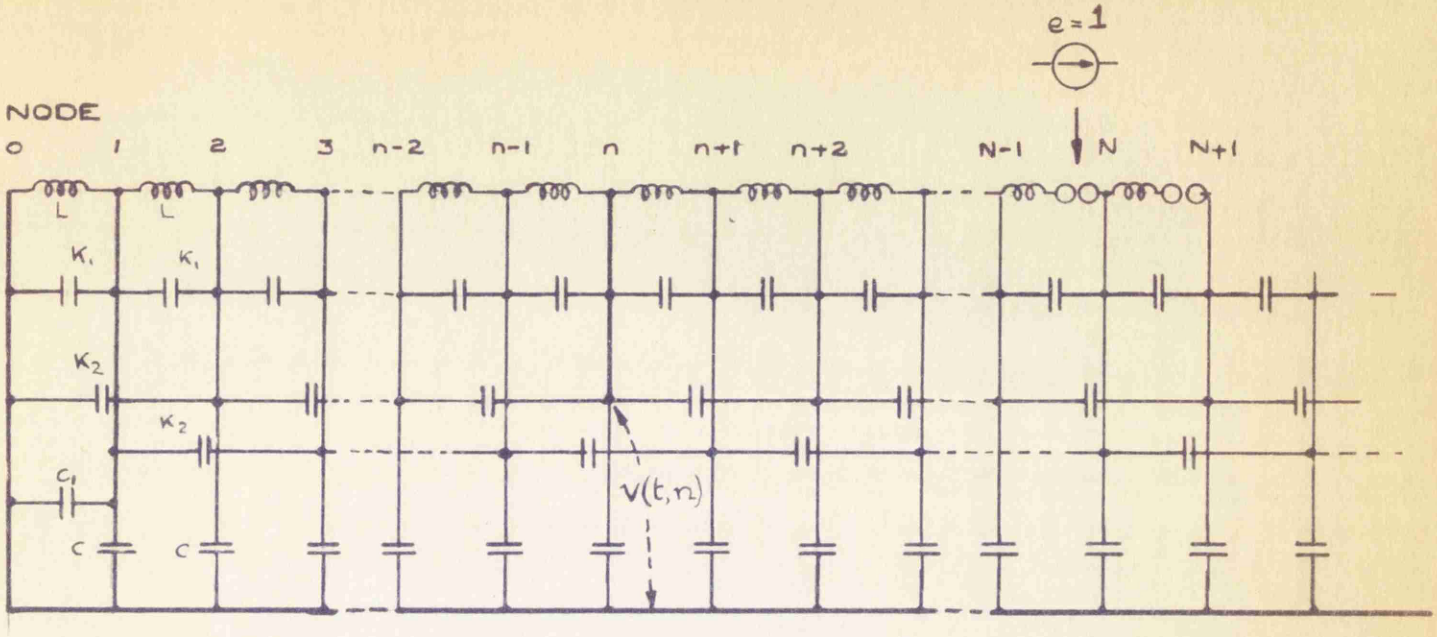

$L = 1.3\ \mu H.$

$K_1 = 10\ pF.$

$K_2 = 33\ pF.$

$C = 30\ pF.$

$C_1 = 33\ pF.$

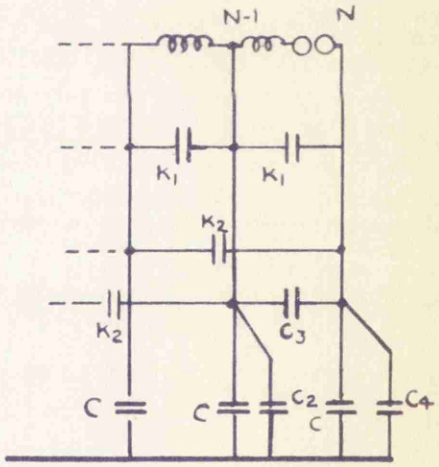

C_2, C_3, C_4 equivalent to remaining unfired stages and terminal load.

LATTICE EQUIVALENT CIRCUIT OF EXTENDED GENERATOR. FIGURE 8.

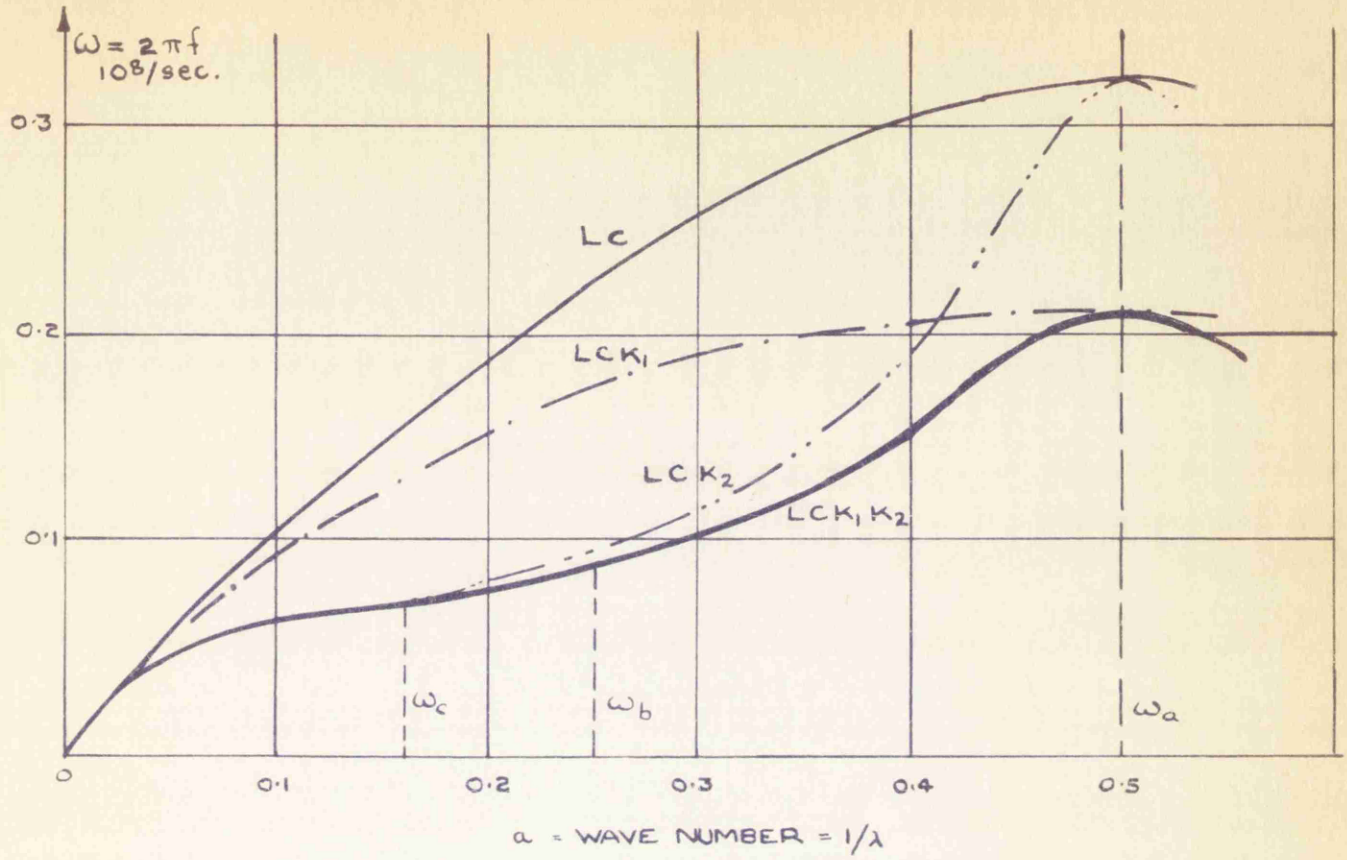

$$\omega^2 = \frac{(1 - \cos 2\pi a)/L}{C/2 + K_1(1 - \cos 2\pi a) + K_2(1 - \cos 4\pi a)}$$

Estimated values

$L = 1.3\ \mu H, \quad C = 30\ pF, \quad K_1 = 10\ pF, \quad K_2 = 33\ pF.$

(Components taken into account shown against curves.)

PROPAGATION CHARACTERISTICS OF LATTICE. FIGURE 9.

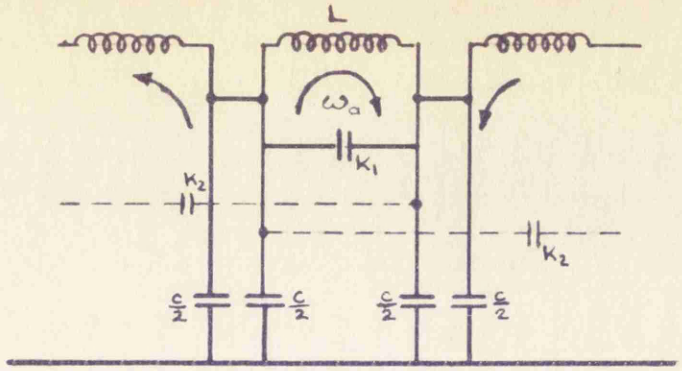

(a)

$$\omega_a^2 = \frac{1}{L(K_1 + c/4)} = \omega_{max}^2$$

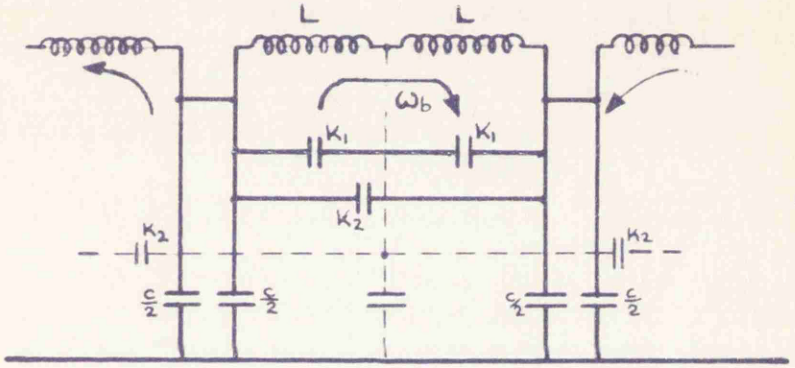

(b)

$$\omega_b^2 = \frac{1}{2L\left(\frac{K_1}{2} + K_2 + \frac{c}{4}\right)}$$

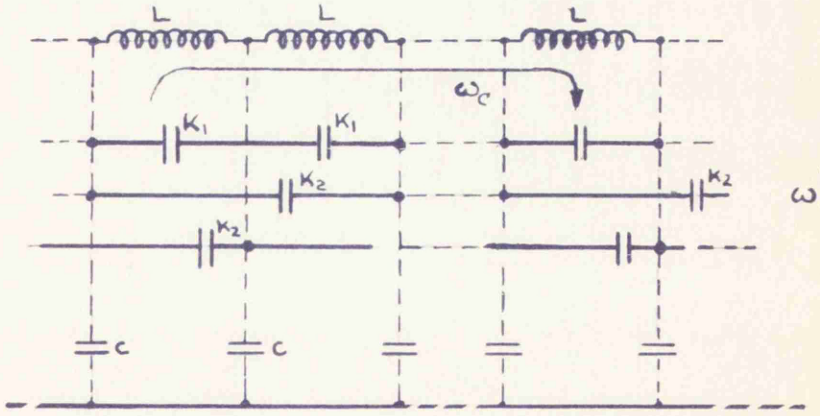

(c)

$$\omega_c^2 = \frac{1}{L(K_1 + 4K_2)}$$

MODES OF OSCILLATION IN LATTICE. FIGURE 10.

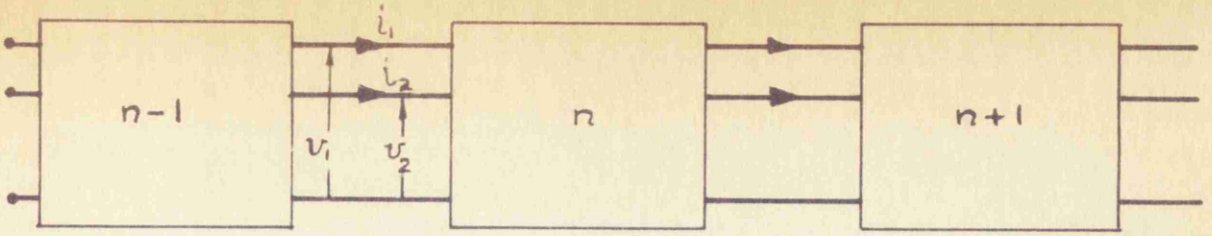

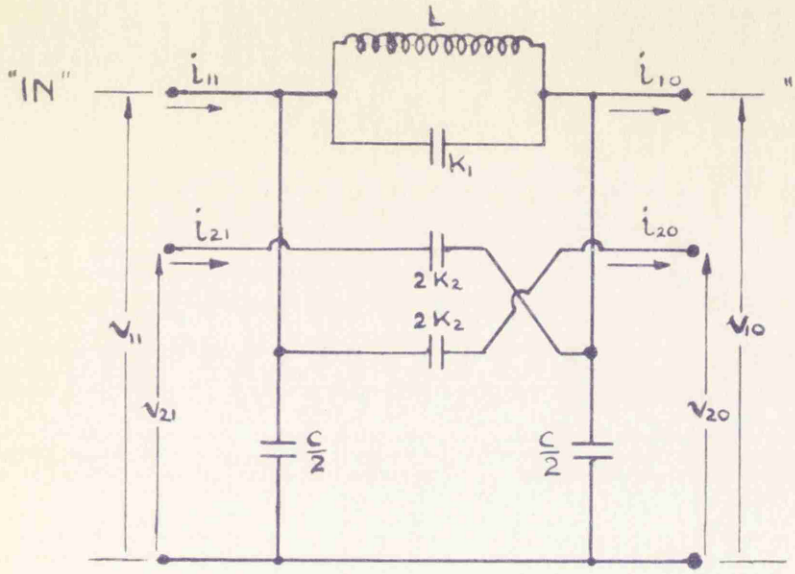

REPRESENTATIVE SECTION AND ADMITTANCE MATRIX.

i_{11}	=	p	$\frac{C}{2}+2K_2+K_1+\frac{1}{p^2L}$	0	$-K_1-\frac{1}{p^2L}$	$-2K_2$	v_{11}
i_{21}			0	$2K_2$	$-2K_2$	0	v_{21}
i_{10}			$K_1+\frac{1}{p^2L}$	$2K_2$	$-\frac{C}{2}-2K_2-K_1-\frac{1}{p^2L}$	0	v_{10}
i_{20}			$2K_2$	0	0	$-2K_2$	v_{20}

v_{11}	=	$\frac{1}{2K_2}$	0	$2K_2$	0	$\frac{1}{p}$	v_{10}
v_{21}			$\frac{C}{2}+2K_2+K_1+\frac{1}{p^2L}$	$-K_1-\frac{1}{p^2L}$	$\frac{1}{p}$	$-\left(K_1+\frac{1}{p^2L}\right)/2pK_2$	v_{20}
i_{11}			$-2K_2\left(pK_1+\frac{1}{pL}\right)$	$2pK_2\left(\frac{C}{2}+K_1+\frac{1}{p^2L}\right)$	0	$-\frac{C}{2}-2K_2-K_1-\frac{1}{p^2L}$	i_{10}
i_{21}			$2pK_2\left(\frac{C}{2}+K_1+\frac{1}{p^2L}\right)$	$-2K_2\left(pK_1+\frac{1}{pL}\right)$	$-2K_2$	$K_1+\frac{1}{p^2L}$	i_{20}

6-TERMINAL SECTIONS IN CASCADE.

FIGURE 11.

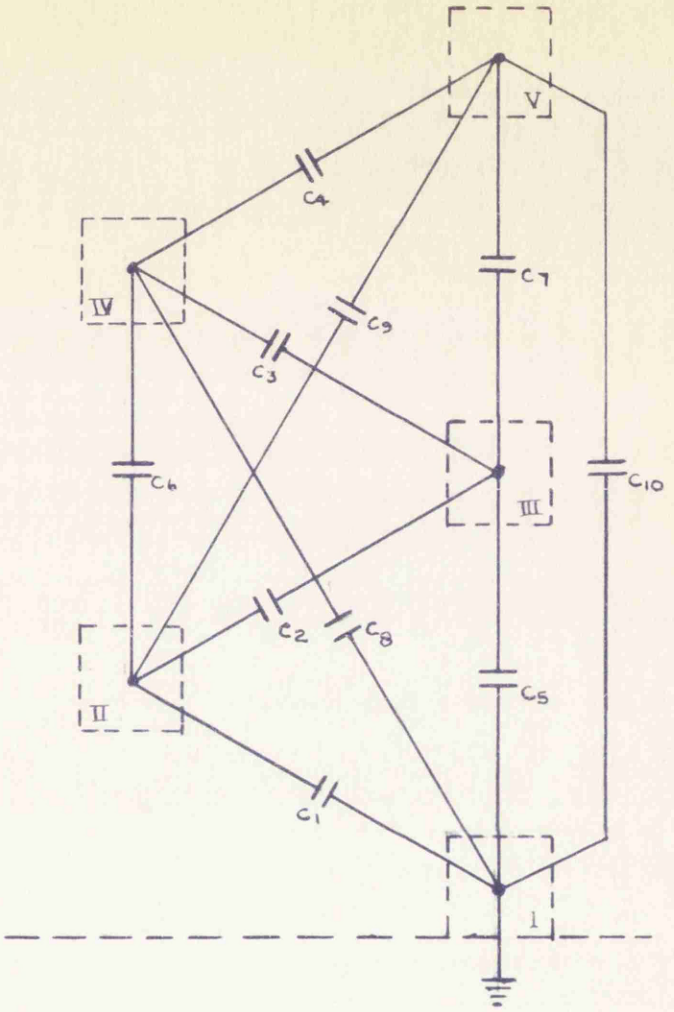

Partial Capacitances. (10^{-12} F)

C_1	C_2	C_3	C_4	C_5	C_6	C_7	C_8	C_9	C_{10}
67.1	8.9	10.5	11.1	56.3	31.9	32.9	35.3	1.2	17.1

(Derived from Bridge Measurements: Fig. 16 and 17)

4-STAGE I.G. PARTIAL CAPACITANCES. FIGURE 12.

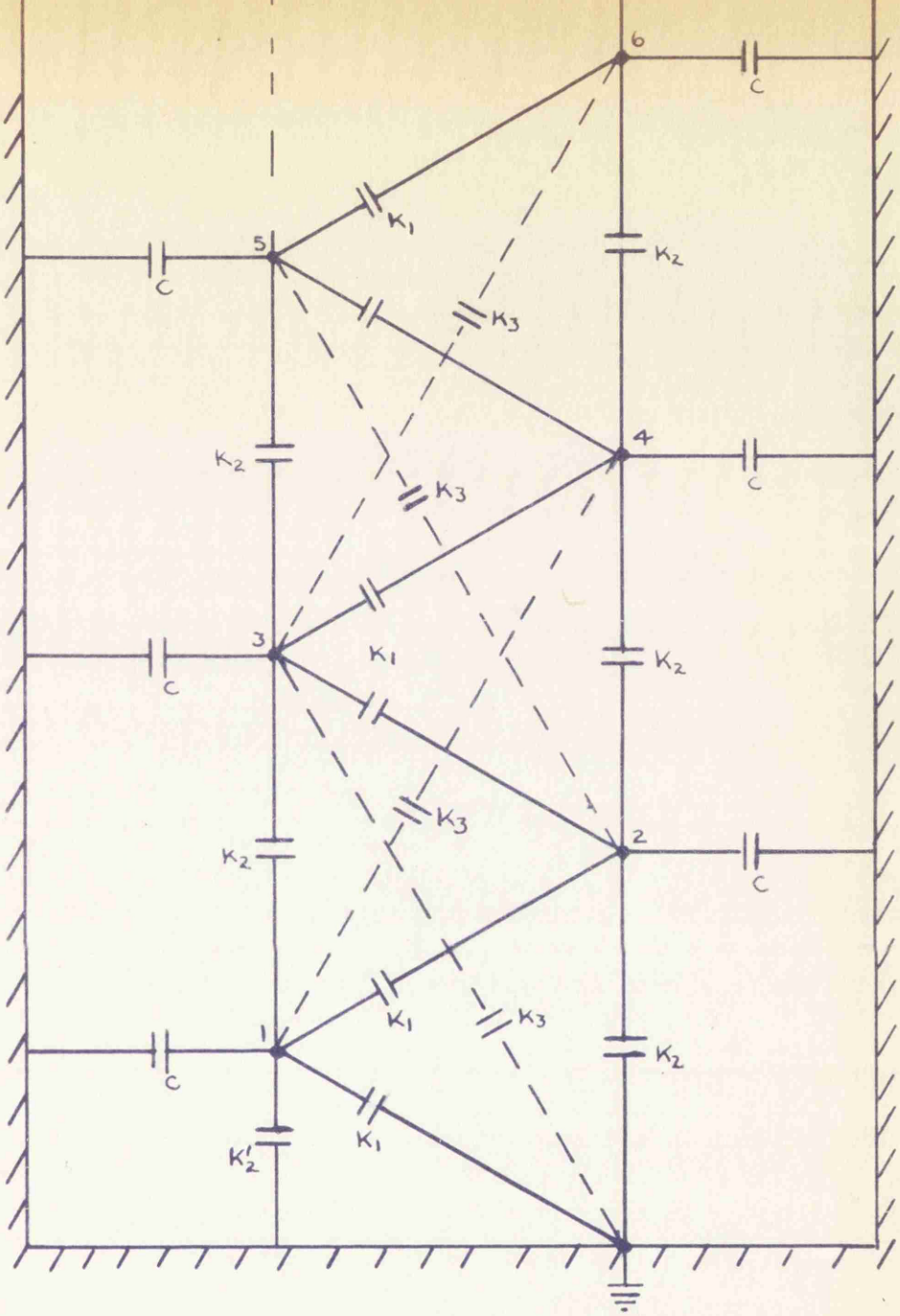

	pF.	Compare Values from Figure 12:-
C	= 30	C_8 = 35 , C_{10} = 17.2 (Flange only)
K_1	= 10	C_2 = 8.9, C_3 = 10.5, C_4 = 11.1
K_2	= 33	C_6 = 31.9, C_7 = 32.9.
K_3	= 0	C_9 = 1.2
$K_2^1 = K_2$	= 33	
$K_1 + K_2^1 + C$	= 73	C_1 = 67.1
$K_2 + C$	= 63	C_5 = 56.3

EXTENDED GENERATOR PARTIAL CAPACITANCES. FIGURE 13.

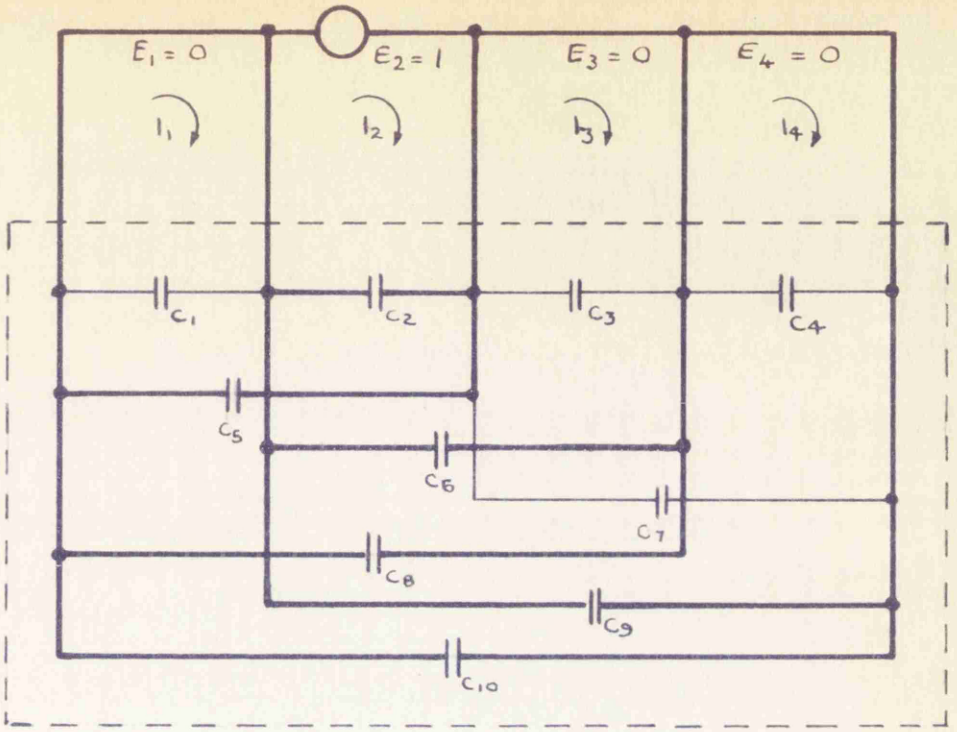

Condition for evaluating terms in 2nd Column of C-matrix.

Ex. $C_{32} = I_3/pE_2 = C_6 + C_8 + C_9 + C_{10}$.

$C_1 + C_5 + C_8 + C_{10}$	$C_5 + C_8 + C_{10}$	$C_8 + C_{10}$	C_{10}
$C_5 + C_8 + C_{10}$	$C_2 + C_5 + C_6 + C_8 + C_9 + C_{10}$	$C_6 + C_8 + C_9 + C_{10}$	$C_9 + C_{10}$
$C_8 + C_{10}$	$C_6 + C_8 + C_9 + C_{10}$	$C_3 + C_6 + C_7 + C_8 + C_9 + C_{10}$	$C_7 + C_9 + C_{10}$
C_{10}	$C_9 + C_{10}$	$C_7 + C_9 + C_{10}$	$C_4 + C_7 + C_9 + C_{10}$

By Substitution of Measured Values from Figure 12:-

C = $(10^{-12}F)$

175	108	52	17
108	150	85	18
52	85	128	51
17	18	51	62

$S = C^{-1}$ = $(10^{10}/F)$

1.07	-0.89	0.24	-0.24
-0.88	1.90	-1.15	0.63
0.24	-1.15	2.01	-1.38
-0.24	0.63	-1.38	2.68

DERIVATION OF CAPACITANCE AND ELASTANCE MATRICES.

FIGURE 14.

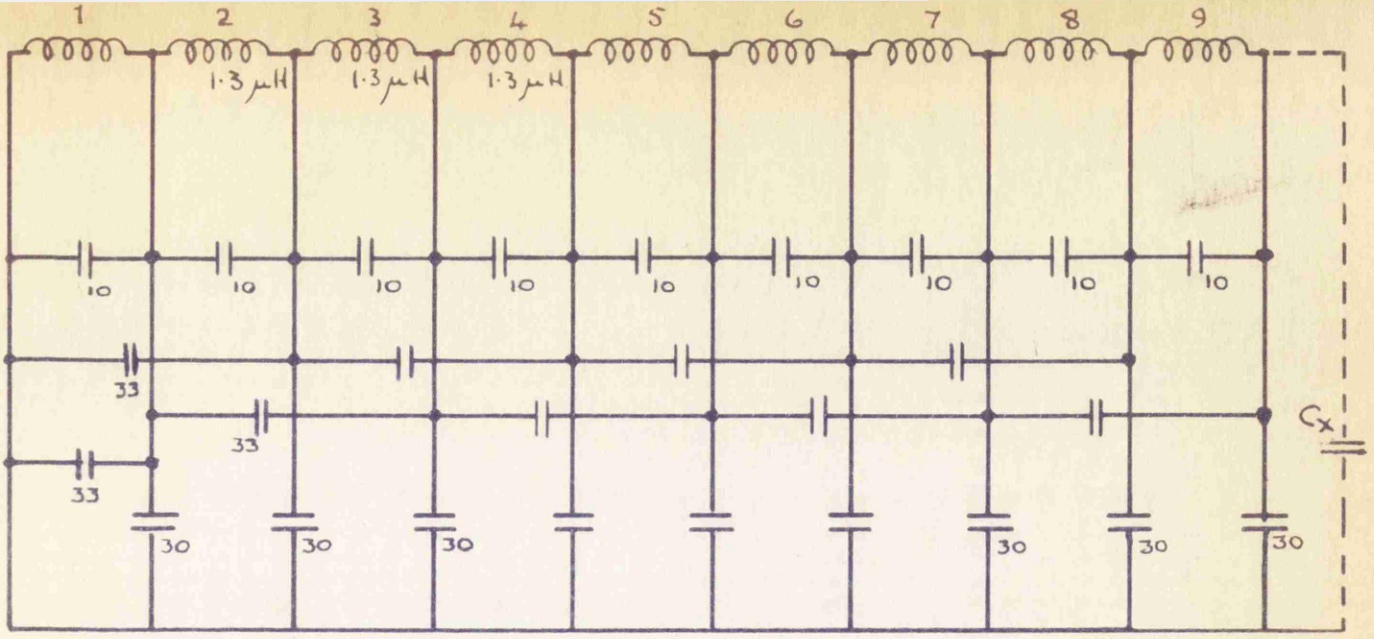

With Load capacitor C_x, matrix is enlarged by one row and column, and all elements increased by C_x. pF-units.

346	273	210	180	150	120	90	60	30	
273	316	243	180	150	120	90	60	30	
210	243	286	213	150	120	90	60	30	
180	180	213	256	183	120	90	60	30	
150	150	150	183	226	153	90	60	30	
120	120	120	120	153	196	123	60	30	
90	90	90	90	90	123	166	93	30	
60	60	60	60	60	60	93	136	63	
30	30	30	30	30	30	30	63	73	

9-STAGE I.G. CAPACITANCE MATRIX. FIGURE 15.

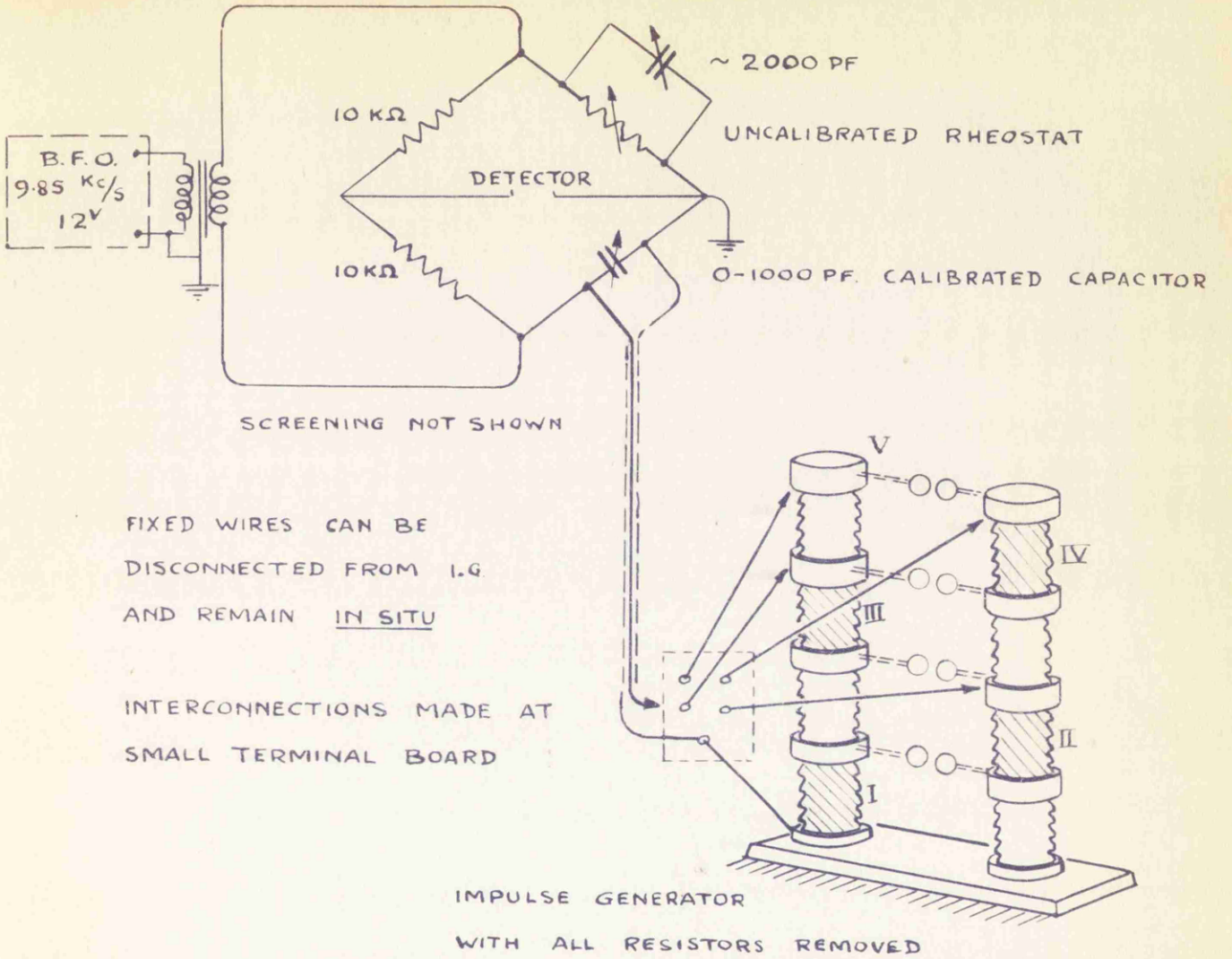

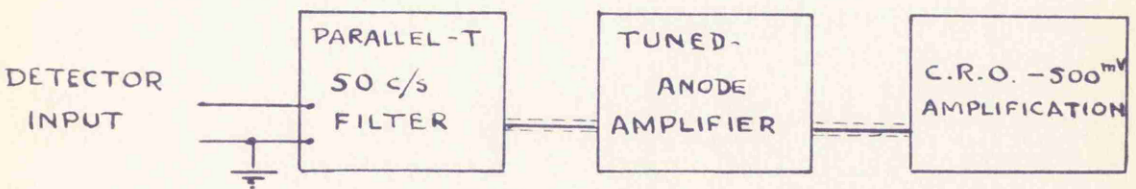

BRIDGE MEASUREMENTS OF PARTIAL CAPACITANCES.

FIGURE 16.

Group	Stages in Group				Partial Capacitances Measured.										Group Capacitance.		
No.	II	III	IV	V	C_1	C_2	C_3	C_4	C_5	C_6	C_7	C_8	C_9	C_{10}	Gross (pF)	Wires (pF)	Net. (pF)
1	*	*	*	*	+1				+1			+1		+1	222.3	46.7	175.6
2	*				+1	+1				+1			+1		119.6	10.6	109.0
3		*				+1	+1		+1		+1				117.3	9.7	108.6
4			*				+1	+1		+1		+1			100.9	12.1	88.8
5				*				+1			+1		+1	+1	76.8	14.3	62.5
6	*	*			+1		+1		+1	+1	+1		+1		220.2	20.3	199.9
7	*		*		+1	+1	+1	+1				+1	+1		156.6	22.7	133.9
8			*	*			+1			+1	+1	+1	+1	+1	155.5	26.4	129.1
9		*		*		+1	+1	+1	+1				+1	+1	129.6	24.0	105.6
10	*	*	*		+1			+1	+1		+1	+1	+1		235.5	32.4	203.1
11	*		*	*	+1	+1	+1				+1	+1		+1	208.5	37.0	171.5
12		*	*	*		+1			+1	+1		+1	+1	+1	187.8	36.1	151.7
13	*	*		*	+1		+1	+1	+1	+1				+1	229.6	34.6	195.0
14	*			*	+1	+1		+1		+1	+1			+1	194.0	24.9	169.1
15		*	*			+1		+1	+1	+1	+1	+1			198.2	21.8	176.4

Wires:- II = 10.6 pF, III = 9.7 pF, IV = 12.1 pF, V = 14.3 pF.

Example: No. 1 represents the equation

$C_1 + C_5 + C_8 + C_{10}$ - (wires II + III + IV + V) = 175.6 pF.

Solutions given in Figure 12.

PARTIAL - CAPACITANCE EQUATIONS. FIGURE 17.

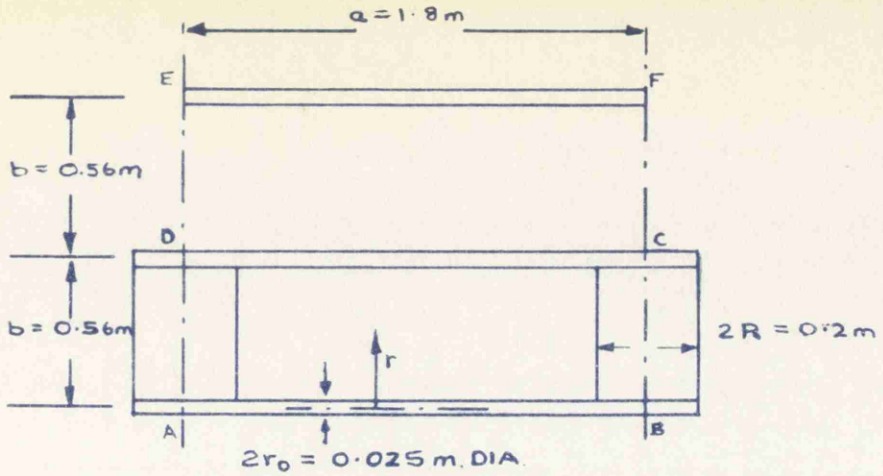

r = radius out from AB.

Mutual Inductance
= 0.16 μH.

Self Inductance
= 1.41 μH/Stage

ORIGINAL CALCULATION OF INDUCTANCE.*

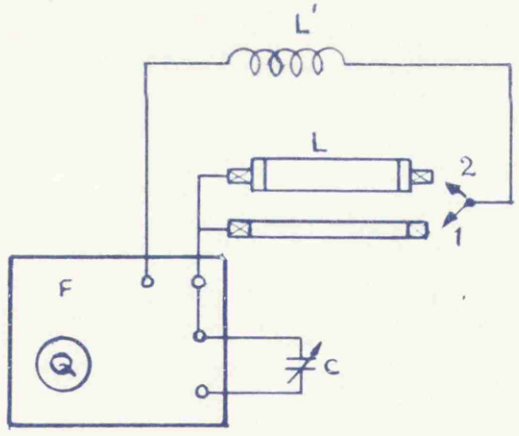

Ballast Inductor

Resistor (R + jωL)

Shorting Link

Variable Capacitor.

Q Meter.

FORMULAE: $R = \frac{1}{\omega}\left(\frac{1}{C_2 Q_2} - \frac{1}{C_1 Q_1}\right)$, $L = \frac{C_1 - C_2}{\omega^2 C_1 C_2}$

L^1(μH)	f(mc/s)	Q_1	Q_2	C_1(pF)	C_2(pF)	L(μH)	R(ohms)
100	1.12	113	~ 20	154	148	5.3	40
50	1.58	127	23	154	144	4.8	25

MEASUREMENT OF INDUCTANCE OF 25 OHM RESISTOR.

* FIGURE 18.
FIGURE 19.

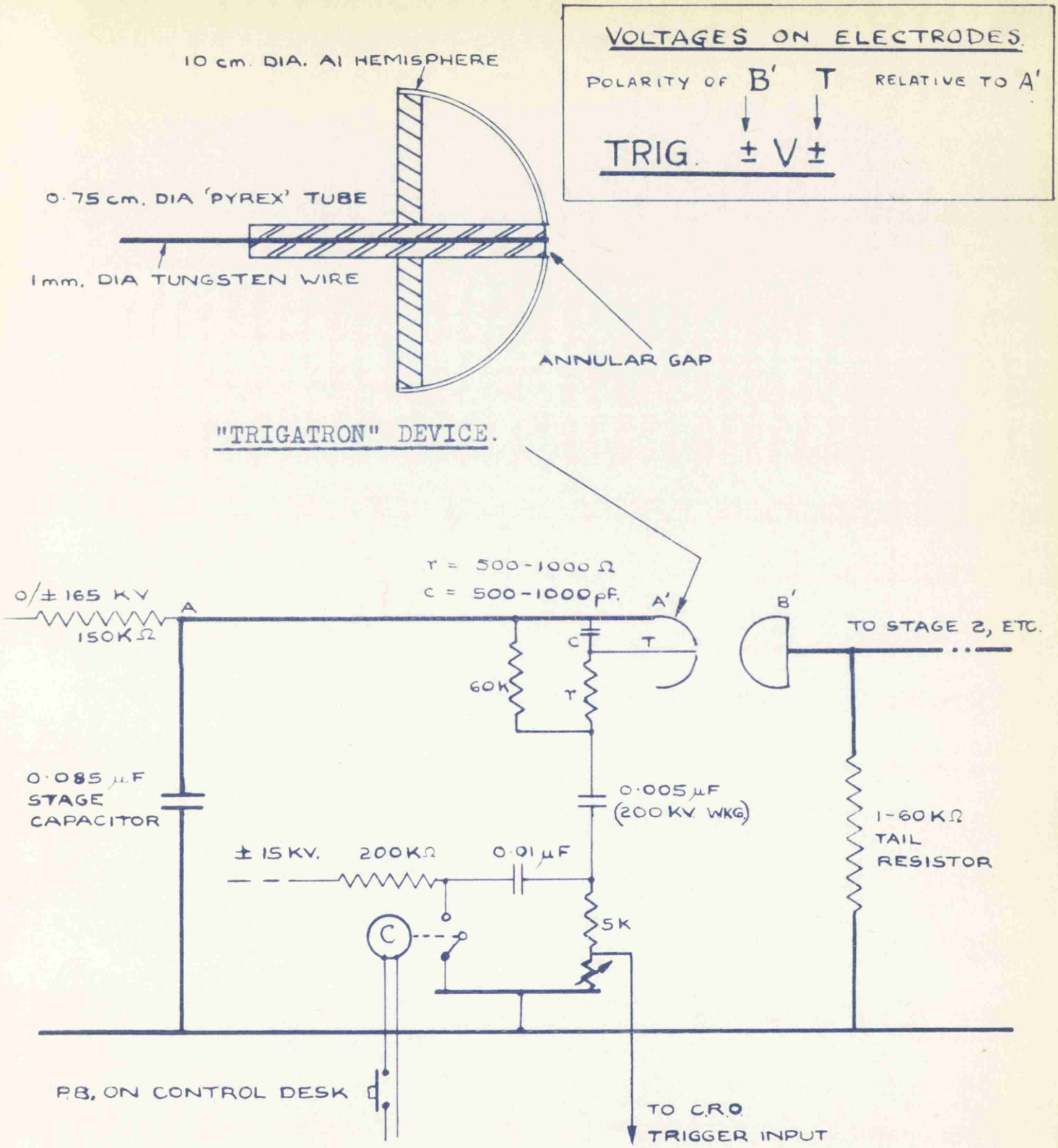

IMPULSE GENERATOR TRIP-CONTROL CIRCUIT.

FIGURE 20.

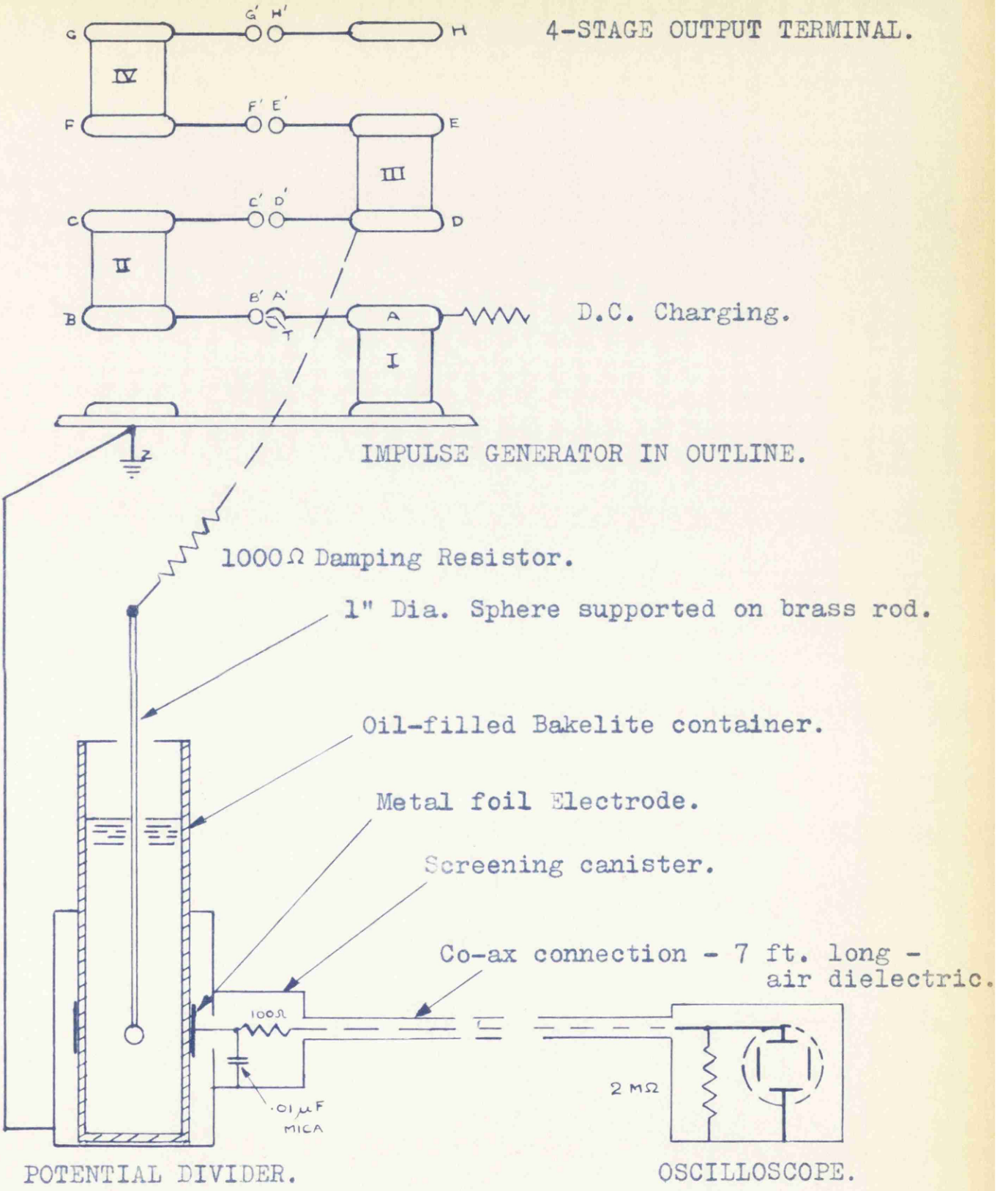

OSCILLOGRAPHIC MEASUREMENT OF VOLTAGES.

FIGURE 21.

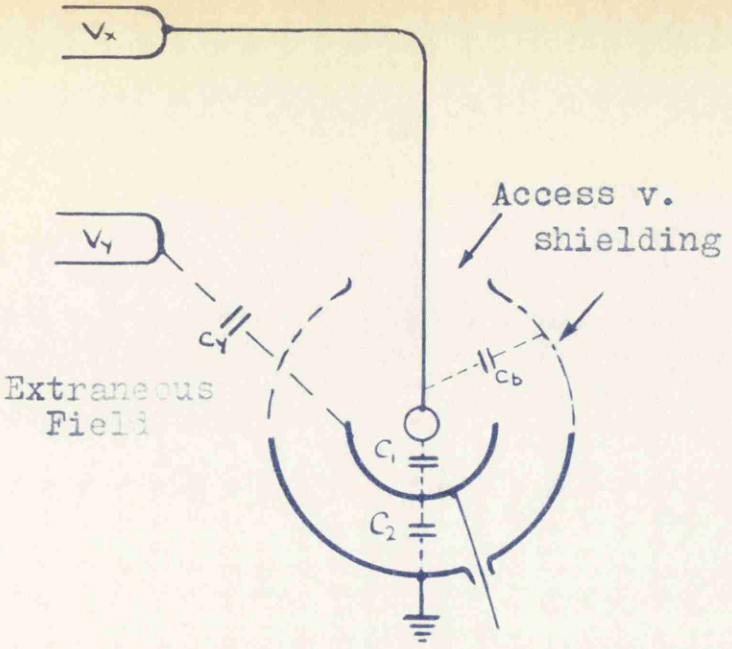

a) Shielding required to make $C_y \ll C_1$.

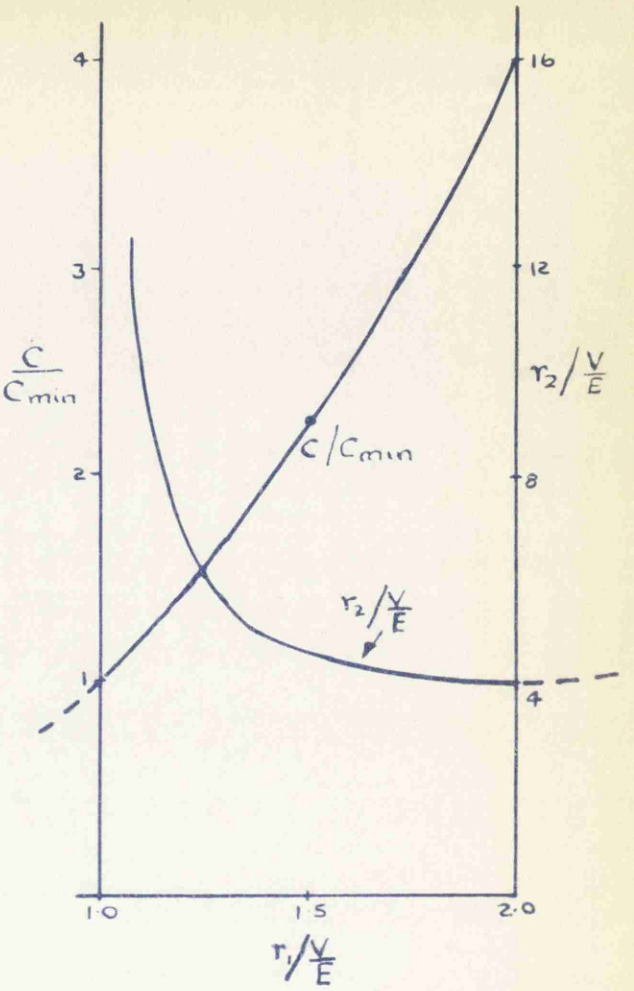

(c) Relative Dimensions.

DIELECTRIC
Permittivity K_1
Dielectric Strength E

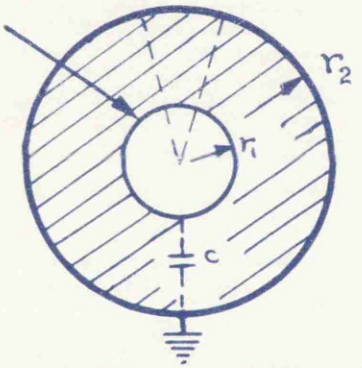

(b) "Transform" of Capacitor.

TABLE: Comparison of Dielectrics. (KV - pF - cm Units)

DIELECTRIC	K_1	Max. E	$\frac{E}{K_1}$	$r_2 = \infty$, $C = C_{min}$		r_2 = min., $C = 4C_{min}$		
				$r_1 = V/E$	C	$r_1 = 2V/E$	$r_2 = 2r_1$	C
AIR	1	30	30	3.3	3.7	6.7	13.3	14.8
OIL	2.5	100	40	1.0	2.8	2.0	4.0	11.0
"PYREX"	4.5	900	200	0.11	0.56	0.22	0.44	2.16
$C.Cl_4$	2.2	660	300	0.15	0.37	0.3	0.6	1.47

DESIGN OF IDEALIZED DIVIDER CAPACITOR.

FIGURE 22

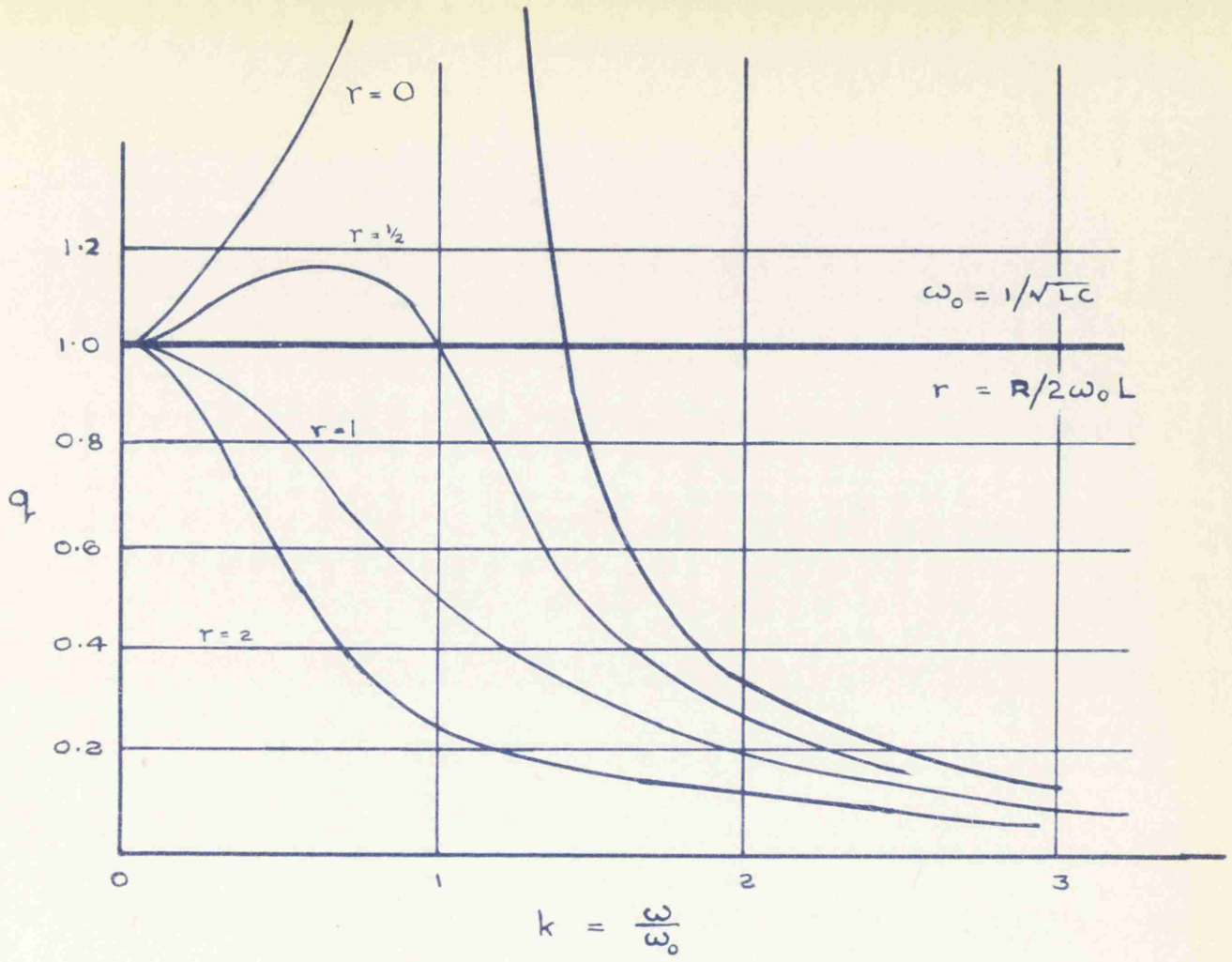

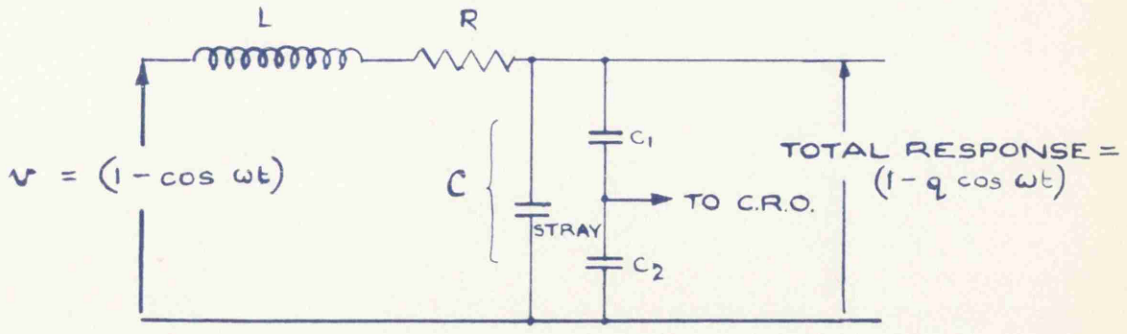

THEORETICAL FREQUENCY RESPONSE OF DIVIDER.

FIGURE 23.

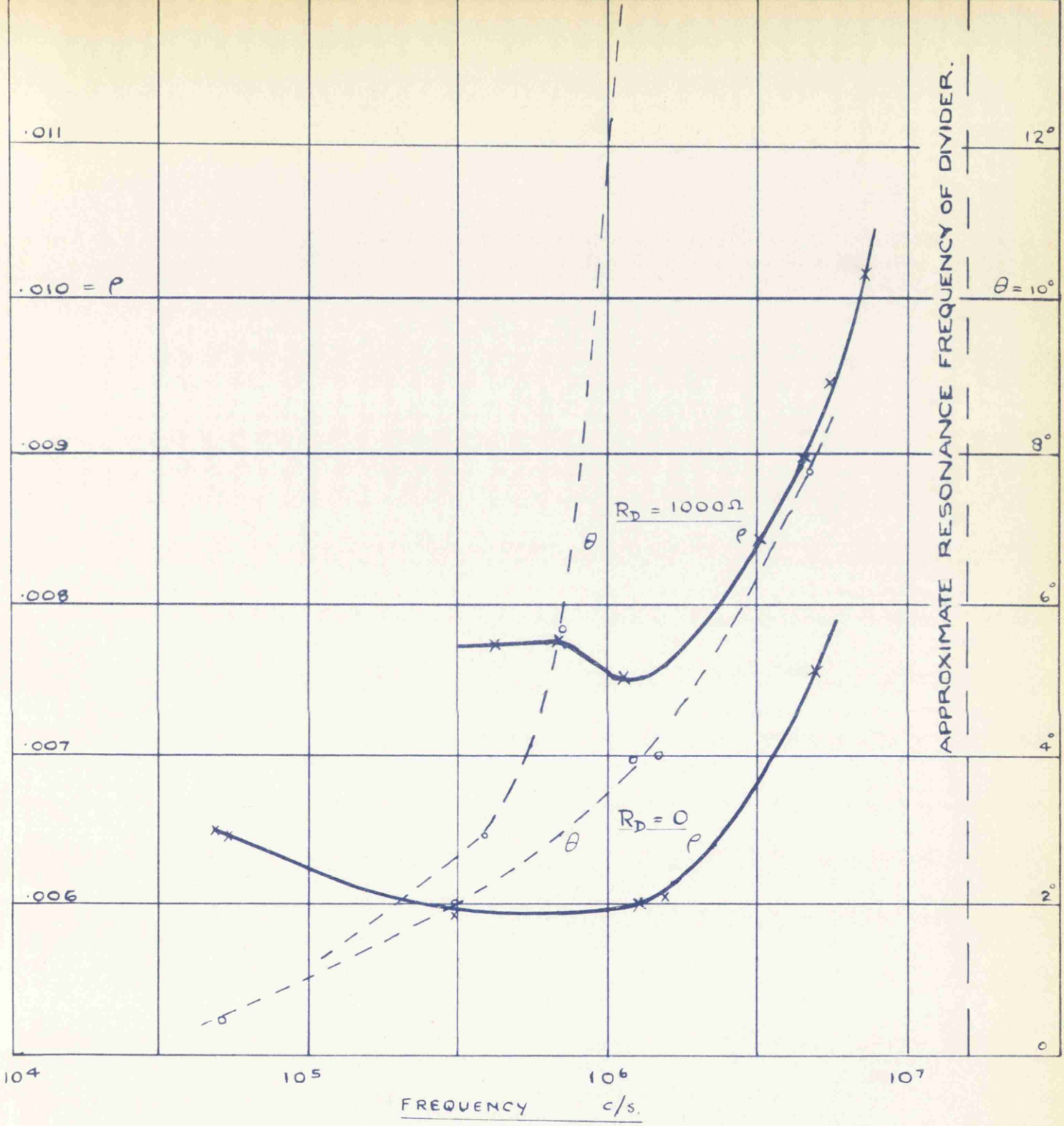

R_D = 0 case measured with original bridge.

R_D = 1000 ohms " " later bridge.

ρ = Ratio output/input voltage.

θ = Phase shift.

MEASURED FREQUENCY RESPONSE OF DIVIDER.

FIGURE 24.

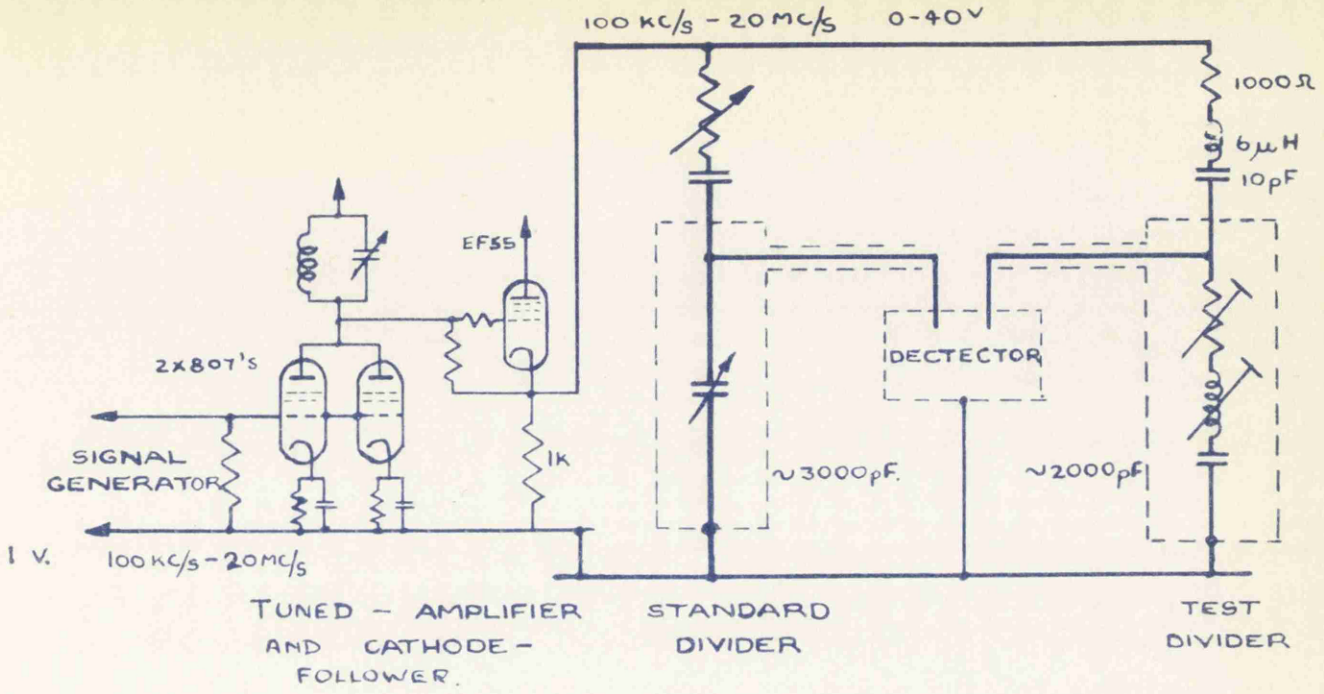

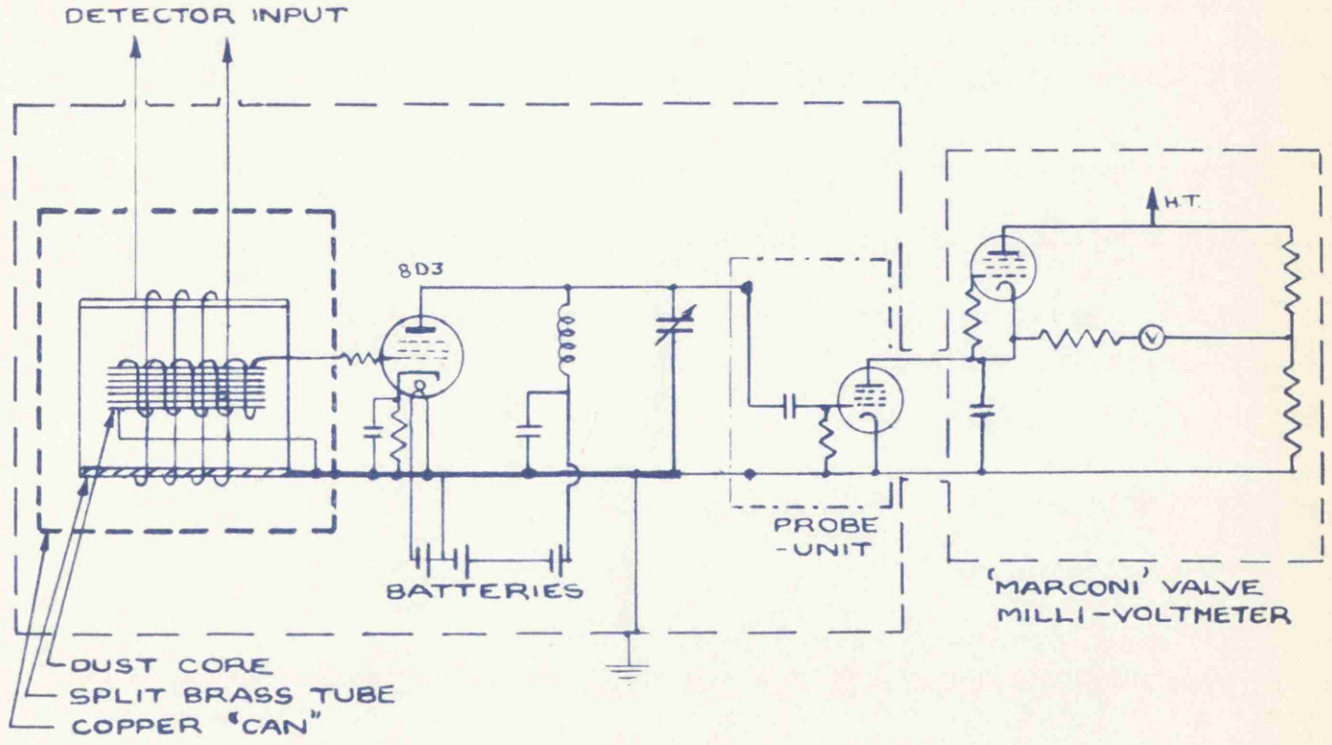

Most Recent Form of Detector.

BRIDGE CIRCUIT FOR CALIBRATION OF POTENTIAL DIVIDER.

FIGURE 25.

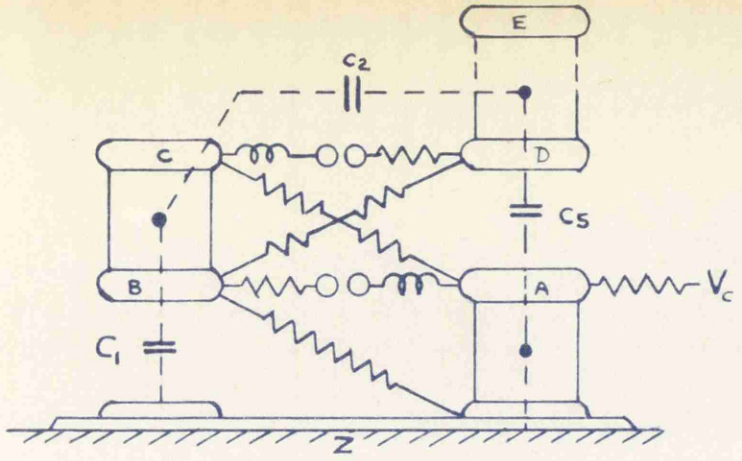

(a) Two Stages of Generator.

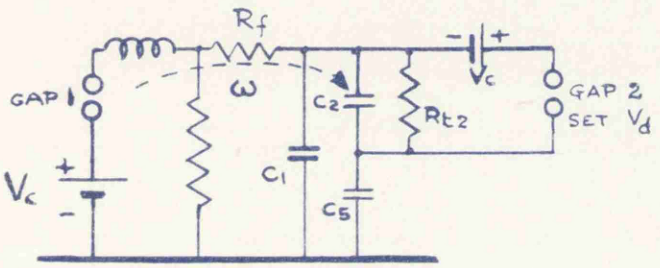

(b) Equivalent Circuit.

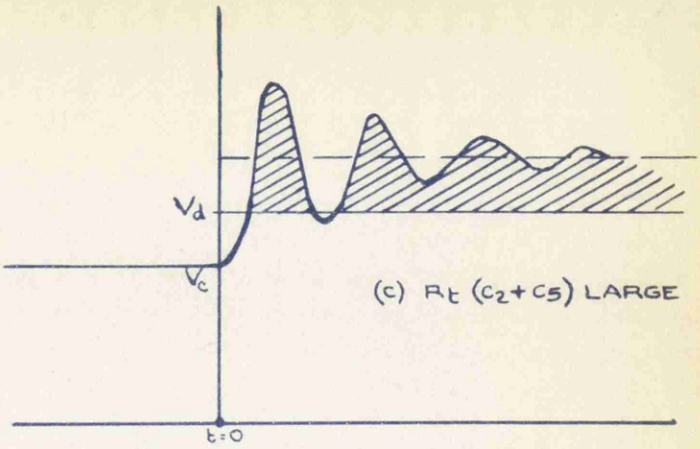

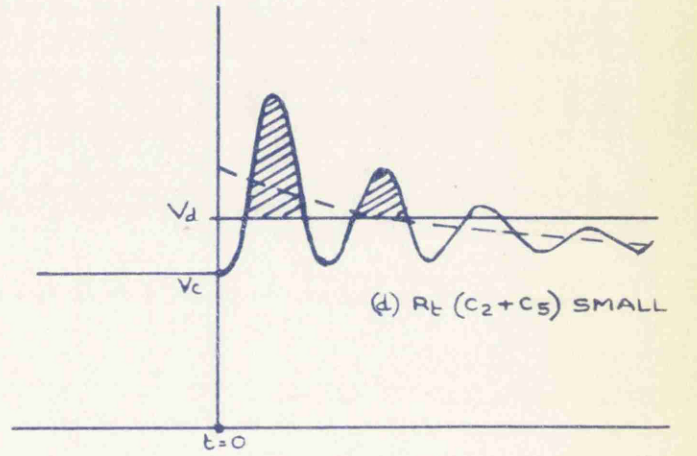

(c,d) Overvoltage Pulses on Gap 2.

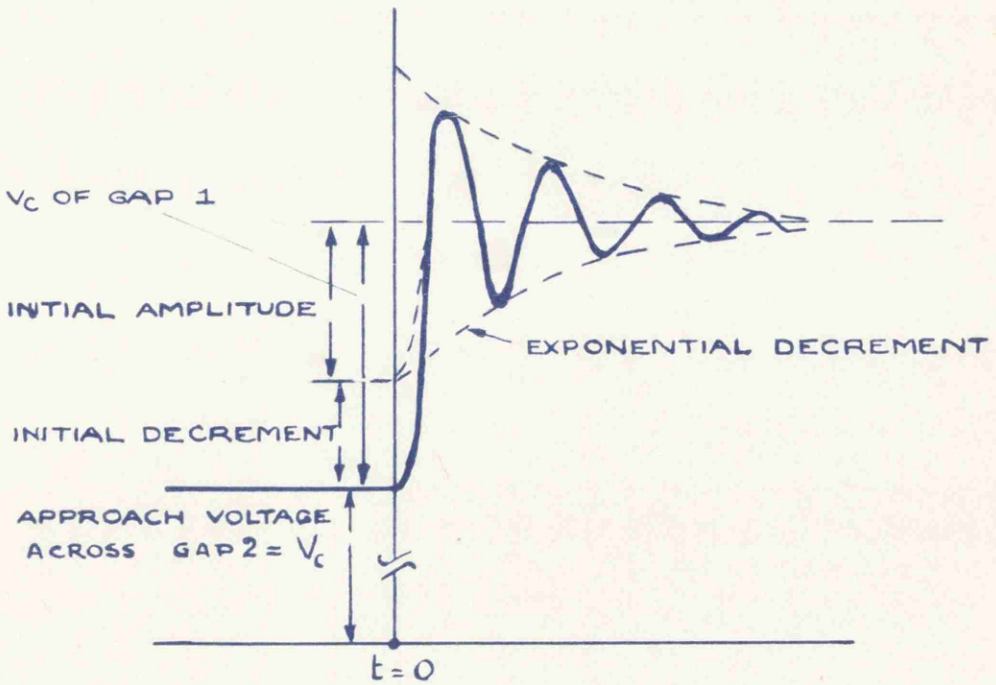

(e) Transient Oscillation due to Gap 1 Firing.

THEORY OF OVERVOLTAGES ON GAP 2.

FIGURE 26.

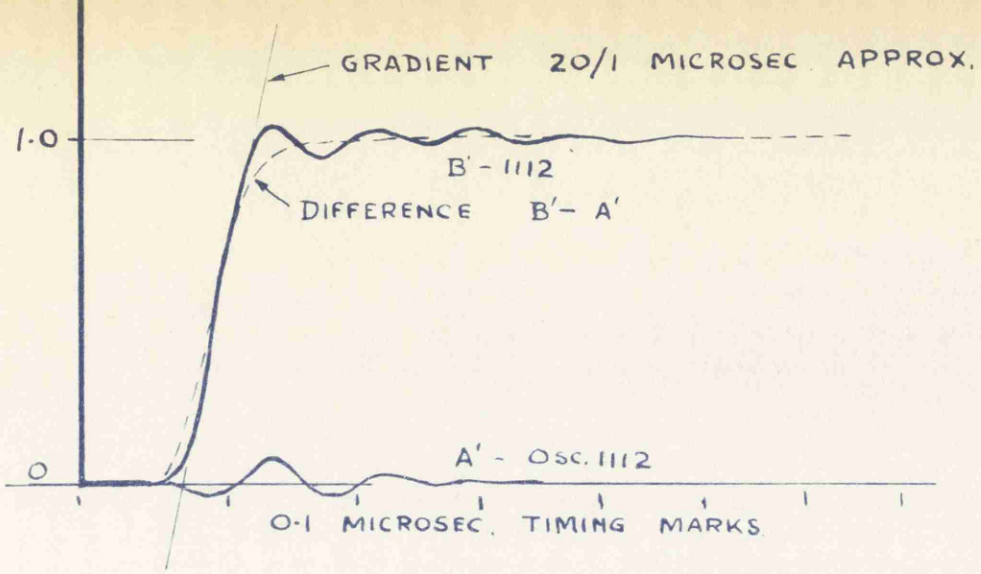

(a) Apparent Voltage-change at Gap 1.

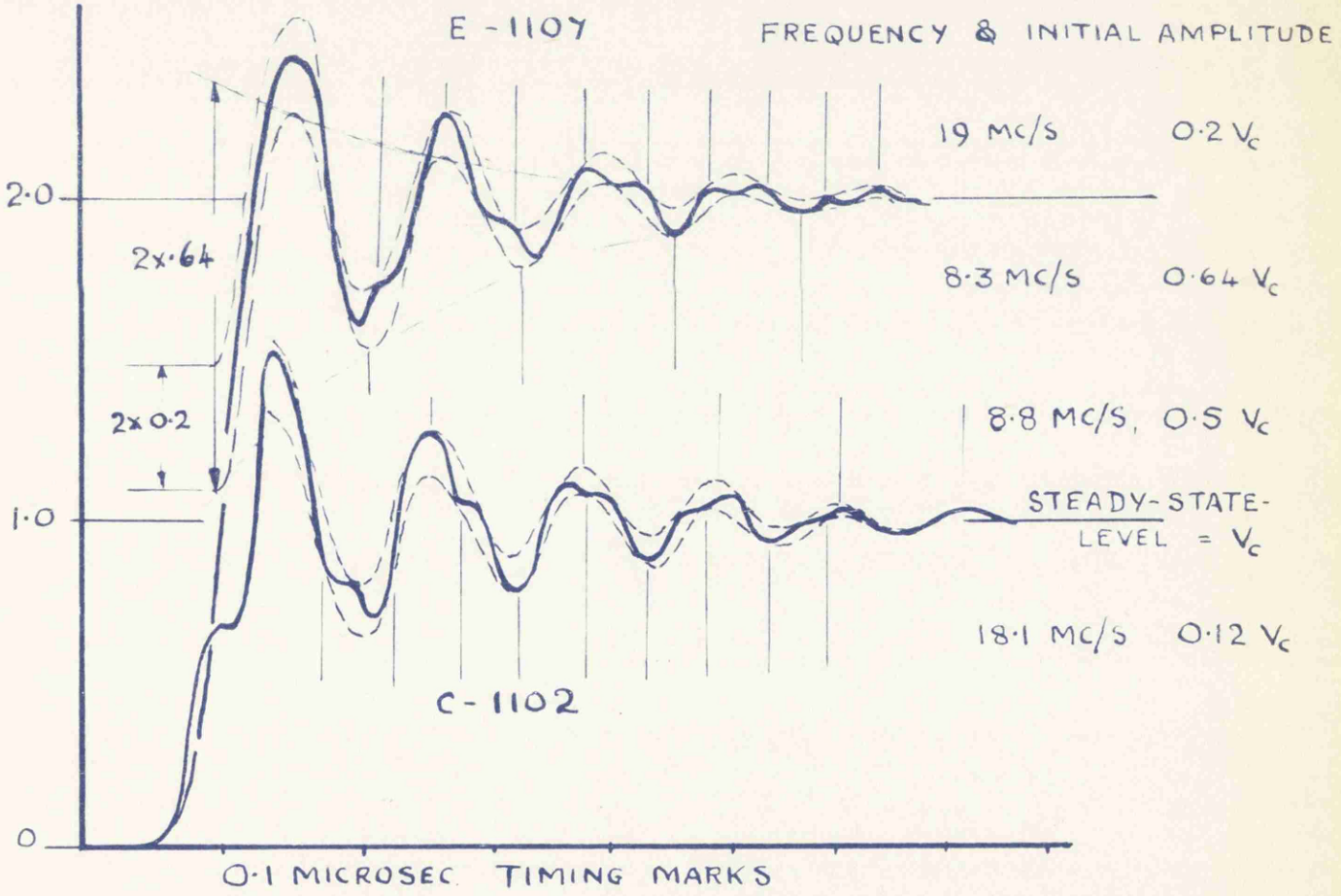

(b) Oscillations in 2-Stage Case.

GRAPHICAL ANALYSIS OF OSCILLOGRAMS.

FIGURE 27.

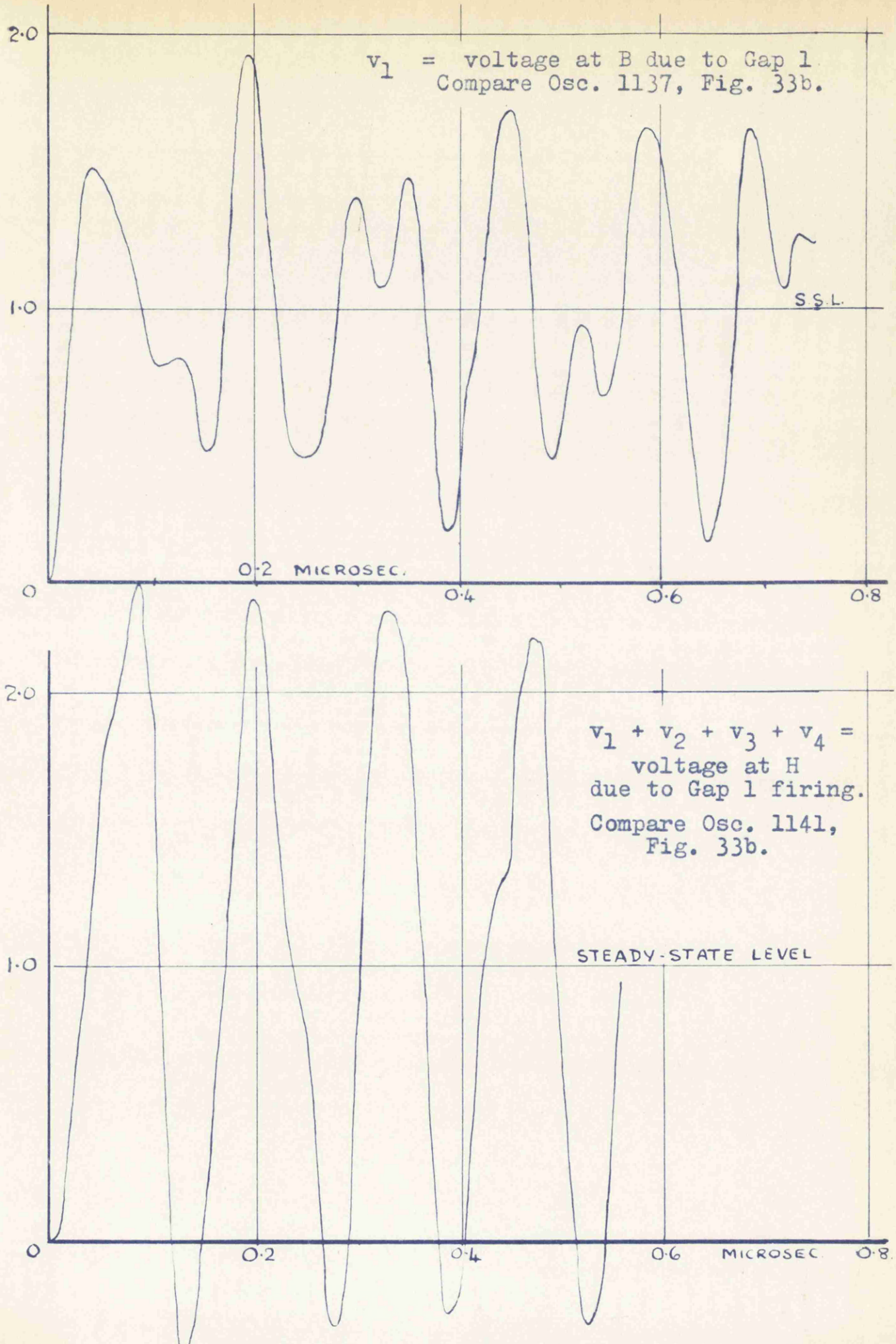

4-STAGE I.G. CALCULATED VOLTAGES.

FIGURE 28.

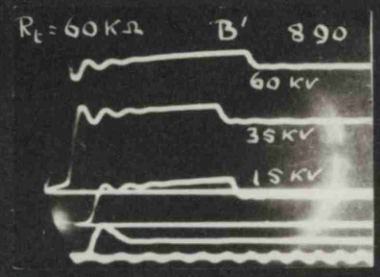

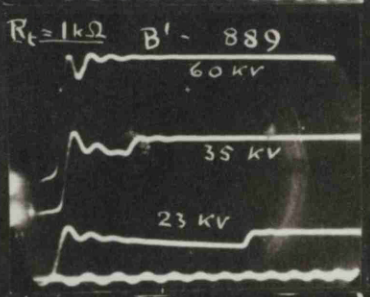

(a)

C.R.O. = 2·5 μs. 5 mc/s. TRIG = −V+

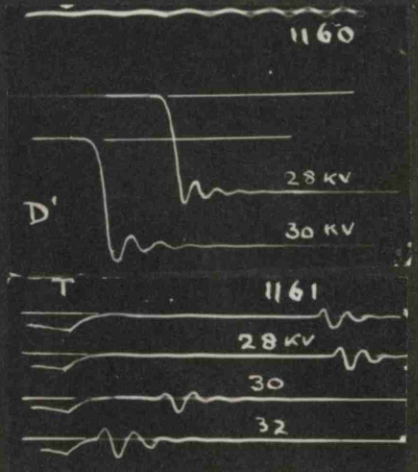

(d) TRIGATRON +V−

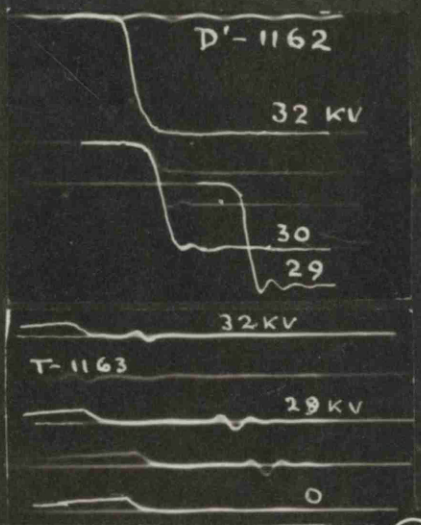

TRIGATRON +V+ (f)

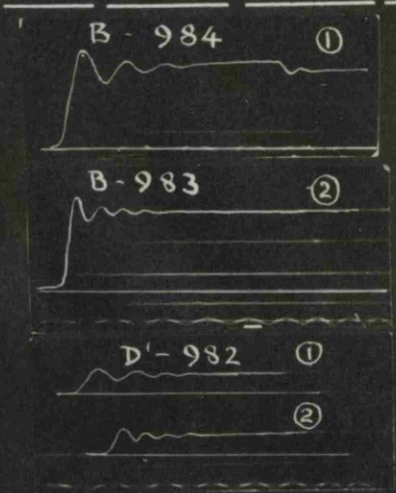

(b)

① Point T, Projecting 1/100"
② " " Withdrawn 1/4"
T, 0, 0, 0 — R_t = 60 KΩ
C.R.O. = 1 μs. 5 mc/s. TRIG = −V+

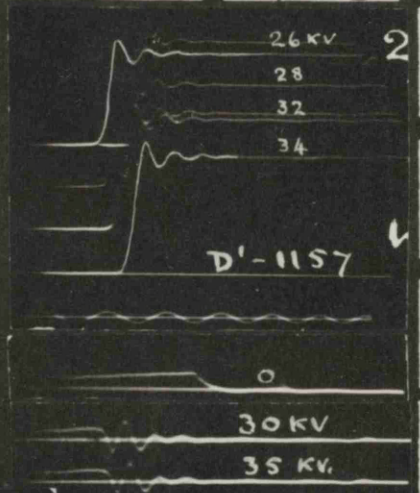

(e) TRIGATRON −V+

Osc. 1157 - 1170

	1	2	3	4
GAPS	S	T	O	O
CM.				
V_d (KV.)				
V_c (KV.)	O	V	O	O
R_t (K.Ω)	60	60	660	660

C.R.O. = 1·5 μs. 5 mc/s. TRIG =

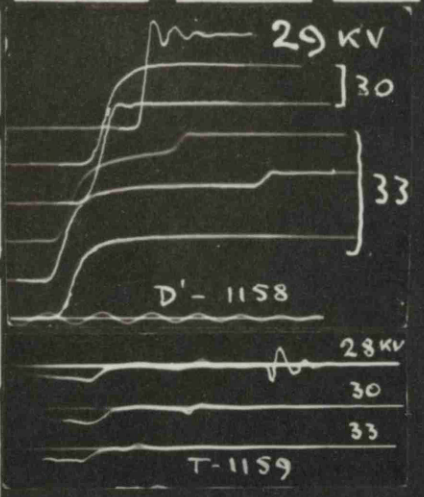

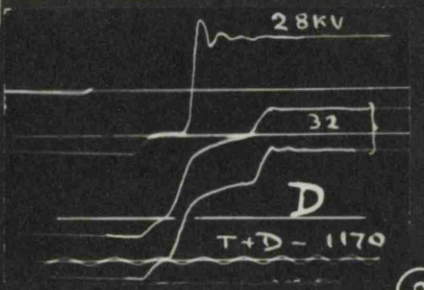

TRIGATRON −V− (g)

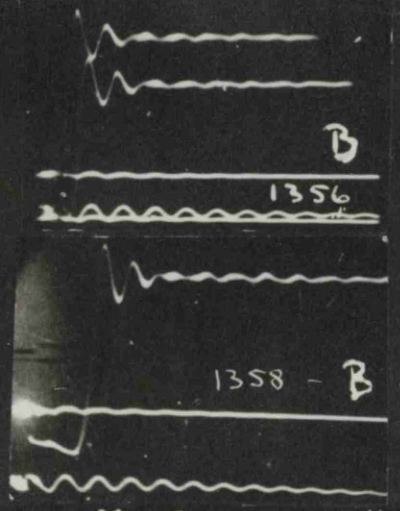

C.R.O. = 2·2 μs 10 mc/s. TRIG = −V− (c)

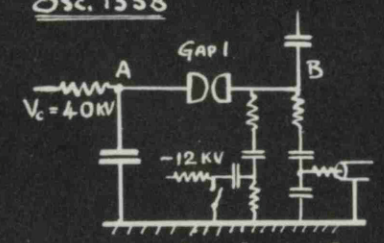

Tripping Gap I by Overvoltage.

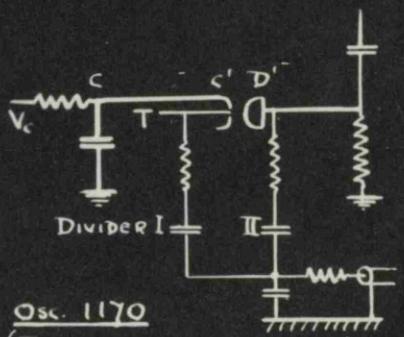

Trigatron Behavior.

Figure. 29.

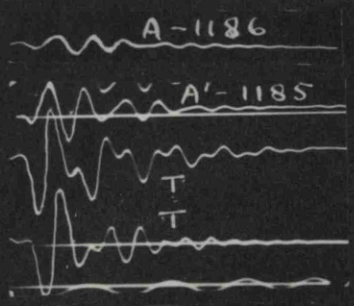

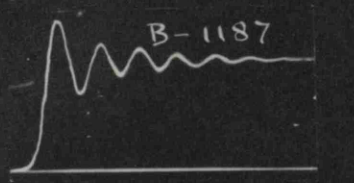

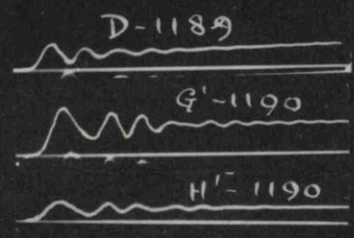

(a)

OSC. 1185 - 1190

	1	2	3	4
GAPS	T	0	0	0
CM.				
V_d (KV.)				
V_c (KV.)	30	0	0	0
R_t (K.Ω)				

C.R.O. = 1 μs. 5 mc/s. TRIG = -V-

OSC. 1215 - 1236

	1	2	3	4
GAPS	T	F	0	0
CM.		1:1		
V_d (KV.)		35		
V_c (KV.)	30	30	0	0
R_t (K.Ω)	60	60	660	660

C.R.O. = 1 μs. 5 mc/s. TRIG = -V-

DIVIDER II USED WITHOUT 1000 Ω DAMPING RESISTOR

(b)

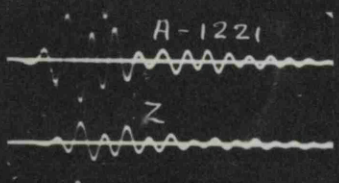

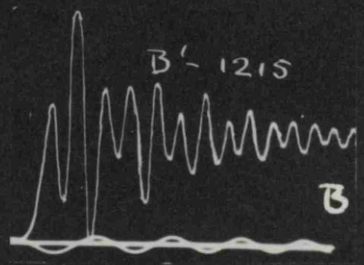

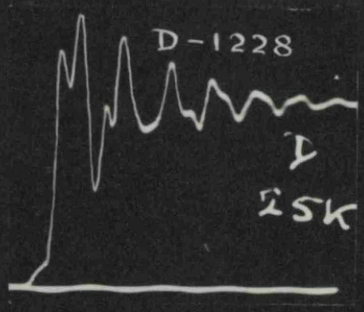

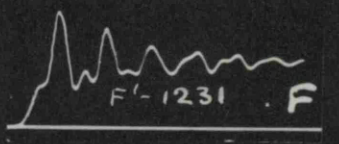

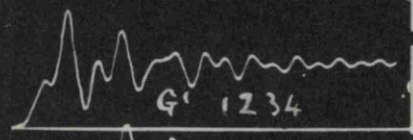

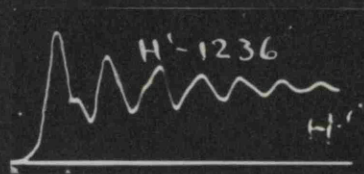

2ND DIVIDER CAPACITANCE CONNECTED TO H'(1236)

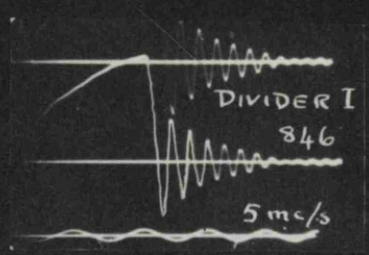

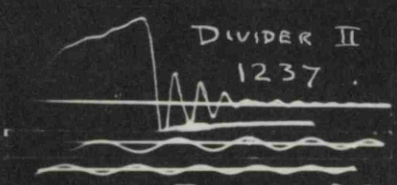

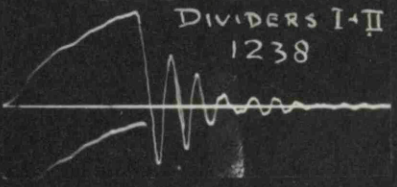

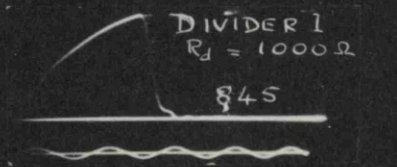

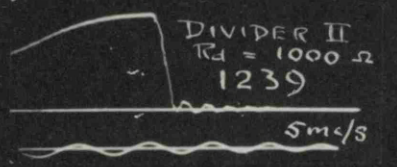

(c)

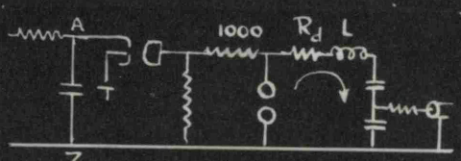

DIVIDER OSCILLATIONS AND DAMPING TESTS.

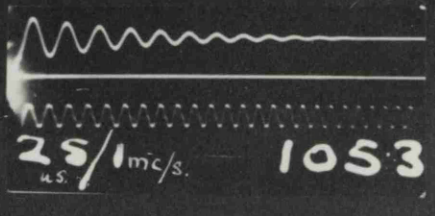

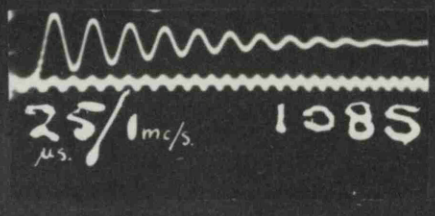

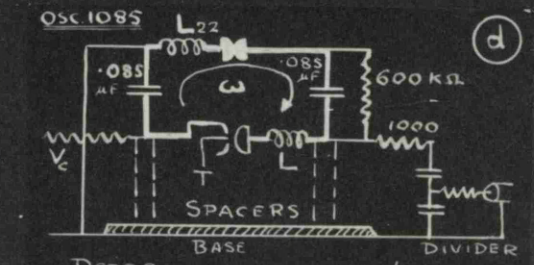

(d)

DETERMINATION OF L_{22}

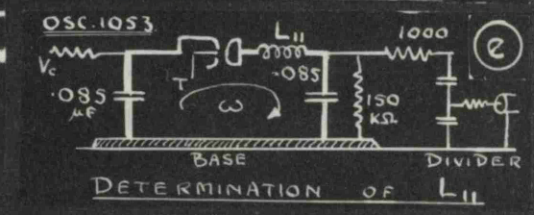

(e)

DETERMINATION OF L_{11}

DIVIDER CONSIDERATIONS AND INDUCTANCE MEASUREMENT FIGURE. 3

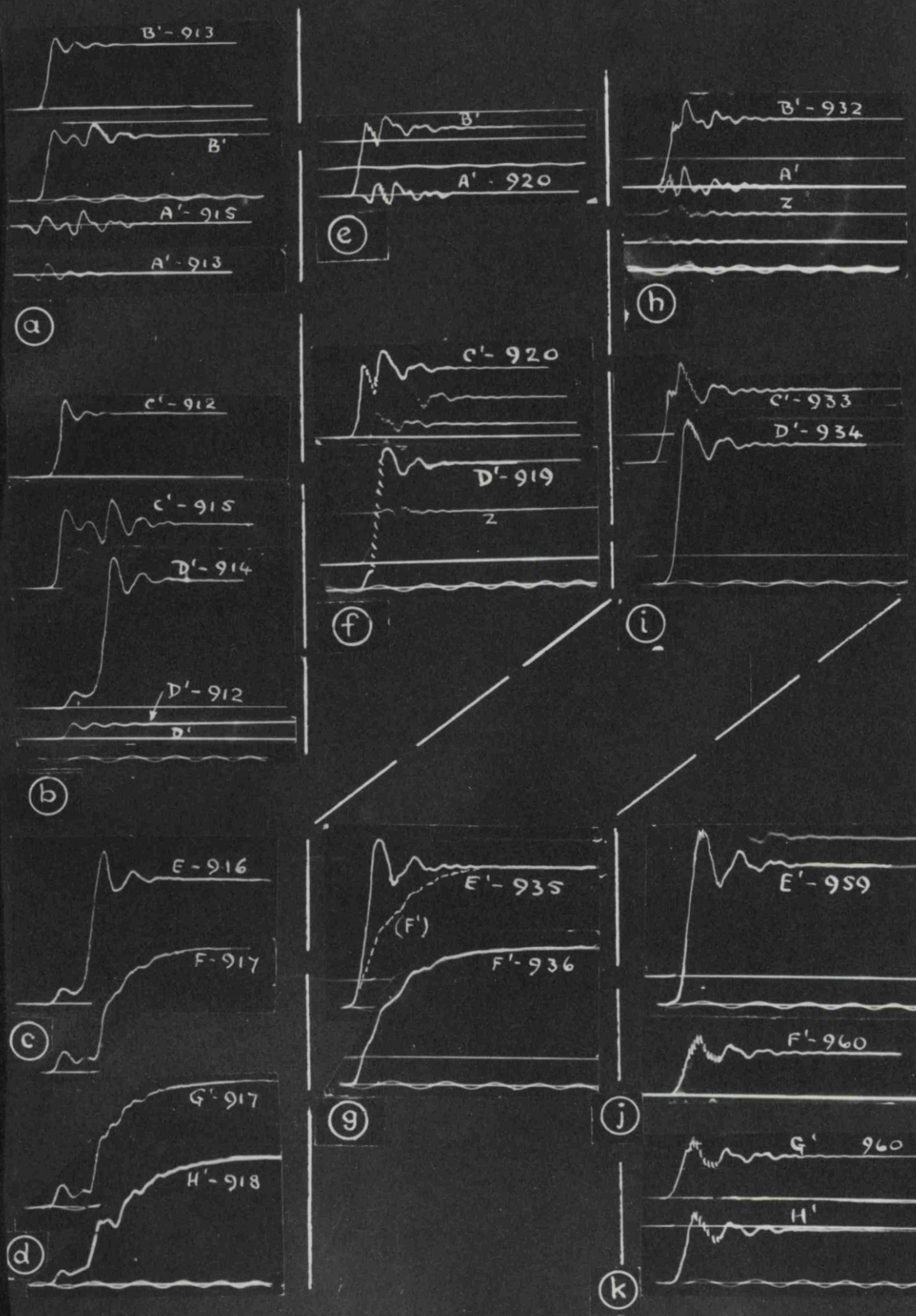

OSC. 959 - 960

	1	2	3	4
GAPS	T	F	0	0
CM.		1·5		
Vd (KV)		46·5		
Vc (KV.)	40	40	0	0
Rt (K.Ω)	60	60	660	660

C.R.O. = 1 μs. 5 mc/s. TRIG = -V-

OSC. 912, 913

	1	2	3	4
GAPS	T	0	0	0
CM.				
Vd (KV)				
Vc (KV.)	41	0	0	0
Rt (K.Ω)	60	60	1	1

C.R.O. = 1 μs. 5 mc/s. TRIG = -V-

914 - 918

1	2	3	4
T	F	0	0
	2·5		
	68		
41	41	0	0
60	60	1	1

OSC. 919 - 920

	1	2	3	4
GAPS	T	F	0	0
CM.		2·0		
Vd (KV)		58		
Vc (KV.)	41	41	0	0
Rt (K.Ω)	60	60	1	1

932 - 936

1	2	3	4
T	F	0	0
	1·5		
	46·5		
40	40	0	0
60	60	1	1

FACTORS INFLUENCING THE FIRING OF GAPS. FIGURE. 31.

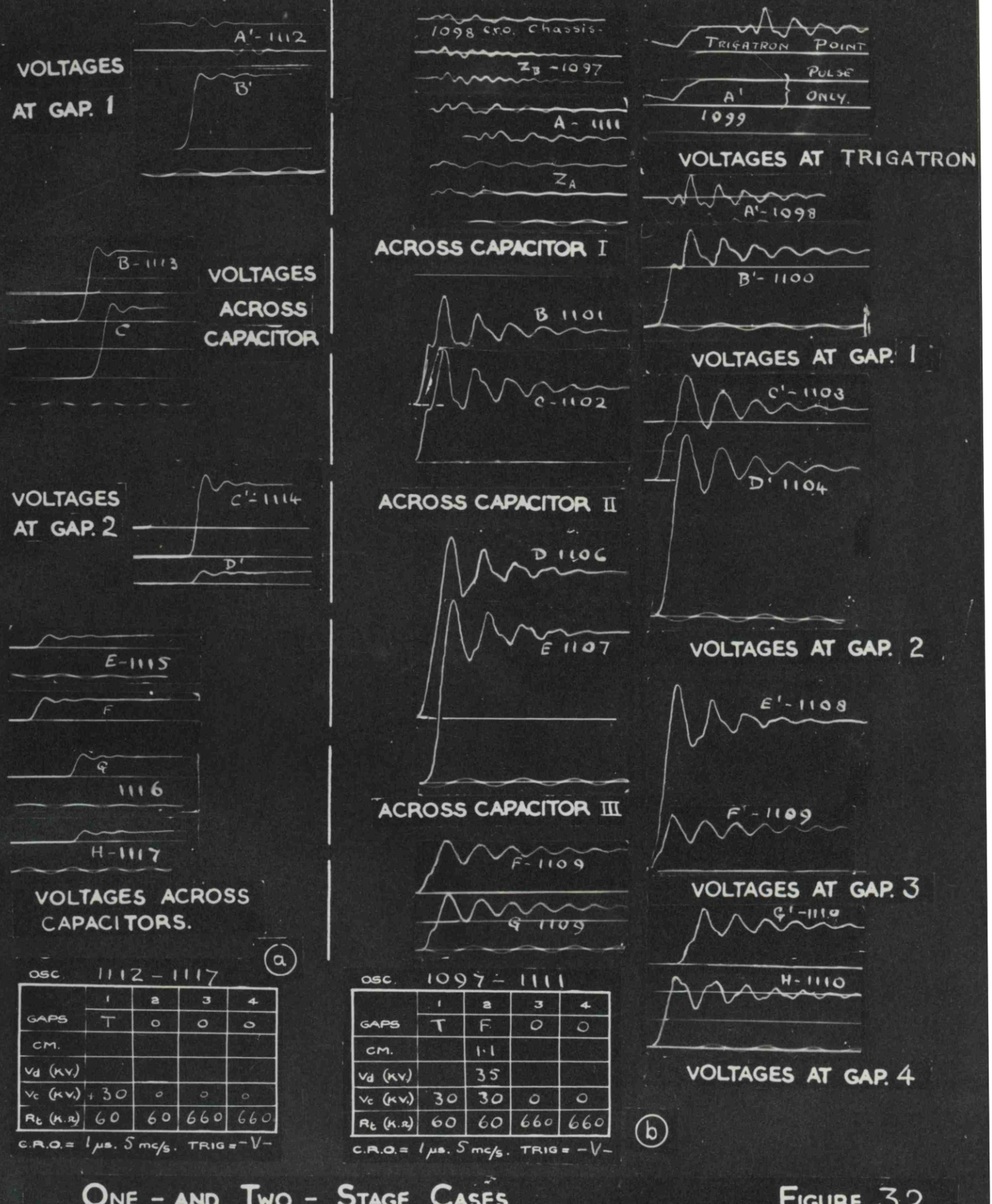

(a)

OSC. 1112 – 1117

	1	2	3	4
GAPS	T	0	0	0
CM.				
V_d (KV.)				
V_c (KV.)	+30	0	0	0
R_t (K.Ω)	60	60	660	660

C.R.O. = 1 μs. 5 mc/s. TRIG = −V−

(b)

OSC. 1097 – 1111

	1	2	3	4
GAPS	T	F	0	0
CM.		1·1		
V_d (KV.)		35		
V_c (KV.)	30	30	0	0
R_t (K.Ω)	60	60	660	660

C.R.O. = 1 μs. 5 mc/s. TRIG = −V−

ONE – AND TWO – STAGE CASES.

FIGURE. 32.

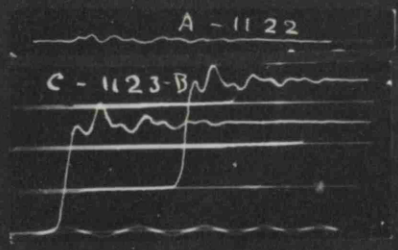

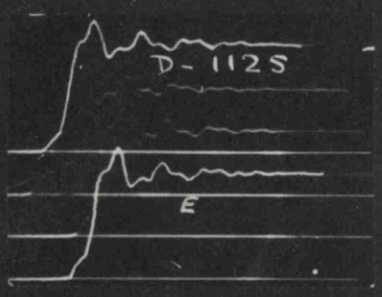

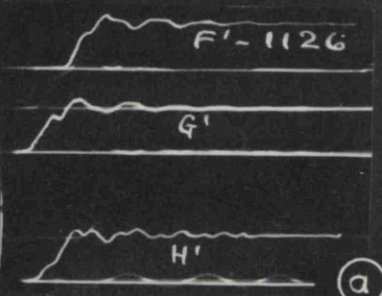

(a)

OSC. 1122 - 1126

	1	2	3	4
GAPS	T	F	0	0
CM.		~0·6		
Vd (KV.)				
Vc (KV.)	30	0	0	0
Rt (K.Ω)	60	60	660	660

C.R.O. = 1 μs. 5 mc/s. TRIG = -V-

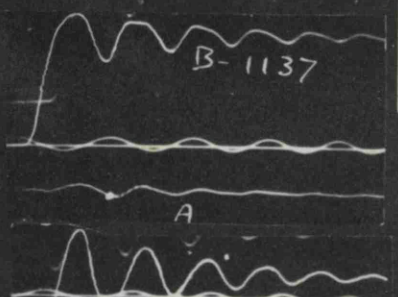

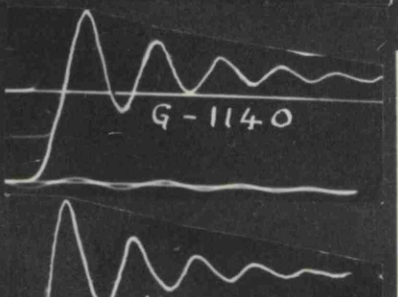

(b)

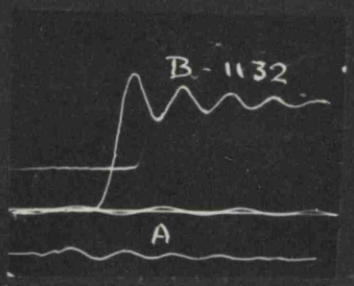

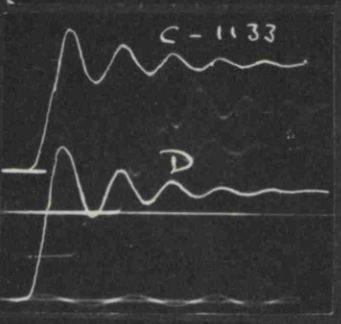

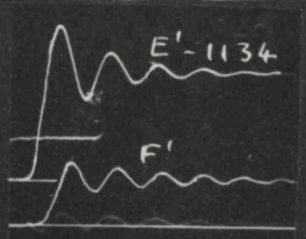

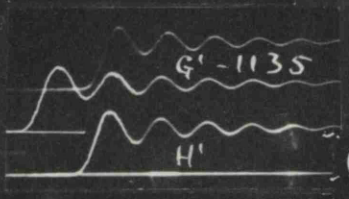

(c)

OSC. 1132 - 1135

	1	2	3	4
GAPS	T	S	0	0
CM.		0		
Vd (KV.)				
Vc (KV.)	30	0	0	0
Rt (K.Ω)	60	60	660	660

C.R.O. = 1 μs. 5 mc/s. TRIG = -V-

OSC. 1137 - 41

	1	2	3	4
GAPS	T	S	S	S
CM.		0	0	0
Vd (KV.)				
Vc (KV.)	30	0	0	0
Rt (K.Ω)	60	60	660	660

C.R.O. = 1 μs. 5 mc/s. TRIG = -V-

OSC. 1142 - 1147

	1	2	3	4
GAPS	S	T	S	S
CM.	0		0	0
Vd (KV.)				
Vc (KV.)	0	30	0	0
Rt (K.Ω)	60	60	660	660

C.R.O. = 1 μs. 5 mc/s. TRIG = -V-

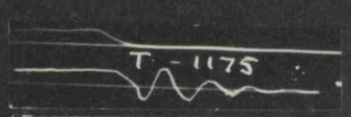

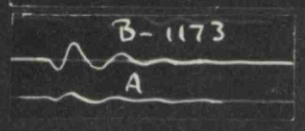

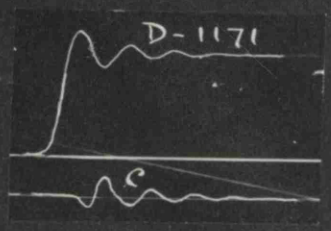

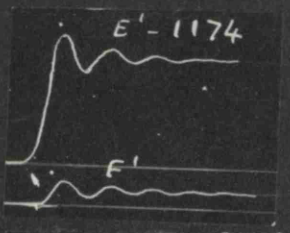

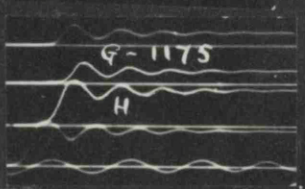

(d)

OSC. 1171 - 1175

	1	2	3	4
GAPS	S	T	0	0
CM.	0			
Vd (KV.)				
Vc (KV.)	0			
Rt (K.Ω)	60	60	660	660

C.R.O. = 1 μs. 5 mc/s. TRIG = -V+

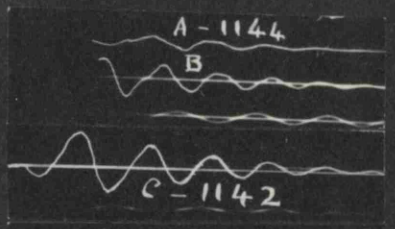

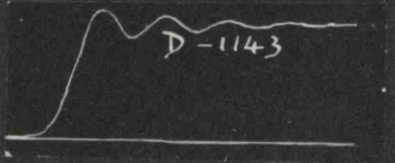

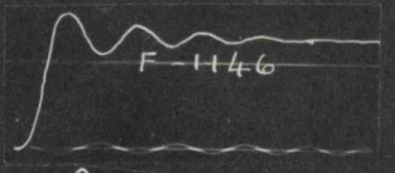

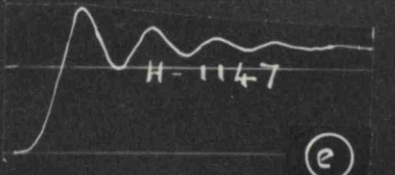

(e)

TWO - AND FOUR - STAGE CASES.

FIGURE. 33.